



# ALMA Band 9 Sideband Separating Upgrade

---

## Study Report

FEND-40.02.09.00-1974-C-REP

Version: C

Status: Released

2023-02-07

<b>Prepared by:</b>		
<b>Name(s)</b>	<b>Organisation/Role</b>	<b>Signature(s) and date(s)</b>
Ronald Hesper	RuG/NOVA	
Jan Barkhof		
Sabrina Realini		
Andrey Baryshev		
Joost Adema		
<b>Approved by:</b>		
<b>Name(s)</b>	<b>Organisation/Role</b>	<b>Signature(s) and date(s)</b>
Carlos de Breuck	ESO	
<b>Released by:</b>		
<b>Name(s)</b>	<b>Organisation/Role</b>	<b>Signature(s) and date(s)</b>
Ronald Hesper	RuG/NOVA	

	<b>ALMA Band 9 Sideband Separating Upgrade</b> <hr/> <b>Study Report</b>	DocID: FEND-40.02.09.00-1974-C-REP Version: C Date: 2023-02-07 Status: Released Page: 2 of 105

## Revision history

Version	Date	Affected section(s)	Change request #	Reason/Initiation/Remarks
A	2022-09-01	All	N/A	Initial document, based on FEND-40.02.09.00-1963-E-REP (ALMA Band 9 Sideband Separating Upgrade—Midterm Study Report)
B	2022-12-01	Many	RIDs	Changes in response to RIDs.
C	2023-02-07	2.2.1; several others (minor)		Clean version after final approval of review panel. Change marks removed. A few typographical corrections and minor changes of wording; some textual relocations to more appropriate places (without change of content); some added (cross-) references. Reformulation of last paragraph in 2.2.1 to close out RIDs 41 and 100.

	<b>ALMA Band 9 Sideband Separating Upgrade</b>	DocID: FEND-40.02.09.00-1974-C-REP
	—	Version: C
	<b>Study Report</b>	Date: 2023-02-07
		Status: Released
		Page: 3 of 105

## Contents

<b>1</b>	<b>Introduction</b>	<b>6</b>
1.1	Scope . . . . .	6
1.2	Scientific driver . . . . .	6
1.3	Outline of historically obtained results . . . . .	6
1.3.1	Noise temperature . . . . .	7
1.3.2	Image rejection ratio . . . . .	7
1.4	Technical overview of the DSB to 2SB transition . . . . .	7
1.4.1	Sideband-separating mixer architecture . . . . .	8
1.4.2	Construction of the 2SB mixer . . . . .	10
1.4.3	Conversion of a DSB CCA to 2SB . . . . .	12
1.5	Tasks in the Study . . . . .	12
1.6	List of acronyms . . . . .	13
<b>2</b>	<b>Study goal 1 — Extending the IF bandwidth</b>	<b>15</b>
2.1	Technical aspects . . . . .	15
2.1.1	Expected SIS mixer IF bandwidth . . . . .	15
2.1.2	Cryogenic IF low-noise amplifiers . . . . .	17
2.1.3	Cryogenic IF hybrid . . . . .	19
2.1.4	IF transport . . . . .	20
2.1.5	Warm IF amplifiers . . . . .	21
2.2	Experimental methods . . . . .	21
2.2.1	Wideband bias-tee . . . . .	21
2.2.2	Cryogenic wide-band LNA . . . . .	24
2.2.3	Cryogenic DSB measurement system . . . . .	26
2.2.4	Band 9 test-bed CCA for 2SB mixer measurements . . . . .	29
2.2.5	Measurement procedure . . . . .	31
2.3	Experimental results . . . . .	32
2.3.1	Initial DSB results with commercial bias-tee . . . . .	32
2.3.2	DSB Results with in-house produced bias-tee . . . . .	33
2.3.3	Sideband-separating results . . . . .	38
2.4	Discussion . . . . .	44
2.4.1	Desired vs. practical IF band . . . . .	44
<b>3</b>	<b>Study goal 2 — Extending the RF bandwidth</b>	<b>46</b>
3.1	Scientific driver . . . . .	46
3.2	Technical aspects . . . . .	46
3.3	Practical implications . . . . .	47
3.4	Costing . . . . .	48
<b>4</b>	<b>Study goal 3 — Availability of SIS mixer devices</b>	<b>49</b>
4.1	Available mixers for the Band 9 2SB upgrade . . . . .	49
4.2	Comparison of average noise with current Band 9 mixers . . . . .	51
4.3	Estimation of the time needed for harvesting . . . . .	54
4.4	Estimation of the time needed for pairing . . . . .	55
4.5	Summary . . . . .	55
4.6	The search for the Golden Wafer . . . . .	56

	<b>ALMA Band 9 Sideband Separating Upgrade</b>	DocID: FEND-40.02.09.00-1974-C-REP Version: C
	<b>Study Report</b>	Date: 2023-02-07 Status: Released Page: 4 of 105

4.6.1	Statistical analysis of I-V curves . . . . .	56
4.6.2	Measurement of additional unknown junctions . . . . .	56
<b>5</b>	<b>Study goal 4 — Improving the polarization purity</b>	<b>58</b>
5.1	Scientific rationale . . . . .	58
5.2	Technical issues . . . . .	58
5.3	Electromagnetic modelling of the Band 9 optics . . . . .	59
5.4	Simulation of the beam squint . . . . .	60
5.5	Simulation of the cross-polarization performance . . . . .	63
5.6	An OMT for Band 9 . . . . .	65
5.6.1	Proposition: Dunning’s OMT . . . . .	66
5.6.2	Straw-man single-horn design . . . . .	68
5.7	Measurement of grid losses . . . . .	69
5.8	Achievable cross-polar level with existing Band 9 optics . . . . .	70
5.9	Cross-polar performance of the bare Band 9 horn . . . . .	72
5.10	Discussion and costing . . . . .	73
<b>6</b>	<b>Study goals 5 and 6 — Upgrade costing</b>	<b>75</b>
6.1	Introduction . . . . .	75
6.2	Parts to re-use, newly procure or discard . . . . .	75
6.3	Cost of full upgrade . . . . .	76
6.3.1	Transport and insurance . . . . .	77
6.3.2	New components . . . . .	77
6.3.3	Spares . . . . .	77
6.3.4	FTE of the upgrade at NOVA . . . . .	78
6.3.5	FTE at JAO . . . . .	78
6.3.6	Summary . . . . .	79
6.4	Expected price increase for optional upgrades . . . . .	79
6.5	Cost of upgrading four CCAs only . . . . .	80
<b>7</b>	<b>Study goal 7 — Upgrade strategies</b>	<b>82</b>
7.1	Technical and logistical issues — introduction . . . . .	82
7.2	Availability during upgrade . . . . .	82
7.2.1	Recombination of USB and LSB during upgrade . . . . .	83
7.2.2	Co-existence of 2SB and DSB receivers during upgrade . . . . .	83
7.3	Logistics of the upgrade procedure . . . . .	84
7.4	Possibilities of a pre-production series . . . . .	85
7.5	Scheduling and FTE issues . . . . .	85
<b>8</b>	<b>Conclusions and outlook</b>	<b>86</b>
8.1	Conclusions . . . . .	86
8.2	Outlook . . . . .	86
<b>A</b>	<b>Appendix — Statistical SIS I-V curve analysis</b>	<b>88</b>
<b>B</b>	<b>Appendix — Polarimetry with ALMA</b>	<b>92</b>
B.1	Analysis cross-pol vs. beam squint . . . . .	92
B.2	Beam squint statistics of the ALMA bands . . . . .	94



<b>C Appendix — Observing during a 2SB upgrade roll-out</b>	<b>97</b>
C.1 Ideal case: per-antenna sub-band configuration . . . . .	97
C.2 Uniform signal path configuration for the whole array . . . . .	98
C.2.1 Relevant correlator capabilities . . . . .	99
C.2.2 Implications on offline processing . . . . .	100
C.2.3 Point-source sensitivity during the upgrade roll-out . . . . .	100
C.2.4 Pros and cons . . . . .	101
<b>References</b>	<b>103</b>

	<b>ALMA Band 9 Sideband Separating Upgrade</b>	DocID: FEND-40.02.09.00-1974-C-REP Version: C
	<hr/> <b>Study Report</b>	Date: 2023-02-07 Status: Released Page: 6 of 105

## 1 Introduction

In this section we formulate the scope, purpose and goals of the study, and present a short overview of past developments leading up to it. Some of the material here is derived from the original Study Proposal [1] and its Amendment [2].

### 1.1 Scope

This Study Report reports on the study titled “Full 2SB Receiver Upgrade for ALMA Band 9: Implementation Study”, performed by the Sub-mm Instrumentation Group, located at the University of Groningen as part of the Netherlands Research School for Astronomy (NOVA), in the framework of the ESO “Advanced Study for Upgrades of the Atacama Large Millimeter/submillimeter Array (ALMA)” (CFP/ESO/16/11115/OSZ). The study is carried out under ESO Collaboration Agreement No. 94866/19/86535/ASP and is formally defined in the Statement of Work (SoW), document nr. ESO-330284.

Several of the topics in this Study Report were already (partially or in full) covered in the Midterm Study Report [3], which passed review, with amendments, in November 2020. The current Study Report supersedes this document.

### 1.2 Scientific driver

The technical feasibility of an ALMA Band 9 upgrade from the existing double-sideband (DSB) configuration to sideband-separating (2SB) was demonstrated in an ESO study by the NOVA Sub-mm Instrumentation Group several years ago [4]. Since then, the design of the sideband-separating mixer has been developed further with significant improvement of the key parameters, namely sensitivity (noise temperature) and image rejection ratio (IRR) [5, 6, 7]. Subsequently, two left-over DSB Band 9 receiver cartridges were converted to 2SB operation [8], one for the SEPIA facility instrument [9] on the APEX telescope in Chile and one for the future LLAMA observatory in Argentina. The former has successfully passed its science commissioning phase, with several key performance parameters far exceeding the specification [10], and is in full operation. These receivers both offer a total IF bandwidth of  $4 \times 8$  GHz, which is double the total bandwidth of the current ALMA DSB and 2SB receivers (with the exception of Band 6, which already exports  $4 \times 5.5$  GHz).

Even without any further widening of the IF bandwidth beyond the demonstrated factor of 2, this upgrade will increase the ALMA sensitivity in Band 9 by 20–30% on average for spectral line observations [6]. This ties in with the Recommended Development Path number 2 (“Larger bandwidths and better receiver sensitivity: enabling gain speed”) in the ASAC recommendations for ALMA 2030 [11]. It also fits in Pathway No. 04 (“2SB B9/B10”) and Pathway No. 05 (“Sensitivity: Lower noise Rx’s”) in the ALMA Development Working Group Report “Pathways to Developing ALMA” [12] and in the ALMA Development Roadmap [13].

### 1.3 Outline of historically obtained results

Here we briefly outline a couple of the key performance results obtained with the SEPIA660 receiver cartridge, which can be considered a baseline prototype for any ALMA Band 9 2SB upgrade.

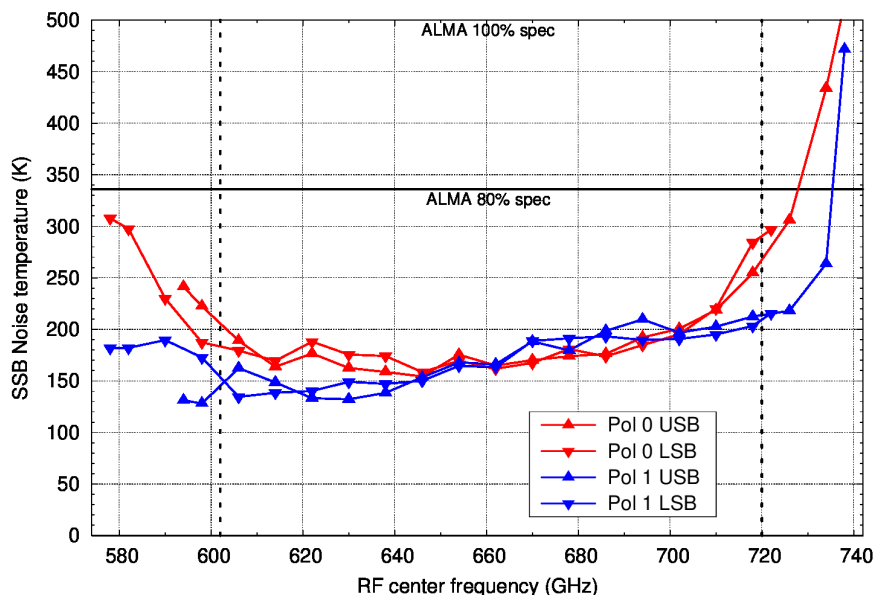


Figure 1: Single-sideband noise temperature integrated over the 4–12 GHz IF band for the delivered SEPIA660 Receiver (lab qualification data). The 80% (336 K) and 100% (500 K) “ALMA specifications” are simply the Band 9 DSB limits multiplied by two. Measurements performed at 4.0 K

### 1.3.1 Noise temperature

The measured SEPIA SSB receiver noise temperature is shown in figure 1. The ALMA Band 9 specifications, adapted to the 2SB case, are shown in the same figure for comparison. At the request of the APEX/SEPIA team the receiver has been characterized over an extended frequency range (580–740 GHz, see also chapter 3). The demonstrated noise performance is well within the SSB-equivalent to the ALMA specifications.

### 1.3.2 Image rejection ratio

The SEPIA660 image rejection ratio (IRR) is presented in figure 2. Measurements were done by using a CW signal source on the background of a wideband Hot/Cold load [14]. The Sideband rejection ratio exceeds 15 dB over most of band, considerably higher than the typical specification for other ALMA bands.

Other key receiver parameters (e.g., stability and IF ripple) also fully meet equivalent ALMA specifications.

## 1.4 Technical overview of the DSB to 2SB transition

Although the principles of sideband-separation are generally known, a brief overview is given here for readers less familiar with the technical aspects, and also to establish some of the nomenclature and details of the chosen implementation. In addition, the conversion from an existing DSB Band 9 receiver to a 2SB version, as performed for SEPIA660, is briefly outlined.

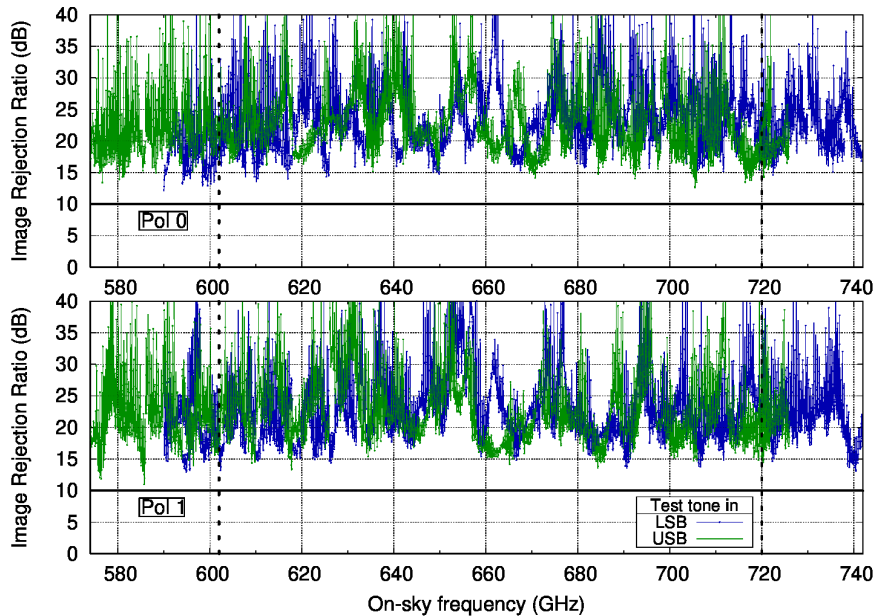


Figure 2: Image rejection ratio measured for the SEPIA660 receiver, as delivered. The LO settings are spaced by 8 GHz, and at each LO frequency the IRR is determined over the full 4–12 GHz IF band.

To set out on the terminology, with  $RF$  we mean the signals coming from the sky at the observational frequency (about 600–720 GHz in case of Band 9), with  $LO$  the tunable frequency of the local oscillator (in roughly the same frequency range) that is mixed with it for down-conversion, and finally with  $IF$  the signals at the difference frequencies of the two (in ALMA currently within a 4–12 GHz range, fully or in part, depending on receiver band). Since this difference can be both positive and negative ( $RF$  above or below the  $LO$ ), we speak of the Upper Sideband (USB) and Lower Sideband (LSB), respectively. In a Double-Sideband (DSB, a.k.a. single-ended) mixer, the two downconverted sidebands are superimposed at the IF output; in a Sideband-Separating (2SB) system, as the name indicates, these are separated from each other and exported at different outputs.

#### 1.4.1 Sideband-separating mixer architecture

The architecture most commonly used to obtain wide-band sideband-separation, schematically shown in figure 3, is based on a so-called I-Q mixer. This consists of two single-ended (DSB) mixers running in quadrature (i.e., with a  $90^\circ$  RF-to-LO phase difference) with respect to each other. For this, either the RF or the LO signal supplied to one of the mixers has to be retarded by one-quarter period, for every frequency within the band of interest. For several reasons, which we will not dwell on here, we choose to shift the RF into quadrature and leave the LO in-phase. The phase-shifting is performed by a so-called (quadrature) hybrid, which is a passive device (typically built in waveguide or stripline technology) that combines the signals from two inputs and divides them again over two outputs, equally in power but, for both channels, introducing a  $90^\circ$  phase difference between the “straight” and “crossed” paths. These two sums are fed into the single-ended mixers which effectively multiply the added RF and LO signals, thereby downconverting them to the IF band. The outputs of the two mixers (containing the difference frequencies in different phase combinations) are then recombined

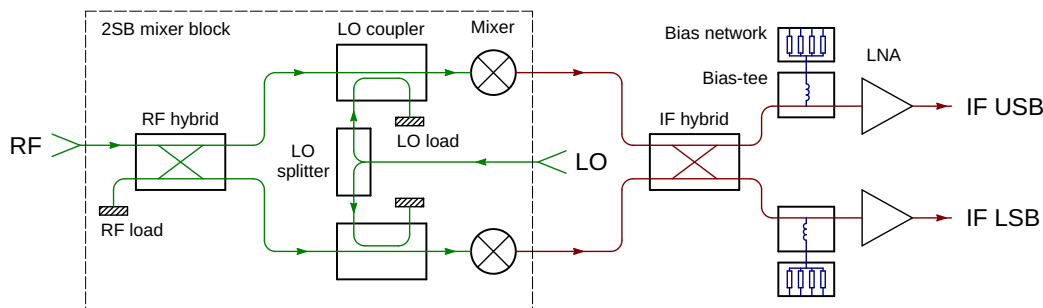


Figure 3: Schematic diagram of the 2SB mixer architecture as used in the SEPIA/LLAMA receivers, as well as in the test-bed receiver described later in this report. Waveguides are drawn in green, IF coaxial cables or (micro)strips in red, DC lines in blue. The RF signal is split equally with  $90^\circ$  phase difference by the RF quadrature hybrid, a small portion ( $\approx -13\text{dB}$ ) of the LO signal (split in-phase) is added in the LO couplers, and in each branch the RF and LO are mixed by the respective (single-ended) mixer. The downconverted IF signals are then recombined in the IF quadrature hybrid into the two sidebands (which may be swapped with respect to the order given in the schematic, depending on details of the phase relations), and are subsequently amplified by the LNAs and exported to the back-end. In between the mixers and the LNAs, bias-tees provide DC bias to the former, which is first conditioned in the bias networks. Critical for the performance are the waveguide loads which terminate the uncoupled LO power (LO loads) and any LO power reflected off the mixers (RF load). All waveguide parts and the mixers are integrated in modular split-block assembly; more details on the latter can be found in, e.g., [5] and [7].

and split again in another hybrid, operating at IF frequencies. When all phase relations are correctly followed through the chain, it turns out that in one of the IF hybrid's outputs the USBs are in phase and therefore reinforce each other, while the LSBs end up in anti-phase and cancel. In the other output the reverse happens. Some more details of the arrangement used in our case are given in the caption of figure 3.

One confusing aspect of the terminology is that both the single-ended mixer device (in our case a superconducting tunnel junction) as well as the entire assembly just described are called a "mixer". In the rest of this report, when there is occasion for confusion, we will try always to talk consistently about DSB (or single-ended) and 2SB mixers.

Also drawn in figure 3 are the components after the IF hybrid. The (cryogenic) LNAs amplifying the IF signals are critical for the noise performance, since they are the first elements in the signal chain providing gain (all preceding components being lossy to some extent). As in the case of the RF loads, the impedance matching of the LNA inputs is critical for the image rejection [6, 7]. Finally, the single-ended SIS mixer devices require a DC bias voltage, which is injected into the IF system somewhere, by a so-called bias-tee. In our case, this happens between the IF hybrid and the IF LNAs, which is possible because the IF hybrid is (crosswise) DC-transparent. The DC bias (which is of the order of a few mV by several tens of  $\mu\text{A}$ ) in turn is generated from higher-level voltages by a resistive bias network. In the case of SEPIA/LLAMA, the bias-tees (with their associated bias networks) were conveniently integrated into the IF LNAs; later there will be some discussion on alternative locations for bias injection.

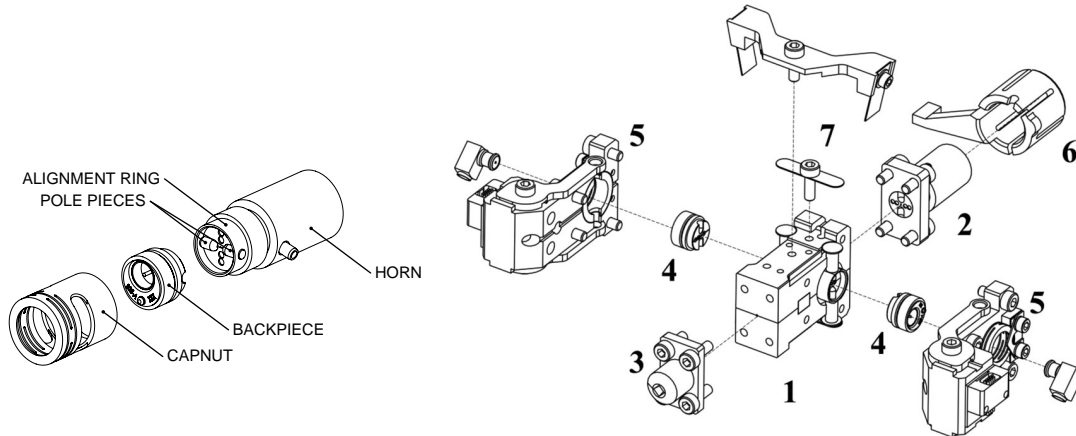


Figure 4: Exploded views of the DSB mixer (left) in the currently deployed Band 9 receivers, and the 2SB mixer (right) as used in SEPIA660 (and proposed for ALMA upgrade in this study). Two important parts of the DSB mixer are re-used. The backpiece (containing the SIS device) becomes position 4 in the 2SB mixer; now two are needed, of course. The horn, after rework and attaching a flange becomes 2SB position 2. The RF hybrid block (1), LO horn (3) and side-pieces (5) are new. The adapter collet (6) gives the 2SB mixer assembly the same interface as the original DSB mixer in its holder (latter not shown). The connector clamp (7) firmly fixes the two GPO connectors of the phase-matched cables leading to the IF hybrid.

#### 1.4.2 Construction of the 2SB mixer

Details of the actual 2SB mixer developed over the years, and deployed in SEPIA660, have been published in several places, e.g., [5], [6] and [7]. Here is a short summary of the actions involved in converting the existing DSB mixers into 2SB ones.

Figure 4 shows exploded views of the two mixer types. Obviously, the 2SB mixer is of much higher complexity than the DSB one (although to be completely fair, there is additional complexity in the DSB mixer *holder*, not shown here). Two important parts are re-used: the mixer backpiece and the corrugated feedhorn (both of which are expensive). Since it is our intention (within the scope of this study, see section 4) to re-use the existing SIS devices, we have to keep the backpieces as well, since it is virtually impossible to remove the devices from the backpieces intact. We therefore made it a design condition that the backpiece interface is fully retained in the 2SB mixer block. This also lets the 2SB mixer inherit the benefits of the DSB backpiece: it is self-contained, robust and very easy to exchange without special tooling. Also, observing some simple procedures, ESD issues are easily handled. In the entire Band 9 production campaign (which involved testing of more than one thousand junctions), to the best of our knowledge not a single one was lost due to ESD. An additional benefit of keeping the backpieces compatible is that it allows pairing of mixers based on DSB measurement data.

The corrugated horn is also re-used, but this requires some modifications. We did not find a technically viable way to keep the existing interface. The solution is to cut off the thread at the back of the horn, and solder on a rectangular flange instead. Although this is a delicate operation, it still turned out to be cheaper by an order of magnitude compared to purchasing a new horn.

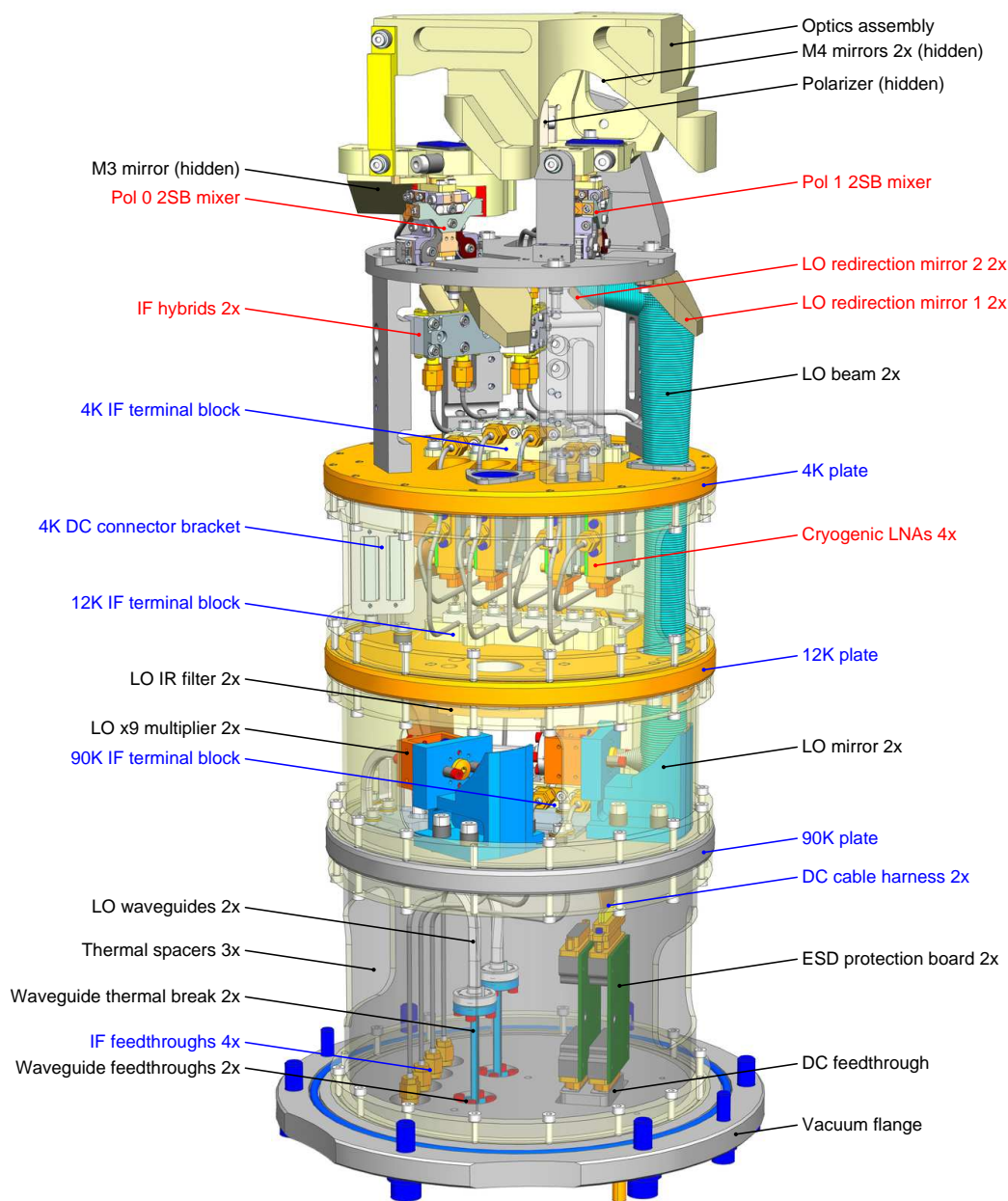


Figure 5: Annotated 3D model of the SEPIA660 2SB CCA (with the fibreglass thermal insulation rings rendered transparent). The basic structure is derived from the Band 9 DSB production cartridge. The optics assembly is retained (with slight reworking to make space for the larger mixers), although it now contains two superfluous LO mirrors that originally projected the LO beams by way of beamsplitters into the mixers. Instead, each LO beam is now re-focused into the bottom of the mixers by a combination of ellipsoidal and hyperboloidal mirrors. Components labelled in red are new key components, in blue are components that, although not key to the conversion, still had to be re-made; black labels indicate parts that were re-used (possibly with some re-working);

	<p><b>ALMA Band 9 Sideband Separating Upgrade</b></p> <p>—</p> <p><b>Study Report</b></p>	<p>DocID: FEND-40.02.09.00-1974-C-REP Version: C Date: 2023-02-07 Status: Released Page: 12 of 105</p>
---	---	--

### 1.4.3 Conversion of a DSB CCA to 2SB

As illustration of the work to be done in order to upgrade a Band 9 DSB CCA to 2SB operation, figure 5 shows an annotated rendering of the SEPIA660/LLAMA660 CCA. The obvious parts to replace or introduce (indicated in red) are the mixers, the IF hybrids and the cryogenic LNAs. Also, because the LO injection geometry of the 2SB mixers is different from the DSB mixers, extra pairs of LO redirection mirrors have to be introduced. Apart from these key components, several other parts have to be re-manufactured because of changed infrastructure (indicated in blue). These have mainly to do with the doubled number of IF transport channels, or are, e.g., brackets for the new components. Finally, several components were re-used (black) either as-is or with minor reworking. Further details of the conversion can be found in [8]. Note that this is the upgrade as performed in the past. In this study we take this as the baseline, and look at developments and improvements beyond this.

## 1.5 Tasks in the Study

In the SoW, the goals, or tasks, in the study are defined to be

1. Investigate the extension the IF bandwidth to at least  $4 \times 12$  GHz (2 sidebands & 2 polarizations), with the goal to achieve as broad a bandwidth as possible without compromising the other performance parameters;
2. Investigate the extension the RF bandwidth beyond 602–720 GHz, without compromising the other performance parameters in this core RF range;
3. Verify the availability of a sufficient number of SIS mixer devices at NOVA to enable a 2SB upgrade of all 73 ALMA Band 9 receivers; if negative, determine the possibilities and cost for new wafer runs in other facilities;
4. At lower priority, investigate the possibility and cost to improve the polarimetric performance beyond that of the currently installed receivers;
5. Determine the expected cost, both in new hardware and labour, to upgrade all existing ALMA Band 9 receivers, including options for increased IF bandwidth and optical performance as mentioned above;
6. Determine the cost for a limited number of pre-production receiver modules (e.g., 4 to 12) to allow field testing of array operations;
7. Investigate the possibility of performing the Band 9 upgrade while keeping the majority of the Band 9 receivers in operations, e.g., by temporary hardware modifications in the IF system of the new 2SB front-ends to allow the correlation of 2SB and DSB receivers; if impossible, a subarray-based solution should be investigated.

In the following chapters we will report on the results we have obtained within each of these tasks.

	<b>ALMA Band 9 Sideband Separating Upgrade</b>	DocID: FEND-40.02.09.00-1974-C-REP
	—	Version: C
	<b>Study Report</b>	Date: 2023-02-07
		Status: Released
		Page: 13 of 105

## 1.6 List of acronyms

2SB	Sideband-separating (processing/exporting both upper and lower downconversion sidebands through separate channels)
ALMA	Atacama Large Millimeter/submillimeter Array
AMC	Active Multiplier Chain
AOS	Array Operations Site (part of ALMA JAO, Chile)
APEX	Atacama Pathfinder EXperiment
BW	Band Width
CCA	Cold Cartridge Assembly (the part of the receiver inside the front-end cryostat, including the vacuum flange)
CW	Continuous Wave
DAC	Digital to Analog Converter
DBS	Detector Bias System
DSB	Double-sideband (processing/exporting both upper and lower downconversion sidebands through one channel, superimposed)
EM	ElectroMagnetic
ESAC	European Science Advisory Committee
ESD	ElectroStatic Discharge
ESO	European Southern Observatory
FE	Front End
FTE	Full-Time Equivalent
FWHM	Full Width Half Maximum
HDPE	High Density PolyEthylene
HEMT	High Electron-Mobility Transistor
IF	Intermediate Frequency (the output frequency band of the receiver)
IRR	Image Rejection Ratio
ISSTT	International Symposium on Space Terahertz Technology
IV	Current-Voltage [characteristic/curve]
JAO	Joint ALMA Office (with facilities SCO, OSF and AOS)
LLAMA	Large Latin American Millimeter Array
LNA	Low-Noise Amplifier
LO	Local Oscillator
LSB	Lower SideBand
M&C	Monitor & Control
NAOJ	National Astronomical Observatory of Japan
NOVA	Nederlandse Onderzoeksschool Voor Astronomie (Netherlands Research School for Astronomy)
OMT	OrthoMode Transducer
OSF	Operations Support Facility (part of ALMA JAO, Chile)
PA	Power Amplifier
PET	PolyEthylene Terephthalate (a.k.a. “Mylar”)
PLL	Phase-Locked Loop
RF	Radio Frequency (the input frequency band of the receiver)
RMS	Root Mean Square
RT	Room Temperature
RuG	Rijksuniversiteit Groningen (University of Groningen), The Netherlands

	<b>ALMA Band 9 Sideband Separating Upgrade</b> — <b>Study Report</b>	DocID: FEND-40.02.09.00-1974-C-REP Version: C Date: 2023-02-07 Status: Released Page: 14 of 105
---	--	---

List of acronyms — continued

SCO	Santiago Central Office (part of ALMA JAO, Chile)
SEPIA	Swedish-ESO PI Instrument for APEX
SIS	Superconductor-Insulator-Superconductor [tunnel junction]
SRON	Netherlands Institute for Space Research
SSB	Single-sideband (processing/exporting either one of upper and lower downconversion sidebands)
SoW	Statement of Work
USB	Upper SideBand
VNA	Vector Network Analyser
WCA	Warm Cartridge Assembly (the part of the receiver outside the front-end cryostat, mating to the vacuum flange of the CCA)
WR	Waveguide Rectangular (with a long side defined in units of 0.01 inch)
WSU	Wideband Sensitivity Upgrade
YIG	Yttrium-Iron Garnet [resonator]
YTO	YIG-Tuned Oscillator

	<b>ALMA Band 9 Sideband Separating Upgrade</b>	DocID: FEND-40.02.09.00-1974-C-REP
	—	Version: C
	<b>Study Report</b>	Date: 2023-02-07
		Status: Released
		Page: 15 of 105

## 2 Study goal 1 — Extending the IF bandwidth

The goal is the determination of the ultimately possible IF bandwidth which a sideband-separating Band 9 receiver could be capable of, using the existing SIS mixer devices. This divides into two main aspects: the bandwidth of the mixer devices themselves and the technological extensions needed to harness this bandwidth and construct a sideband-separating receiver based on these mixers.

Because even the most basic mixer testing in this respect requires an IF infrastructure, these two aspects are closely interwoven at all stages of the experiment.

### 2.1 Technical aspects

We discuss here the most important technical challenges related to the extension of the Band 9 IF bandwidth beyond 4–12 GHz. It should be noted that for any increase in the IF bandwidth only the AlN-barrier mixers should be considered. The older AlO<sub>x</sub>-barrier junctions show a clear evidence of IF bandwidth limitations in the 4–12 GHz range [15]. These junctions have a natural limit in the current density achievable, while the main quality parameters, e.g., subgap resistance  $R_J$  over normal resistance  $R_N$ , are still high enough to make a good mixer. This limits the  $R_N$  value to  $\sim 20 \Omega \mu\text{m}^2$ . With  $0.5 \mu\text{m}^2$  junctions,  $R_N$  would become very high ( $\sim 40 \Omega$ ) and the source impedance at IF would be in the range 200–400  $\Omega$ . This consideration, combined with a larger junction area (given by the need to lower  $R_N$  to better match a 50  $\Omega$  line) limits the IF frequency. In addition, for the end-loaded stub tuning that we use, the overlap area of the tuner to match a higher- $R_N$  junction is also approximately 2 times larger, and that leads to an additional limit in the IF frequency. In total, 30 AlO<sub>x</sub>-barrier junctions are still employed in the existing Band 9 array, and these will have to be replaced in any case (further details in chapter 4).

#### 2.1.1 Expected SIS mixer IF bandwidth

Employing the vastly increased numerical simulation power, we reimplemented the models for our production Band 9 SIS devices<sup>1</sup>. These show an actual IF bandwidth which is much larger than the original design goal of 4–12 GHz, perhaps by a factor of up to two.

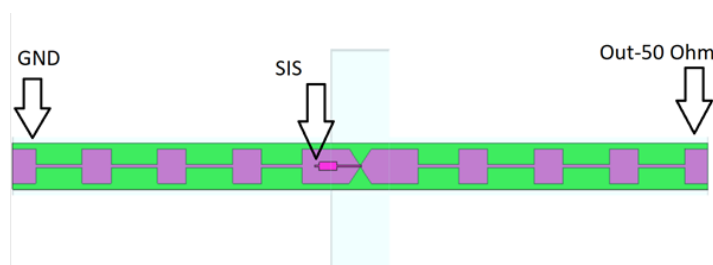


Figure 6: View of the 3D layout which was used to calculate IF performance of the ALMA Band 9 mixer using CST Microwave Studio.

A view of the 3D electromagnetic model of the mixer is presented in figure 6. The model includes a short stretch of waveguide and a waveguide backshort cavity, the mixer substrate,

<sup>1</sup>Co-author for this subsection: Kirill Rudakov



	<b>ALMA Band 9 Sideband Separating Upgrade</b>	DocID: FEND-40.02.09.00-1974-C-REP Version: C
	<b>Study Report</b>	Date: 2023-02-07 Status: Released Page: 17 of 105

the metal layers. Representative values of the key parameters for the IF performance are given in Table 1. For the real part of the IF source impedance we take a value of five times the normal resistance of the SIS junction, which represents well the observed dynamic resistance of the SIS mixer operating at Band 9 frequencies. For the IF circuitry’s input impedance we use a  $50\ \Omega$  approximation, since we plan to use amplifiers which are well matched to a  $50\ \Omega$  line within the IF band. Using matched amplifiers allows us to use flexible lengths of semi-rigid cable as well as to avoid bulky (and lossy) IF isolators.

The result of the simulation of the SIS mixer power coupling to the  $50\ \Omega$  IF port is shown in figure 9, demonstrating a good match up to at least 20 GHz IF frequency. The  $-3\ \text{dB}$  point in the power coupling is actually located at about 24 GHz. One of the two main aspects of this study goal is the experimental verification of these simulations.

These simulations were performed by Kirill Rudakov as part of the ESO study project to adapt ALMA Band 9 mixer layout to the technological capabilities of the GARD group at Chalmers University, Sweden. These results are also included in Rudakov’s PhD thesis [16].

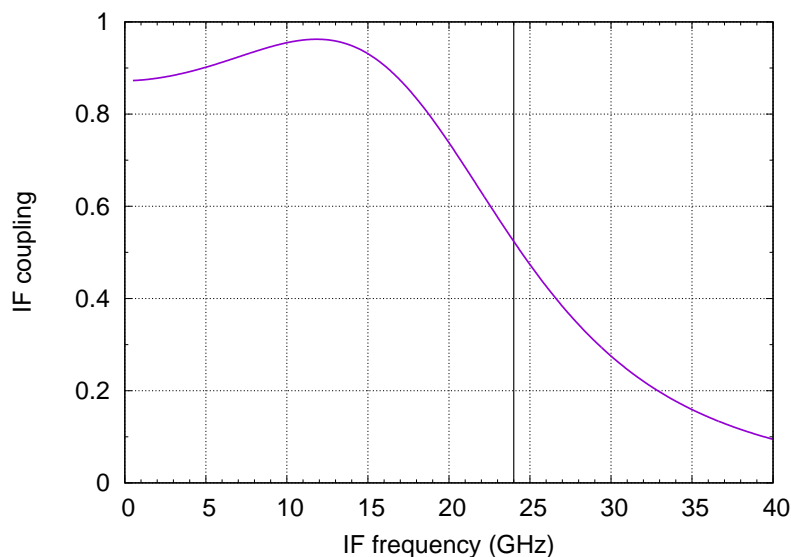


Figure 9: Simulated IF power coupling of the Band 9 SIS junction at the operating point.

It should be noted that the model only contains the SIS device and its direct embedding. For instance, the further transition to a coaxial transmission line for the IF is not modelled, which could lead to a somewhat steeper roll-off at high frequencies.

### 2.1.2 Cryogenic IF low-noise amplifiers

Assuming that the mixers indeed deliver the expected bandwidth, by far the greatest technical challenge is obtaining cryogenic low-noise amplifiers (LNAs). The key performance requirements are the following:

- A bandwidth covering the desired IF band;
- A gain in the 30–40 dB range;



- An equivalent input noise temperature not exceeding, say, 7 K, preferably a bit lower, to minimize the impact on the overall receiver noise temperature;
- A maximum input reflection ( $|S_{11}|^2$ ) of at most  $-10$  dB, preferably below  $-15$  dB for most of the band. Apart from reducing the standing waves in the IF passband, this is crucial for obtaining a good image-rejection ratio [6, 7];
- A maximum dissipation of 9 mW per LNA to stay within the 4 K-stage heat dissipation specification of ALMA.

Note on the location of the LNAs: these are located at the 4 K stage to get the lowest LNA noise and the tightest mixer-LNA coupling in terms of pre-LNA loss (since otherwise a lossy stainless-steel cable would be required between the mixers and the LNAs). Also, any standing pattern gets faster with frequency, and therefore more difficult to compensate, with a longer electrical mixer-LNA distance. A cold LNA also reduces the risk of elevating the mixer temperature. For these reasons, all versions of the Band 9 CCA built by NOVA have their LNAs at 4 K. Alternatively, the LNAs could be strapped thermally to the 15 K level to allow an increased dissipation. For the reasons mentioned above, and the fact that we have no legacy in this respect, the option to thermally strap to 15K stage was not considered for this study.

Note on the noise temperature requirement of the LNA: due to Friis' formula, the noise contribution of the LNAs to the total noise temperature of the receiver is of course inversely proportional to the mixer gain (and any other gain in front of it). Since the Band 9 mixer gain is (on average) about  $-6$  dB, each Kelvin of LNA noise translates into about 4 K on the receiver level.

Our main partner on the LNA side is the Observatorio Astronómico de Yebes, Spain (“Yebes” in short), who have a long track-record constructing cryogenic low-noise amplifiers. For instance, they developed the 4–12 GHz IF amplifiers currently integrated in ALMA Band 9 (and 4–8 GHz ones for other bands), and the “third generation” ALMA-style LNAs deployed in SEPIA660 and LLAMA660. The top-level performance characteristics of the latter are shown in figure 10. They combine the low noise ( $\approx 5 \dots 7$  K) wide-band characteristics of the DSB Band 9 LNAs with sufficiently low input return loss ( $-19 \dots -12$  dB for most of the band, rising to  $-10 \dots -8$  dB in the lowest GHz) to couple them directly to the mixer (without isolator) even in a sideband-separating configuration. Currently, Yebes is involved in the further

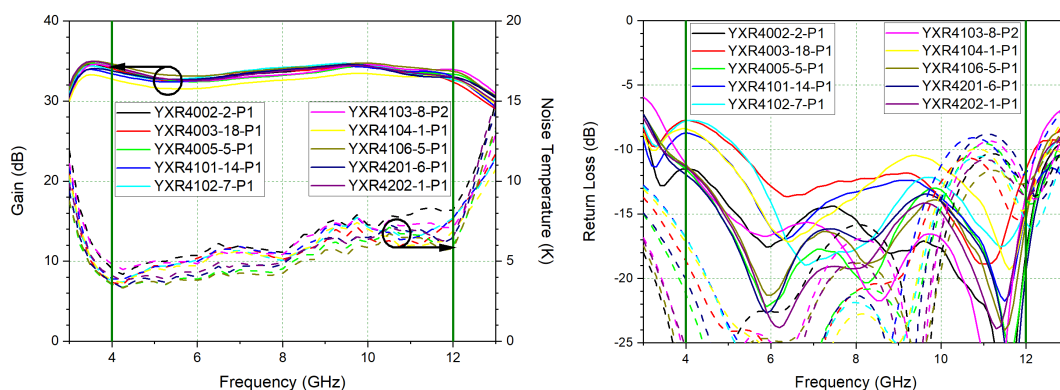


Figure 10: The gain and noise temperature (left) and the input and output matching (right,  $S_{11}$  solid,  $S_{22}$  dashed) of ten cryogenic Yebes 4–12 GHz LNAs (YXR4000 series). Eight of these have been integrated into the Band 9 2SB CCAs for SEPIA and LLAMA. Graphs courtesy of R.I. Amils Samalot, Observatorio Astronómico de Yebes.

	<p><b>ALMA Band 9 Sideband Separating Upgrade</b></p> <p>—</p> <p><b>Study Report</b></p>	<p>DocID: FEND-40.02.09.00-1974-C-REP</p> <p>Version: C</p> <p>Date: 2023-02-07</p> <p>Status: Released</p> <p>Page: 19 of 105</p>
---	---	--

development of this type of amplifiers, especially towards larger bandwidth and better input matching, supported by a dedicated ESO technology development program. In the course of the study, several of these successive-generation LNAs were provided by Yebes on loan. Details on them will be covered in later sections.

Apart from the LNAs developed at Yebes, there are alternatives available, either from institutes or on the commercial market. Of the latter, one of the most interesting and well-known is Low-Noise Factory (LNF) in Sweden. Two of their types seem to fit an extended ALMA IF band: LNF-LNC4.16C (4–16 GHz) and LNF-LNC6.20D (6–20 GHz). Either type could be suitable, depending on the desired final bandwidth. There used to be another type, LNF-LNC4.23A (4–23 GHz), but this is apparently discontinued.

The LNF-LNC4.16C (when operated cryogenically) offers very low noise (2.5–5 K over 4–16 GHz) with a gain of about 38 dB and a dissipation of 17 mW.<sup>2</sup> The dissipation can be halved by reducing the bias settings with hardly any impact on the noise temperature, although with a few dB loss in gain. Depending on the bias settings, there is also a gain rolloff by 4–6 dB above 14 GHz. One potential issue with this type is that the input matching, while being around –15 dB in the lower part of the band, rises rather sharply to –10 dB above 13 GHz and ends up at –3 dB at 16 GHz. As in all devices in this class, tradeoffs have to be made between bandwidth, noise temperature, input matching, etc. It may therefore still be possible to match this LNA better at the input (e.g., by modification of the bias settings) with some sacrifice of other performance parameters. Another interesting type being offered by LNF is the new LNF-LNC6.20D, with noise in the same range (but now from 4–20 GHz, even a bit wider than the nominal band) and a gain of 32–34 dB at a typical dissipation slightly above 20 mW. With the settings published in the datasheet, the input matching also here rises above –10 dB above 13 GHz (ending up around –3 dB at 20 GHz). But again, this could possibly be mitigated somewhat by adjusting bias parameters.

As stated above, in the current study we decided to benefit from the synergy with Yebes’ LNA development project. In the future, alternatives like LNF could be considered as well, although it is likely that also here application-specific attention to specific parameters (like the input matching) is required.

### 2.1.3 Cryogenic IF hybrid

Another component that Yebes has a very good reputation with is wide-band cryogenic quadrature hybrids, in this case needed to construct a side-band separating mixer out of two DSB mixers. The high image-rejection ratio (IRR) obtained in the SEPIA660 receiver is due for a significant part to the excellent 4–12 GHz hybrid.

Recently, Yebes extended this range considerably, and for the purpose of this study, loaned us one of their 4–20 GHz IF hybrids. Fig. 11 shows some key characteristics, measured at cryogenic temperature. The performance is quite comparable, and in some aspects even slightly better, over the 4–20 GHz range than the 4–12 GHz hybrids used in the SEPIA660 and LLAMA660 receivers over their nominal range.

These 4–20 GHz IF hybrids use normal copper conductors, and therefore introduce some extra resistive loss. As can be seen in fig. 11 (lower right panel), a maximum of about 0.2 dB could be recovered by using superconducting striplines in the hybrid, corresponding to about

<sup>2</sup>The LNF performance parameters mentioned in this section have been taken from datasheets downloaded on 2022-09-26 from their web site (<https://lownoisefactory.com/product-category/cryogenic-amplifier/>).

	<b>ALMA Band 9 Sideband Separating Upgrade</b>	DocID: FEND-40.02.09.00-1974-C-REP
	<b>Study Report</b>	Version: C Date: 2023-02-07 Status: Released Page: 20 of 105

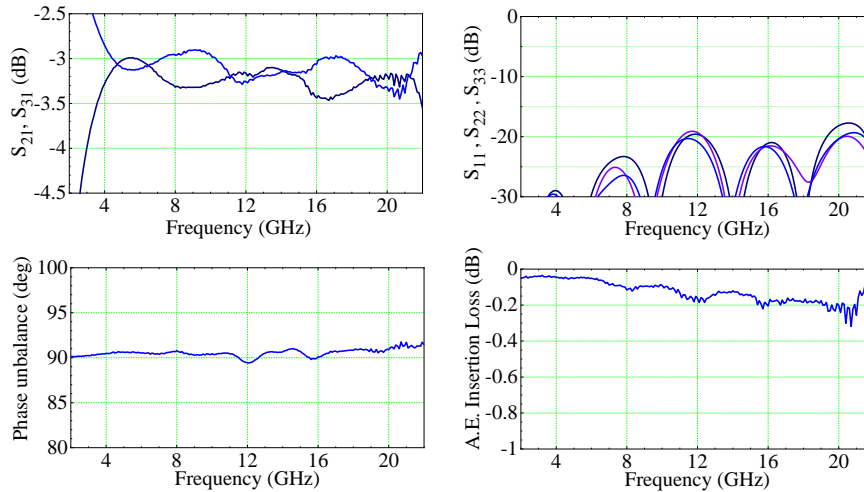


Figure 11: Key characteristics of the YH90420 quadrature hybrid, measured at 16 K. Top left:  $S_{21}$ ,  $S_{31}$ , the  $0^\circ$  and  $90^\circ$  transmission coefficients. Bottom left: phase difference between these two channels. Top right:  $S_{11}$ ,  $S_{22}$ ,  $S_{33}$ , input/output reflections. Bottom right: Average Effective Insertion Loss,  $|S_{11}|^2 + |S_{12}|^2 + |S_{13}|^2 + |S_{14}|^2$ . Graphs courtesy of Observatorio Astronómico de Yebes.

4–5 K of receiver noise temperature. The downside is that this is not easy to implement technologically in the coupled stripline architecture used by Yebes, since superconducting high-frequency PCB material is not readily available, very difficult to contact, etc. Nevertheless, other receiver groups (e.g., IRAM and GARD) *do* employ superconducting microstrip-based IF hybrids (typically photolithographically defined Lange-type couplers); it would be interesting to explore this further as an alternative in a later stage. Note that, to reap the full benefit of a zero-loss hybrid, also the coaxial cables up to the LNAs should be made superconducting.

#### 2.1.4 IF transport

All IF cables, connectors and vacuum feedthroughs that are used in the Band 9 cartridge typically are specified at least up to 18 GHz, some up to 26.5 GHz. We did not investigate this point in detail, because it was not a goal of this study to build a full demonstration receiver. Such system analysis should be part of any future in-depth upgrade study, however. The main issue that can be expected is a general roll-off towards the top of the band because of frequency-dependent losses in the stainless-steel semirigid cables between the temperature stages. Because of the required thermal isolation between the stages we don't have many options to reduce this loss; it should simply be compensated with sufficient gain in the cryogenic LNAs. If the slope would start limiting the total dynamic range of the frontend-backend chain, room-temperature gain equalizers (or slope-corrected warm IF amplifiers) could be employed in the WCA.

On the lower side of the IF transport range, most of the passive components in the IF chain work down to DC, with exception of the bias-tee (which can be made much lower than 1 GHz, though) and the IF hybrid, which is difficult to make much wider than a decade. A well-matched, low power dissipation amplifier is also difficult to achieve with frequencies below 2 GHz with 20 GHz upper frequency.

	<b>ALMA Band 9 Sideband Separating Upgrade</b> <hr/> <b>Study Report</b>	DocID: FEND-40.02.09.00-1974-C-REP Version: C Date: 2023-02-07 Status: Released Page: 21 of 105
---	---	---

### 2.1.5 Warm IF amplifiers

The warm IF amplifiers in the WCA should obviously be matched to any extension in the bandwidth. Nowadays, several commercial suppliers (e.g., Miteq-Narda, B&Z Technologies to name a few) offer amplifiers with the required bandwidth (4–20 GHz), gain (25–30 dB), noise (NF 3.5–4 dB) and compression (P1dB 10 dBm) specifications. Note that the specs mentioned here are only indications; for a real production receiver a detailed design analysis should be performed, of course.

Another interesting option is procuring a custom-tailored type, as was done for the Band 5 production. This typically implies a non-recurring cost of several k€, but since the requirements can then be fit more tightly, the per-unit cost may be attractive. It should be expected, however, that their price will be at least as high as the 4–12 GHz amplifiers employed up to now. All our cost estimates are based on prices in 2020, but it is known that material and components prices can change significantly in few years time.

## 2.2 Experimental methods

The main experimental challenge of this goal is the fact that up to now almost all our IF infrastructure has been limited to the ALMA 4–12 GHz IF standard for DSB bands. The absolute minimum required IF infrastructure for a DSB noise temperature measurement consists of (following the signal path) a bias-tee, a cryogenic LNA, cryogenic IF transport, a warm IF amplifier and finally a detector. Note that in this list a cryogenic isolator is absent; isolators with a bandwidth wider than 4–12 GHz are reported to exist in an experimental stage, but not in a state that we can simply buy one. For that reason, and also because we committed ourselves to isolator-less designs for production receivers, we have to combat standing waves in the IF system by other means, i.e., good impedance-matching of the components.

### 2.2.1 Wideband bias-tee

Unlike the 4–12 GHz LNAs used in the SEPIA and LLAMA cartridges, the amplifiers we could get on loan for this project (see section 2.2.2) do not have a built-in bias-tee to supply the required DC bias to the mixer device. For this reason we were forced to insert a discrete bias-tee into the signal path between the mixer and the LNA.

Initial measurements were performed with a commercial off-the-shelf room temperature bias-tee specified for 4–14 GHz. This was verified (by VNA up to 20 GHz, and above that by synthesizer and spectrum analyser), at room temperature, to give a reasonable performance up to about 27 GHz. Because we do not have a VNA with a frequency range above 20 GHz, the upper part of the band was only tested for transmission, not for details of input matching. Without doing a detailed analysis, we cannot expect this bias-tee to yield a very flat IF response. During the first measurements we indeed suffered from strong standing waves, part of which were likely to be caused by bad matching of the bias-tee, especially at 4 K, for which it was not intended.

Because of the high level of standing waves observed in the initial measurements (section 2.3.1), it was decided to construct a new wide-band (goal 1–24 GHz) cryogenic bias-tee in-house. It is based on the same types of conical inductors with iron-powder cores (figure 12) that Yebes uses in the bias-tees integrated in their LNAs. Because of their small size (due to the high

	ALMA Band 9 Sideband Separating Upgrade	DocID: FEND-40.02.09.00-1974-C-REP
	—	Version: C
	Study Report	Date: 2023-02-07
		Status: Released
		Page: 22 of 105

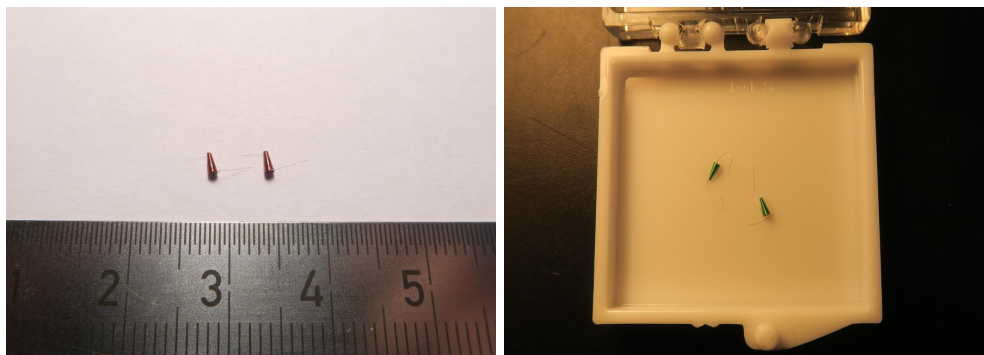


Figure 12: Photographs of the conical inductors of Coilcraft (BCL-122JL,  $1.2 \mu\text{H}$ , left) and Piconics (CC45T47K240G100,  $0.84 \mu\text{H}$ , right). These were provided by both suppliers as free samples.

$\mu_r$  of the core), these inductors work over a large bandwidth. Alternatively, with air-coils for instance, it is our experience (during construction of the CHAMP+ array) that these are very difficult to get working above, say, 8 GHz, probably due to their relatively large intra-winding capacitance. The inductor couples to the top of a single straight  $50 \Omega$  microstrip on thin Rogers TMM10i dielectric over a continuous ground plane. Since all current Yebes amplifiers have DC blocking capacitors at their inputs, a DC break in the bias-tee is not needed, which simplifies the design. The bias-tee includes the DC mixer bias network as well, copying the scheme successfully applied in the SEPIA660 LNAs. Further design goals: minimization of (thermal) mass, possibility of extra heatsinking (since it couples directly to the mixer) and free choice of male and female connectors to minimize the number of extra transitions in the IF chain.

A 3D rendering of the design is shown in figure 13. The IF connectors are of K-type, mated to

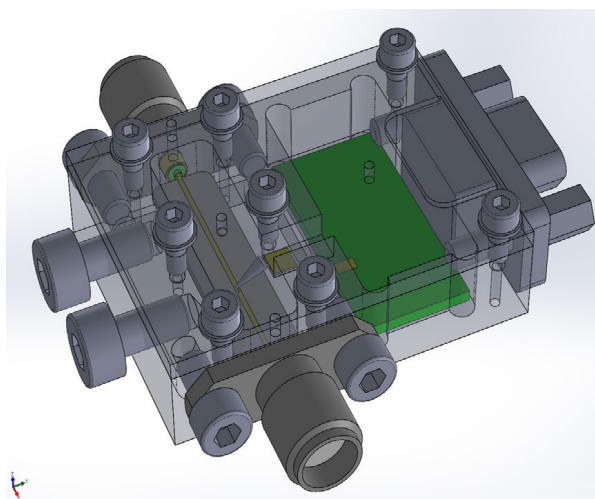


Figure 13: 3D rendering of the ultra-wide-band bias-tee. The IF cavity (left) contains a  $50 \Omega$  microstripline coupled to two K-type connectors for input and output. A conical inductor couples in the DC voltage coming from the DC bias network board in the DC cavity (right). The six-point bias connection to the outer world is by MDM connector (far right). The large screws on the left are for mounting or additional heatsinking.

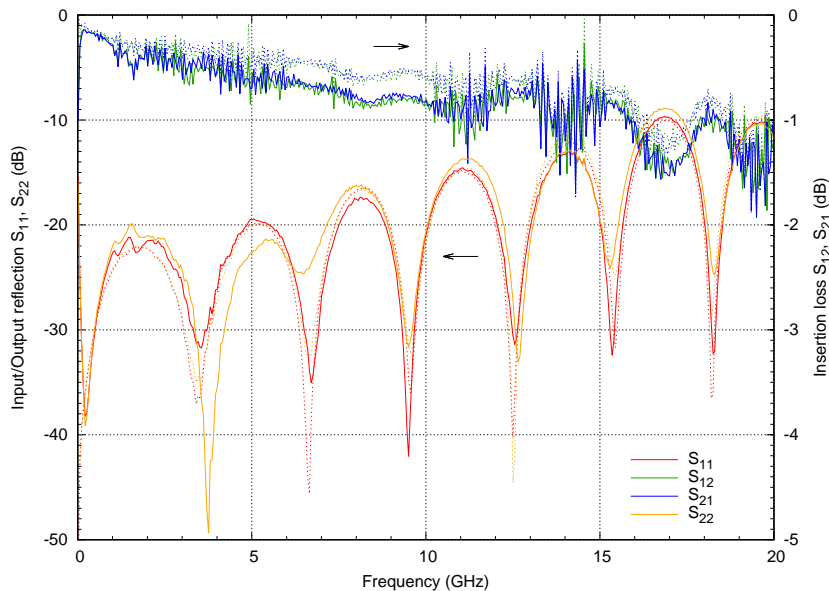


Figure 14: The S-parameters of the new bias-tee, first version before retuning, measured by VNA at room temperature. The insertion loss rises gradually up to about 1 dB (expectedly lower at cryogenic temperature), while the input and output reflections go up to about  $-10$  dB. The dotted and solid traces are measured without and with the conical inductor, respectively. As can be seen, the inductor introduces an additional insertion loss of about 0.2–0.3 dB, while it hardly affects the return losses.

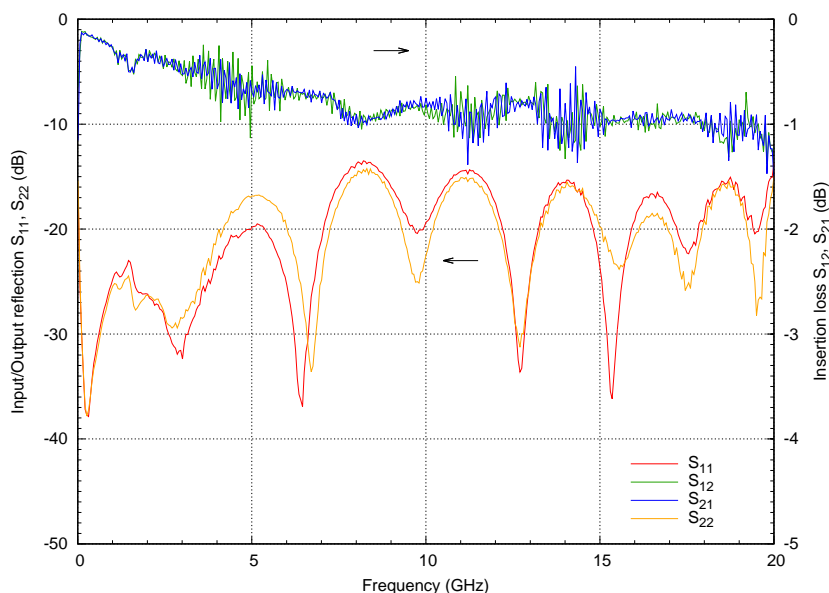


Figure 15: The S-parameters of the second new bias-tee (with conical inductor), after retuning, at room temperature. Now the input and output reflections are reasonably uniform at a  $-15$  dB level

	<b>ALMA Band 9 Sideband Separating Upgrade</b> <hr/> <b>Study Report</b>	DocID: FEND-40.02.09.00-1974-C-REP Version: C Date: 2023-02-07 Status: Released Page: 24 of 105
---	---	---

glass beads conductively glued or soldered into the housing, which should give low return loss at high frequencies (spec up to 40 GHz) and allows free choice of male/female connectors. The 9-pin MDM bias connector has the same pinout as the bias network boxes used in the DSB Band 9 cartridges, which makes it plug-in compatible both with our test-bed CCA as with the cable harness of our wet cryostats.

In the end, two of these bias-tees were constructed (first one for the DSB measurements in the wet cryostat, and later a second one to enable the 2SB experiment). The room-temperature S-parameters of the first one are shown in figure 14. The insertion loss rises to about 1 dB at high frequency, but this is expected to go down considerably upon cooling. In this version, which was used for the DSB measurements, the input and output reflections are still disappointingly bad at high frequencies, however. The second copy was constructed with some careful adjustments and after tuning out some parasitic inductances performed considerably better, as shown in figure 15. The input/output reflections are still a bit higher than hoped (about  $-15$  dB rather than below  $-20$  dB), but since this is comparable to the input return loss of the LNAs, we consider it acceptable for the moment. After the lessons learned from the construction of the second bias-tee, the first was also retuned to about the same level, and together they were used for the 2SB measurements.

As it turned out, obtaining a decent performance from these bias-tees was a non-trivial operation that absorbed a disproportionate amount of effort within the project. Since its design and performance are not central to the questions of this study, the path towards the shown performance will not be detailed here. If there is interest, some particulars could be reported in a later stage, or in private communication.

We argue that for an operational receiver, the bias-tee, rather than being implemented as a discrete component, should be integrated either in the LNA, the IF hybrid or the mixer block (basically anywhere between the SIS device and the first DC-blocking capacitor in the LNA). With the current IF architecture, the most favourable location is in the LNA itself, since this is the only place where microstrips are being used. Neither the backpiece (coaxial) nor the IF hybrid (embedded stripline) are very accommodating for components like inductors. On the other hand, any LNA that is likely to be used in a receiver like this (whether discrete or MMIC-based) will have microstrip (or maybe CPW) structures at its input, and is therefore the natural place to introduce a bias-tee. During our consultations with the people from Yebes, this was confirmed: although integration of a high-quality bias-tee may be non-trivial, similar structures already exist in the LNAs to bias the transistors. Of course, if the IF hybrid were to be constructed in microstrip technology, this could be a viable location as well. This was done, for instance, in ALMA Band 5, but even there a multi-substrate solution was needed, increasing complexity again.

### 2.2.2 Cryogenic wide-band LNA

For the purpose of the study, several cryogenic LNAs were provided on loan by Yebes. For the initial DSB measurements one (type Y214G) with a nominal bandwidth of 2–14 GHz, modified for higher frequencies, and an older model (YK22) covering 20.5–24.5 GHz to study the upper part of the IF response. And, for the final 2SB measurements, two nominal 4–20 GHz amplifiers of the Y420G series, with improved input matching.

The Y214G model used in most of the DSB measurements is based on the design of a three-stage 2–14 GHz discrete HEMT amplifier, modified experimentally with a narrow-gate input transistor to extend the band up to about 20 GHz. It has a gain of around 33 dB and an

equivalent noise temperature of 7.5 to 10 K. The input return loss ( $|S_{11}|^2$ ) varies from  $-20$  dB at 14 GHz to about  $-5$  dB at 18 GHz, and to  $-3$  dB towards the 4 GHz lower band edge. The typical power dissipation is 19 mW. Figure 16 shows some key performance plots of the LNA: the gain, noise temperature and input/output return loss.

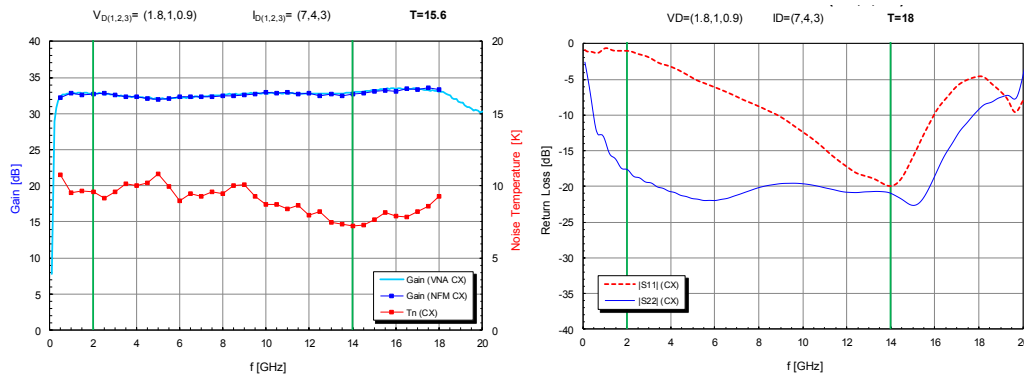


Figure 16: The gain and noise temperature (left) and the input and output matching (right) of the extended-band cryogenic 2–14 GHz LNA (Y214G 1027) used for the ultra-wide IF DSB measurements, at low temperature. Images courtesy of Observatorio Astronómico de Yebes.

As mentioned before, since we do not have cryogenic isolators available for this wide band, we are forced to couple the mixer to the LNA directly, although this LNA is clearly not optimized for that. From our SEPIA660 experience, an  $S_{11}$  of around  $-15$  dB over the entire band is required for a sufficiently flat IF response and for obtaining a good image rejection ratio.

The 20.5–24.5 GHz LNA (model YK22) has similar performance, in its own band, compared to the Y214G type. The key characteristics of YK22 are shown in figure 17. Since it turns out, as shown below (see, e.g., figure 25), that the Y214G actually performs at least as good up to 24 GHz, we only tested the YK22 once.

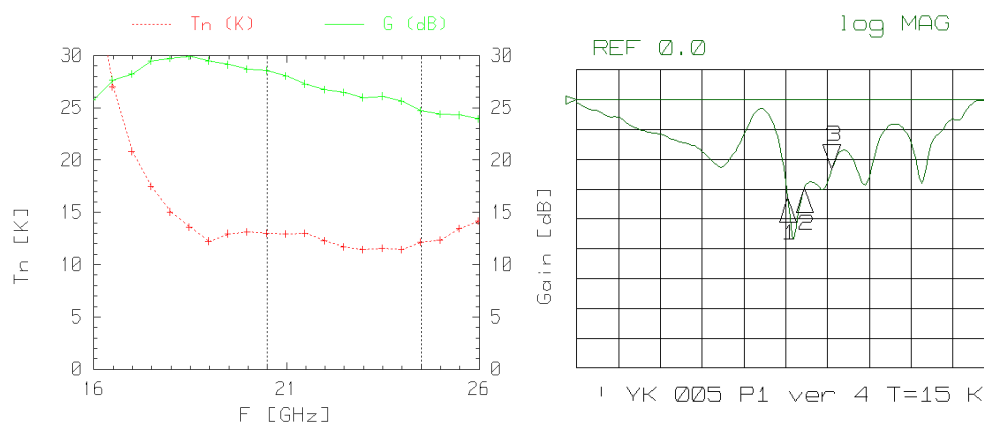


Figure 17: The gain and noise temperature (left) and the input matching (right) of the cryogenic 20.5–24.5 GHz LNA (YK22 005) used for some of the the ultra-wide IF DSB measurements, at low temperature. The axes of the right panel: horizontally 0–40 GHz, vertically 10 dB/div, 0 dB at the triangle on the right. Images courtesy of Observatorio Astronómico de Yebes.

	<b>ALMA Band 9 Sideband Separating Upgrade</b>	DocID: FEND-40.02.09.00-1974-C-REP
	—	Version: C
	<b>Study Report</b>	Date: 2023-02-07
		Status: Released
		Page: 26 of 105

The final set of amplifiers, used for the 2SB measurements, are a further development especially targeting an improved input matching over the full 4–20 GHz band. Figure 18 shows the S-parameters of these amplifiers at cryogenic temperature. As can be seen, the input matching compared to the Y214G improved significantly, especially over the bottom half of the band, and is now typically around  $-15$  dB and, except below 5 GHz, everywhere better than  $-10$  dB. The noise temperature (not shown here) also improved, to about 5–6.5 K. The power dissipation of these amplifiers is about 16 mW. Although smaller than the Y214G type, this is obviously still too high for a real upgrade. It should be noted, however, that these are development models to prove the bandwidth and matching performance. For operational LNAs additional effort should be invested in order to reduce power dissipation.

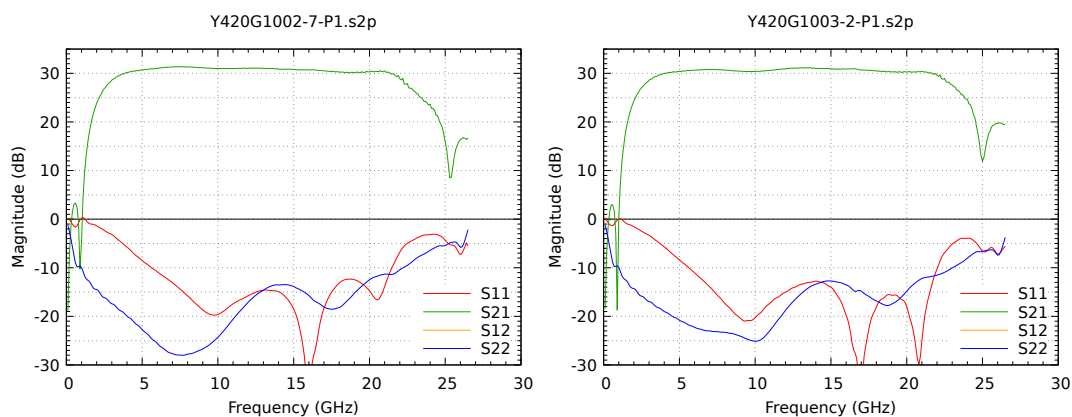


Figure 18: S-parameters of the two Yebes 4–20 GHz amplifiers (Y420G series) used in the 2SB measurements, obtained at 5.5K physical temperature. Compared to the earlier upgraded 2–14 GHz amplifier (Y214G, see fig. 16), the crucial improvement for our purpose is in the input matching ( $S_{11}$ , red curves). Data courtesy of Observatorio Astronómico de Yebes.

### 2.2.3 Cryogenic DSB measurement system

Since integration of experimental components is not very convenient in an ALMA-style receiver cartridge, the first set of double-sideband (DSB) measurements were performed in a conventional Infrared-Labs 8” liquid-helium (“wet”) cryostat, at 4.2K. As the focus of the measurements is the determination of the IF bandwidth, the system was not particularly optimized to obtain the lowest noise temperature. For instance, it uses a warm table-top LO and a relatively thick beamsplitter for easy pumping of the mixer. Also the infrared filters in the cryostat are not really state-of-the-art.

The DSB setup, schematically depicted in figure 19, is quite conventional. The signal chain, following the RF and IF signal path, consists of the following parts, with their most important characteristics:

- 300/77 K hot-cold load optimized for Band 9 wavelength
- 12.7  $\mu\text{m}$  Mylar beamsplitter (shared with LO path, see below)
- Cryostat window (Band 9 quartz), Goretex IR filters at 77 K and 4 K
- Dual-mirror cryogenic relay optics

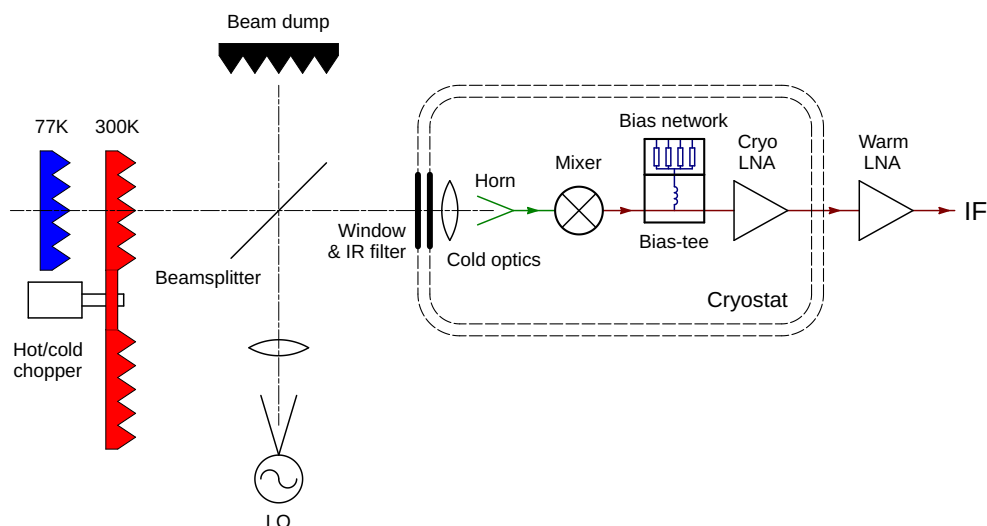


Figure 19: Schematic diagram of the DSB measurement setup. The hot and cold black-body signals from the hot/cold chopper are combined by beamsplitter with the LO, enter the cryostat through a vacuum window and set of IR filters, and are imaged by the cold optics onto the mixer horn. The downconverted IF signal is amplified both at cold and ambient temperatures. Between the mixer and the LNA, the DC mixer bias is injected by the bias-tee after being conditioned by the bias network. Colour codes inside the cryostat as in figure 3.

- Band 9 SIS mixer 2803C48 with standard Band 9 feedhorn Either
  - M/A-Com bias-tee (nominal BW 4–14 GHz, verified 4–27 GHz), or
  - In-house built wide-band bias-tee with integrated bias network
- Either
  - Yebes cryogenic LNA Y214G 1027 (nominal BW 2–20 GHz), or
  - Yebes cryogenic LNA YK22-005 (nominal BW 20.5–24.5 GHz)
- Copper-nickel IF cables from 4 K to 300 K (slope 0–3 dB for 0–30 GHz)
- B&Z RT LNAs BZR-02002650-351328-182323 (Gain 28 dB, BW 2–26.5 GHz)
- Spectrum analyser Rohde & Schwarz FSP30 (9 kHz–30 GHz)

And the LO path:

- Rohde & Schwarz SMP22 signal generator
- Spacek AKKa-2X active doubler
- Band 9 lab LO T09-1
- Double HDPE lens
- 12.7  $\mu\text{m}$  Mylar beamsplitter (about 10% LO coupling), shared with signal path

The parts for which alternatives are listed were replaced in the course of the experiments, as described elsewhere. Figure 20 shows an overview of the experimental setup in the lab.

The tested mixer (SIS2803C48) was a recently re-measured left-over Band 9 production mixer. Its noise performance is in spec but not great (figure 21); in other respects it is representative for typical AlN-barrier Band 9 mixers, and has a 4–12 GHz IF passband free of unusual features.

The two existing IF cables in the cryostat were checked by cross-connecting them at 4 K and measuring the S-parameters when cold by VNA up to 20 GHz, and signal generator/spectrum

	<b>ALMA Band 9 Sideband Separating Upgrade</b> <hr/> <b>Study Report</b>	DocID: FEND-40.02.09.00-1974-C-REP Version: C Date: 2023-02-07 Status: Released Page: 28 of 105
---	---	---

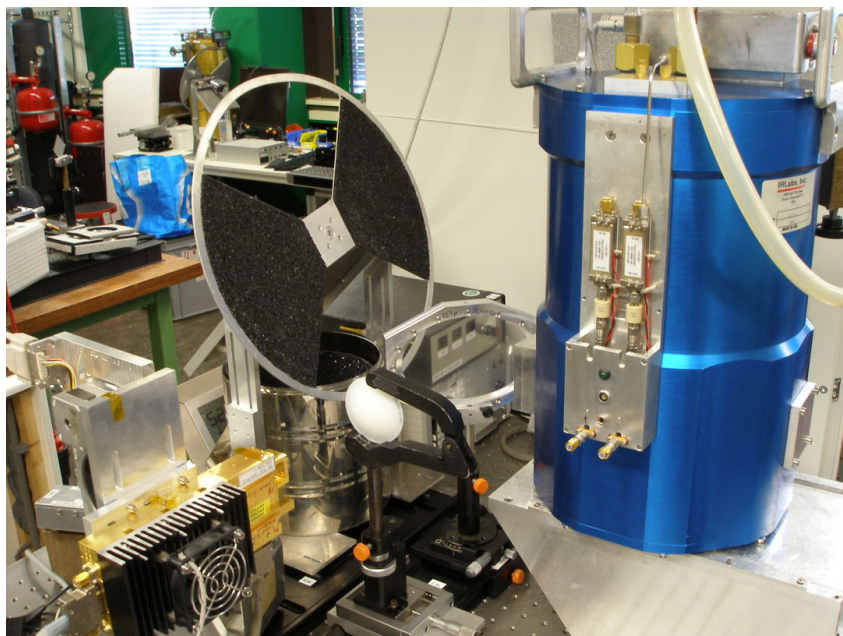


Figure 20: Photograph of the double-sideband (DSB) measurement setup. Cryostat (blue) on the right, in front of the cryostat window (left side) is the  $12.7\ \mu\text{m}$  Mylar beamsplitter, then the hot/cold load (two-bladed chopper and bucket with liquid nitrogen, both covered with absorber). The golden block with heatsink on bottom left is the LO, the beam of which is projected onto the beamsplitter by an HDPE lens (centre). The warm IF amplifiers mounted on the side plate of the cryostat are still of the old 4–12 GHz type used in ALMA. Partially visible through the beamsplitter are the bias and read-out boxes for the cold LNAs that were used initially before the DSB system was fully operational.

analyser further up to 30 GHz. This yielded a slope of about 0 to 3 dB loss (per cable) when going from 0 to 30 GHz. No glaring misbehaviour was observed in this range, although the frequency resolution above 20 GHz was not high enough to catch narrow suck-outs.

All devices in the cryostat are controlled through our Detector Bias System (DBS), which was co-developed together with SRON several years ago. The DBS is functionally comparable to the ALMA bias module, but built with higher flexibility for lab use in mind and with improved specifications. An important activity during the preparation for these measurements was the full coupling to the NOVAsoft engineering software, developed as part of the “Advanced Tuning” study performed recently under ESO contract [17]. Especially the automatic suppression of the Josephson effect means that these measurements can now be performed very efficiently and reproducibly. Apart from the mixer (through the DBS), NOVAsoft also controls the LO (frequency and power) and the hot/cold chopper, so all measurements can be fully scripted.

Note that the DBS-NOVAsoft integration was under development during the current study, so some of the initial measurements were partially done with older equipment. At the time of the last reported measurements (section 2.3.2), the full system was in place and operational.

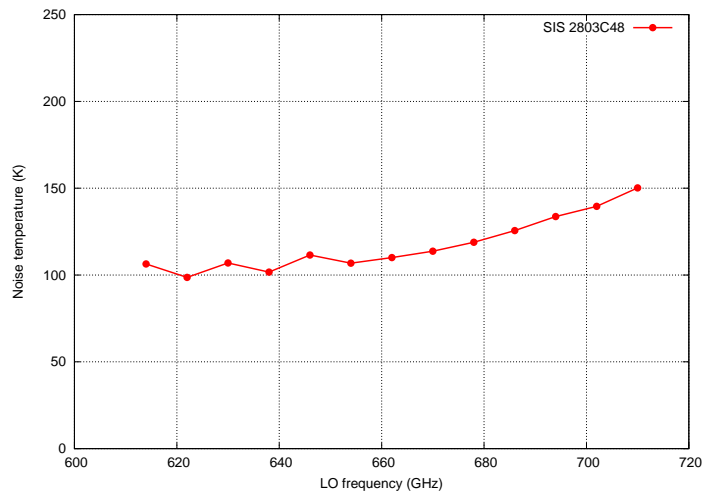


Figure 21: DSB Noise temperature of the used test mixer, as recently measured in ALMA Band 9 cartridge #99.

#### 2.2.4 Band 9 test-bed CCA for 2SB mixer measurements

During the DSB measurements in the wet cryostat, it became clear that the final step, the demonstration of a wide-band 2SB mixer assembly, would face some serious handicaps when performed in the same system. The most important was the bad coupling of the LO power into the mixer cryostat. After a significant effort to optimize this, it turned out that even the DSB mixer could barely be pumped to its optimal level at the upper half of the band. A 2SB mixer assembly, which needs at least twice the LO power (two mixers to pump plus additional losses in the mixer block), would very likely become LO-starved. Even the common workaround of increasing the thickness of the beamsplitter (at the cost of some noise temperature) could not be applied, as the LO coupling ratio is fixed in the 2SB block at about  $-13$  dB, already 3 dB lower than the beamsplitter used in most DSB measurements. Together with some smaller issues (stability of the cabling, availability and effort to convert the 10" Infrared-Labs cryostat to wide-band operation, effort of building up a table-top test-tone system) led to the decision to conduct the 2SB test campaign in an ALMA-type Cold Cartridge Assembly (CCA). For this purpose, our test-bed Band 9 CCA #99, which had been configured to DSB operation for additional SIS device tests (subject of section 4) was rebuilt for 2SB operation. This was done more or less along the lines of the SEPIA660 upgrade (for a short summary see section 1.4.3), although for one polarization only, and in a slightly improvised way.

Because the wideband 2SB IF system is quite different from the one used in DSB Band 9 CCAs (mixer-isolator-LNA), and no hardware from the SEPIA/LLAMA 2SB construction remained, some new hardware had to be produced to patch the IF system into CCA #99. The bias-tees and LNAs are now in the positions formerly occupied by the IF isolators, as can be seen in figure 22. This construction leads to relatively short cable runs from the IF hybrid to the LNAs, and allows us to re-use the existing interface of the the 4K level to the rest of the CCA (which therefore does not require any modification). The 4–20 GHz Yebes IF hybrid itself (figure 23) is mounted on an intermediate bracket because its form factor differs from the earlier 4–12 GHz model. The IF Hybrid and cryogenic LNAs are hard-bolted to the metal of the 4 K structure, which should provide sufficient thermalization to avoid unwanted heat input to the mixers. The top part of the 4K level is built around the original one-off optics cradle that was produced for the very first Band 9 2SB ESO study. Since the IF infrastructure below

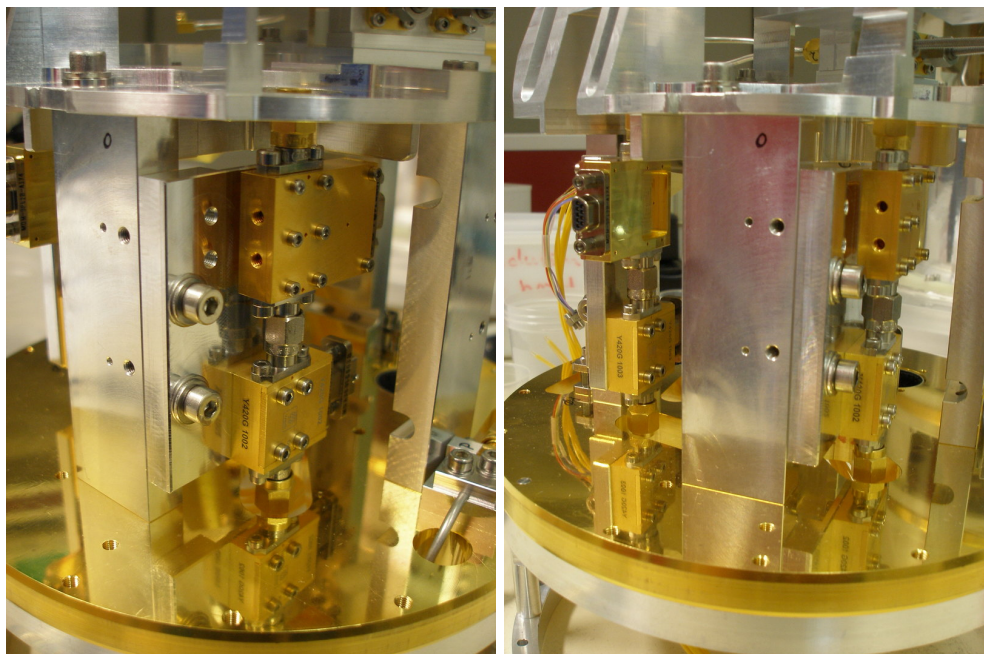


Figure 22: Left: one of the 4–20 GHz IF chains mounted in roughly the position of the former IF isolator in Band 9 CCA #99. The LNA is below, the bias-tee on top. Right: overview, with both IF chains visible.

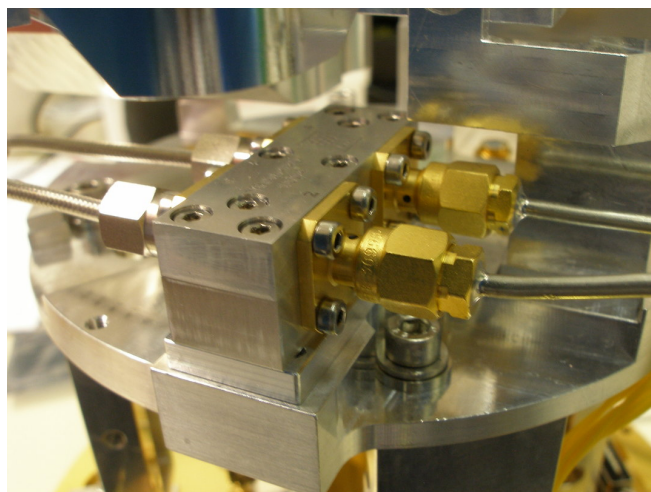


Figure 23: The 4–20 GHz IF quadrature hybrid mounted on an intermediate bracket to make it compatible with the earlier 4–12 GHz one. The two semi-rigid phase-matched cables on the right lead to the mixer (not mounted here yet).

the 4K level consists of two channels only, the resulting CCA observes just one polarization.

With this, apart from its IF bandwidth, single polarization and minor cabling differences, the CCA is fully compatible with the configuration of the SEPIA/LLAMA 2SB CCAs, and therefore all test procedures used in the SEPIA/LLAMA qualification campaign are available. The Warm Cartridge Assembly (WCA) is a standard (2-channel) Band 9 one, except that the 4–12 GHz room-temperature LNAs were replaced by the same B&Z 2-26.5 GHz types as used

	<b>ALMA Band 9 Sideband Separating Upgrade</b> <hr/> <b>Study Report</b>	DocID: FEND-40.02.09.00-1974-C-REP Version: C Date: 2023-02-07 Status: Released Page: 31 of 105
---	---	---

in the DSB experiments.

The mixers selected for the experiment were a pair left over from the test campaign, showing excellent image rejection over 4–12 GHz (comparable to the ones in SEPIA). The devices had shown some difficulty in Josephson-suppression, however, which was the reason they were not selected for delivery then.

### 2.2.5 Measurement procedure

Both for the DSB and 2SB tests, we performed standard heterodyne measurements, very similar to those used to qualify mixers in receiver cartridges. The mixer is defluxed and Josephson-suppressed in its first minimum, and subsequent IF spectra are recorded while alternatively looking at a hot (300 K) and cold (77 K) load, from which the noise temperature is calculated by Y-factor formula. One hot-cold measurement cycle takes about 6 seconds, much shorter than the typical Allan time of a Band 9 receiver (about 10 s, although this is of course not completely representative for the wet cryostat setup where it is expected to be longer). A spectrum analyser is used here as “back-end”. This immediately provides the noise temperature as function of the IF frequency at high resolution. Since we are primarily interested in the IF response, rather than the RF one, this has benefits over the conventional combination of a YIG filter and power meter in terms of speed, spectral resolution and dynamic range. In addition, during most of the study (until the Band 2 project got underway), a YIG filter covering the full IF range was not available. For reference, in the spectrum analyser, the RMS detector was used for the noise temperature measurements with a resolution bandwidth of 3 kHz, and the power level was kept around or below 10 dBm/MHz (this also applies to the later IRR measurements).

In the initial measurements, four LO frequencies were tested (at 621, 648, 675 and 702 GHz equally spaced over the band), and per LO frequency up to 30 hot-cold cycles were recorded. For later measurements, when the full DBS/NOVAsoft control was implemented, standard 8 GHz-interval sets of LO frequencies were obtained.

At various moments during the experiments we determined both IF noise temperature and IF gain by the shot-noise method. For this, the mixer is biased above the gap (typically at 4 and 8 mV), where it shows normal Ohmic behaviour. Since the level of the shot noise caused by the passing of the electrons through the tunnel barrier can be determined from the current, the mixer is used as a “calibrated” two-level noise source, analogous to the hot/cold load used to determine the RF noise temperature. Although this method is used routinely to characterise the IF chain in receivers (e.g., during production cartridge qualification), there is an important caveat: in the normal state, where the mixer is biased for this purpose, its output impedance is typically very different from its design value in the superconducting state. Because of this, the results of this method should be considered with careful judgment when the actual interaction of the mixer with the rest of the IF system is under consideration, as it is in these experiments.

The image rejection ratio (IRR) is determined by injecting a weak test-tone into one sideband and measuring its leak-through into the opposite one. Calibration of the test tone power and other gains in the system is done according to the method described by Kerr et al. [14].

All measurements performed on the ALMA-type cartridge were done at a stabilized temperature of 4.0 K of the 4K-stage of the cryostat, in compliance to the ALMA specifications. For comparison, this also applies to the original SEPIA lab qualification data shown in figures 1 and 2.

## 2.3 Experimental results

### 2.3.1 Initial DSB results with commercial bias-tee

Figure 24 shows the noise temperature obtained with the commercial bias-tee as function of IF frequency, for four different LO frequencies. From the IF noise temperature plots it is clear that this mixer performs at least up to about 17–18 GHz, after which the noise starts increasing gradually. Unfortunately, the standing waves that diverge rapidly above 20 GHz obscure the precise noise development in this region. Nevertheless, when looking at the lowest parts of the standing wave pattern, where the coupling is supposed to be optimal, we can at least get a qualitative idea of the mixer’s IF coupling there. Actual measures taken to mitigate the standing waves could raise this level somewhat. With this in mind, it appears that the useful band, seen in the noise temperature, may extend up to about 24 GHz for the lowest three LO frequencies. In section 2.3.2 we will see that the excess noise at 702 GHz is probably due to problems with the LO. Note that these measurements were done with the Y214G cold LNA which is specified up to 20 GHz only.

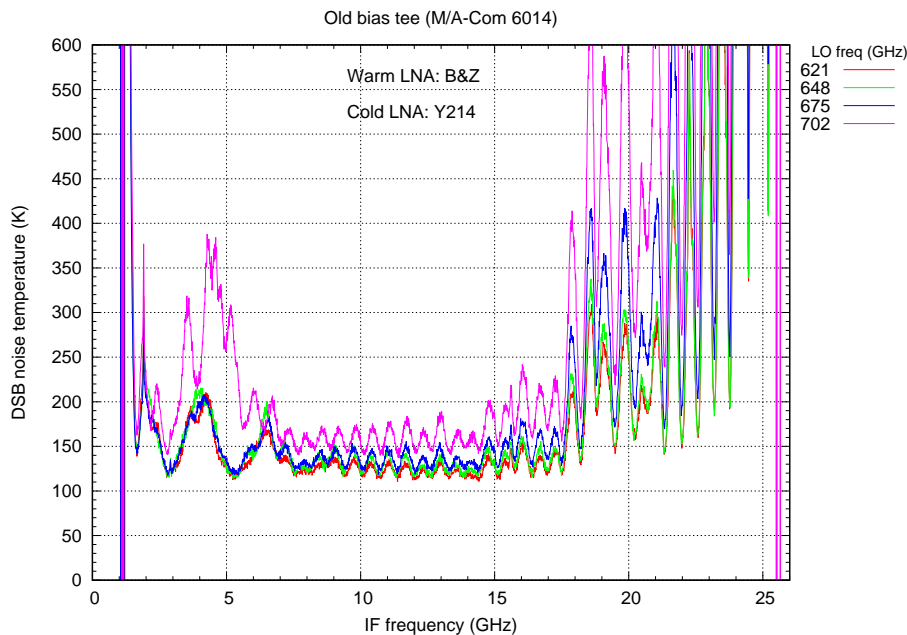


Figure 24: DSB noise temperature of the reference mixer as function of IF frequency, 4 LO frequencies using the old bias-tee.

Next, the YK22-005 LNA (20.5–24.5 GHz) was built into the cryostat and the measurements repeated, shown for one LO frequency in figure 25. Surprisingly, up to about 24 GHz, the noise temperature seems to be higher than for the Y214 amplifier, although the amplitude of the standing waves is slightly smaller indicating a better impedance match. Because of this, all further measurements were performed with the Y214 amplifier exclusively.

Shot-noise measurements were performed on these configurations as well, but since it was decided by now to replace the commercial bias-tee with the in-house developed one, we will show and discuss the IF gain results in section 2.3.2.

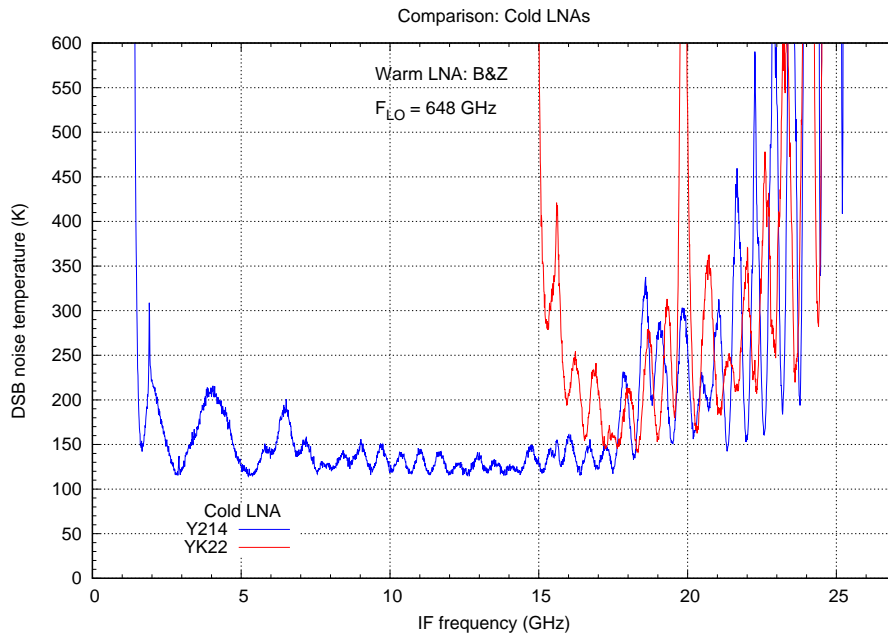


Figure 25: The DSB mixer noise temperature with both cold Yebes LNAs (Y214: 2–20 GHz, YK22: 20.5–24.5 GHz, nominally) and the old bias-tee.

At this point, our interim conclusion is that the SIS devices indeed could have an IF coupling that extends up to 24 GHz, as predicted by the simulations of Kirill Rudakov. Since we also observe a clear increase in the noise temperature towards the upper edge, the practical IF band is probably limited to about 18–20 GHz. It is also clear that without proper input matching of the LNAs, this range is not available yet for actual use. Another handicap is the absence of a built-in bias-tee, as this is also likely to be responsible for part of the standing waves.

### 2.3.2 DSB Results with in-house produced bias-tee

Despite the standing waves still visible in the VNA measurements of the new bias-tee, a set of noise temperature curves was obtained using the same mixer as in the previous tests. This time, instead of just four LO frequencies, the same set frequencies, 8 GHz apart, as in ALMA/SEPIA was used. This is much easier to do than before as the entire wet-cryostat setup is now controlled by NOVAsoft through the DBS system.

The cold LNA used is the same Y214G as before. Figure 26 shows the results with all curves plotted on top of each other. To study the noise behaviour of the individual LO settings more closely, figure 27 shows the same curves as figure 26 (except for the highest LO frequency), but now with progressive vertical offsets. In figure 28 the IF output power at the output of the warm LNA is shown, with the mixer looking at the 300 K hot load. Also here with the individual curves offset to separate them.

There is clearly still a problem with standing waves (although not the 3 GHz ones seen in the bias-tee itself). The overall noise temperature is better, and the standing waves in the 18–20 GHz are clearly reduced. The most striking observation, however, is that the noise temperature in most cases is quite constant (apart from the standing-wave ripple) down to

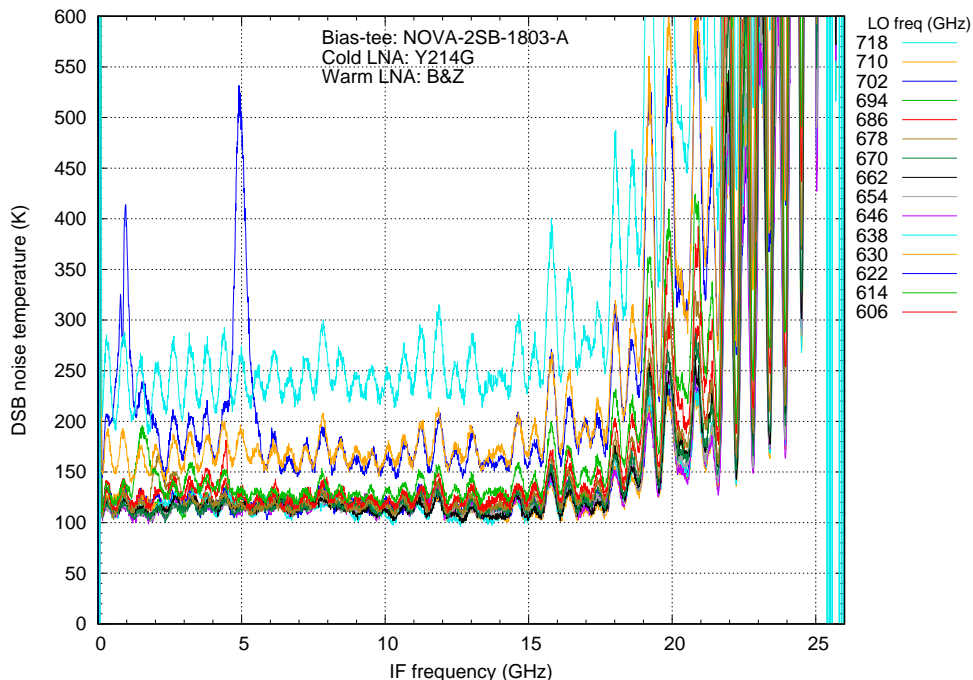


Figure 26: DSB noise temperature of the reference mixer as function of IF frequency, for 15 LO frequencies using the new bias-tee.

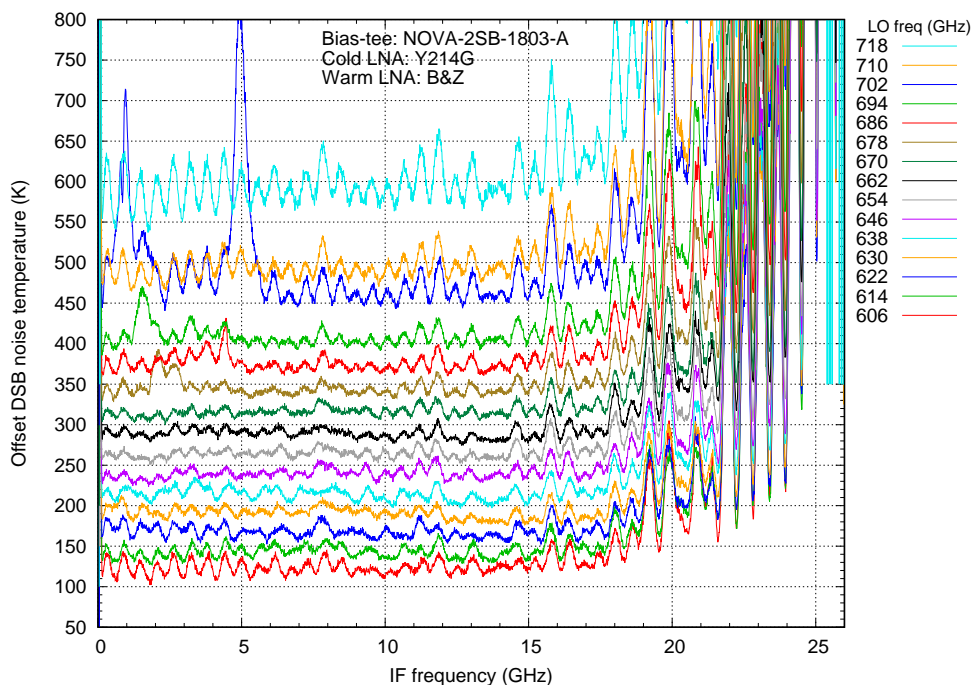


Figure 27: The DSB noise temperatures as function of IF frequency using the new bias-tee. Each curve offset vertically by a multiple of 25 K to separate them. The bottommost curve (606 GHz) is at the original level.

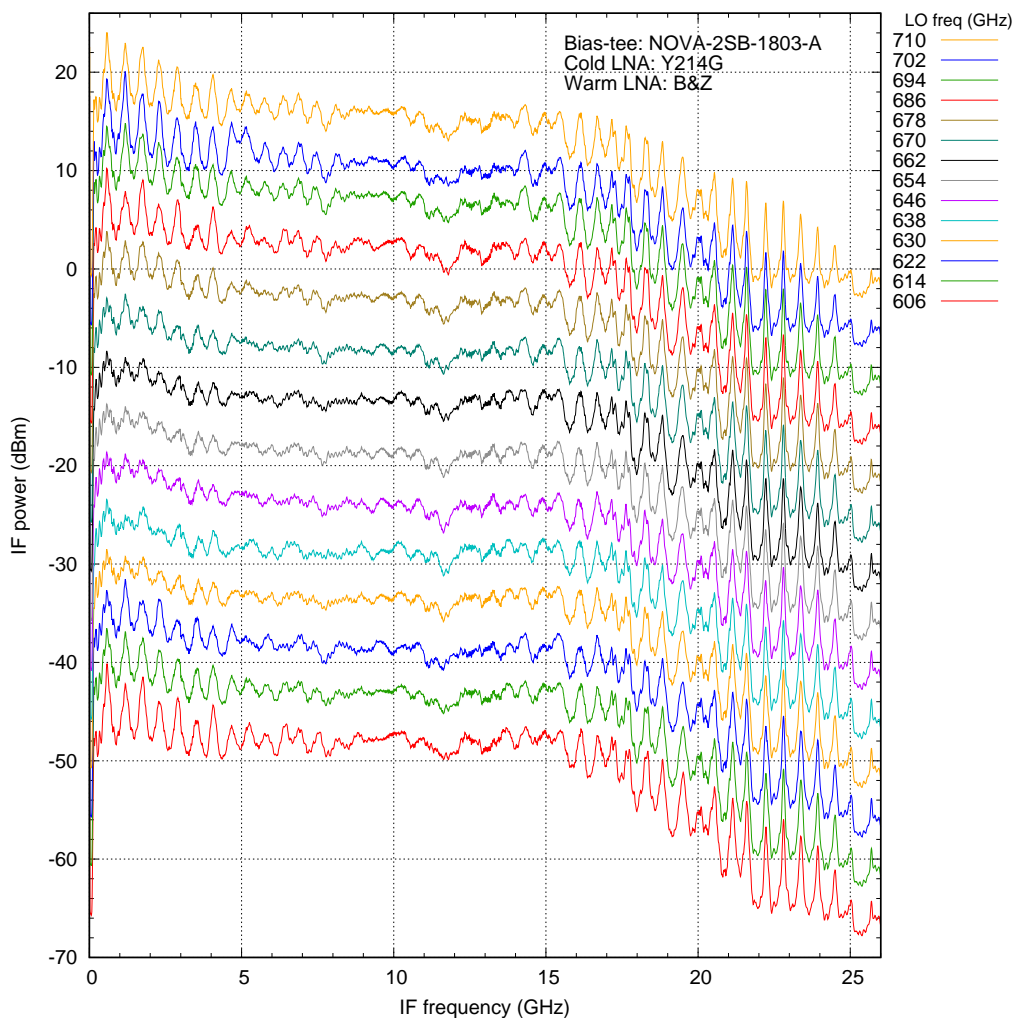


Figure 28: IF power with the new bias-tee and the Y214G LNA, and the mixer looking at a 300 K load. Each curve offset vertically by a multiple of 5 dB.

very low IF frequencies, roughly 100 MHz. For the mixer device itself this should actually not come as a surprise, since there is no physical limitation of the IF frequency on the lower end. It shows, however, that all other IF components perform here as well, far beyond their nominal bandwidth (below 1 GHz for the Yebes Y214G and 2 GHz for the B&Z warm LNA). Especially the noise matching of the the 2–14 GHz LNA seems very good down to the lowest frequencies, despite  $S_{11}$  rising to essentially 0 dB around there.

The more narrowly-spaced LO frequencies also reveal that the extra noise features at around 5 GHz and below for the 702 GHz trace, which were a bit puzzling in the previous four-frequency measurements, are probably due to misbehaviour of the LO, as they are virtually absent in adjacent frequencies. The overall noise temperature averaged over the 4–12 GHz part of the IF band goes up consistently with the historical data (figure 21) for the corresponding LO frequencies (614–710GHz), namely about 50 K.

The standing wave pattern is even more pronounced if we look at the pure IF noise and

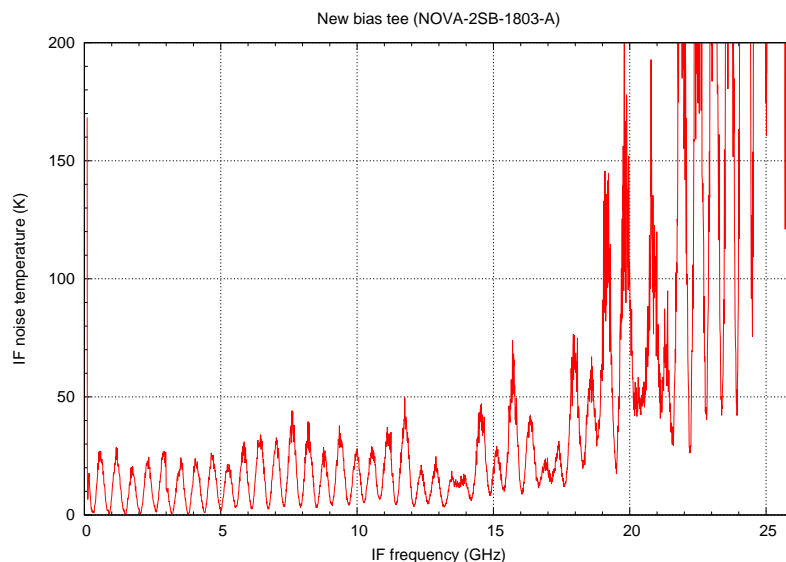


Figure 29: IF noise temperature measured by shot-noise method.

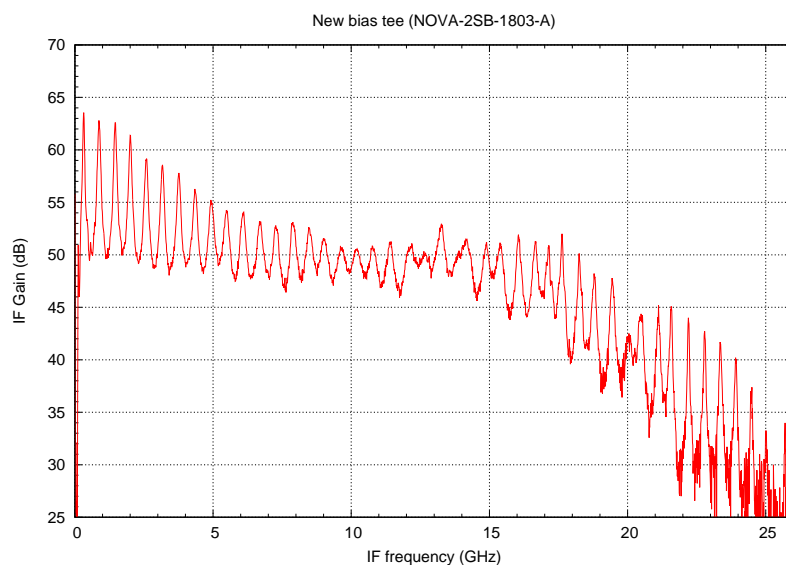


Figure 30: The IF gain measured by shot-noise method.

gain contributions, obtained by shot noise measurement, and shown in figures 29 and 30, respectively. As usual, there is the caveat that the mixer, biased above the gap for this measurement, presents quite a different output impedance compared to its normal operation, and so any present standing wave pattern is likely to be enhanced. It is interesting to note that the standing wave amplitude is indeed lowest between 10 and 15 GHz, where the LNA's input match is best (less than about  $-12$  dB return loss, see figure 16). Also, since the amplitude of the standing wave is indeed larger than in the superconducting state, it is suggestive that the mixer itself constitutes one of the endpoints of the resonator.

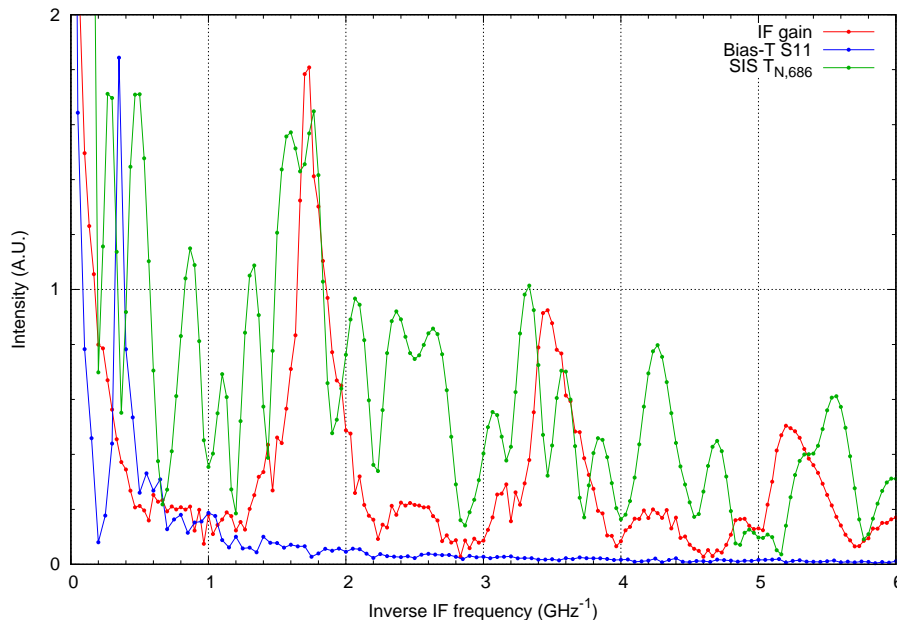


Figure 31: Fourier transforms of the IF gain (by shot noise), the input reflection ( $S_{11}$ ) of the bias-tee and the mixer noise temperature for one arbitrary LO frequency.

To compare the IF ripple with the overall periods found in the noise temperature curves, the IF gain, total IF power for one arbitrary LO frequency (686 GHz), and the  $S_{11}$  of the bias-tee have been Fourier-transformed and plotted together in figure 31. The idea is that any standing waves within the bias-tee should show up here. We considered  $S_{11}$  because it is the most sensitive parameter to anything happening in the bias-tee, rather than, say,  $S_{21}$ , which is a very small (and noisy) number. Somewhat surprisingly, the standing wave period of the bias-tee (about  $0.34 \text{ GHz}^{-1}$ ) is not really visible in the mixer noise temperature. This strengthens our belief that the dominant reflections are elsewhere. The lowest (inverse) frequency component in the IF gain is at about  $1.7 \text{ GHz}^{-1}$ , corresponding to an electrical round-trip length of about 510 mm. With an estimated group velocity of  $2/3 \cdot c$  in the IF cables, this would be a mechanical distance of 170 mm between reflections. This is considerably longer than the total mechanical length of the mixer—bias-tee—LNA chain (about 80–90 mm).

Because of increasing time pressure (due to COVID, Band 2 effort, etc.), and despite the fact that the origin of the standing waves was not fully explained at this point in the study, it was decided to push forward from here to obtain 2SB results as quickly as possible. One final DSB test was done, now with one of the new 4–20 GHz LNAs that Yebes had delivered for the 2SB configuration (see last paragraph of section 2.2.2). The same measurement procedure was followed, resulting in the data shown in figures 32 (noise temperature) and 33 (IF power).

Concerning the standing waves, these turn out to be markedly lower than with the Y214G amplifier as can be clearly seen when comparing the IF powers of figures 28 and 33. Without rigorous analysis, we ascribe this to the improved input matching of the LNA. Indeed, the strongest remaining standing waves are below 5 GHz and above 21 GHz, where the input return loss exceeds -10 dB (figure 18).

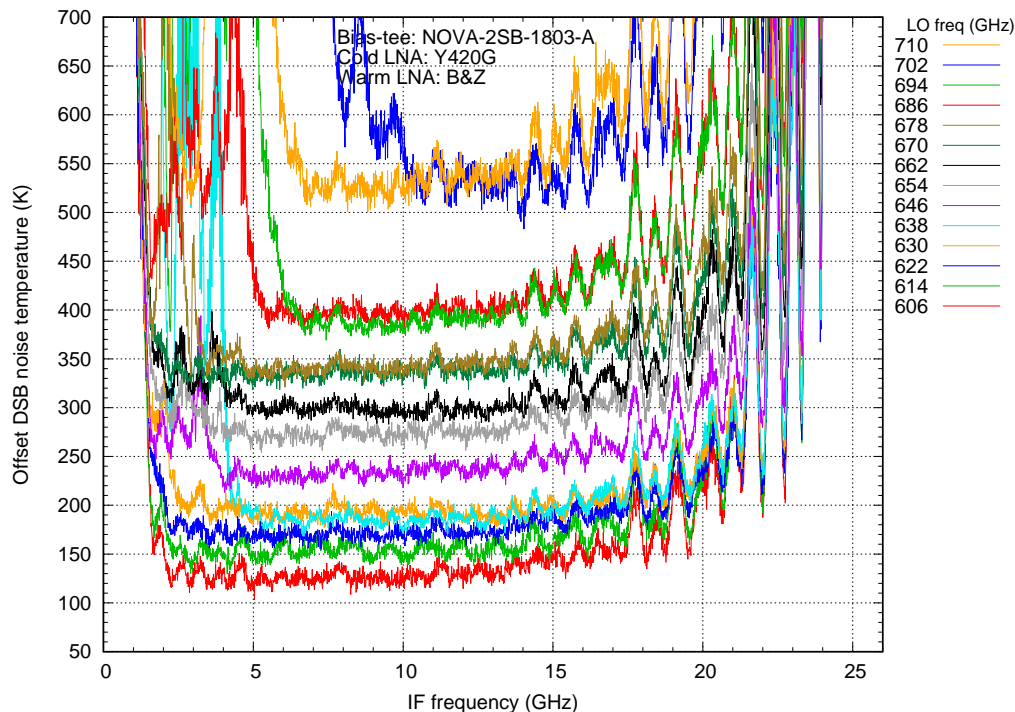


Figure 32: DSB noise temperature, as in figure 27, but with the new Yebes Y420G LNA. The measurement data (taken by spectrum analyser) looks more noisy than in the former measurement due to averaging over fewer SA sweeps. Also, in this measurement the mixer was clearly underpumped at several LO frequencies resulting in excess noise. Each curve from bottom to top is offset by 25 K from the preceding one (the 606 GHz curve is at its “native” level).

### 2.3.3 Sideband-separating results

The sideband-separating mixer built into CCA #99 was tested for the two most interesting properties: the image rejection ratio (IRR) and the noise temperature over the IF band.

The IRR is presented in two ways, in figures 34 and 35. The first shows the individual IRRs over the full IF band of 2-20 GHz, each at a different LO setting. Clearly visible is that the IRR is pretty high and flat over most of the central part of the IF band. As a tentative usable range, we propose 4–18 GHz here, which are the limits between which most of the traces are above 10 dB, the traditional ALMA requirement for the 2SB bands. Over most of this sub-band the IRR is close to or above 15 dB, actually. It should be noted that most (perhaps even all) of the strong isolated negative spikes observed within the 4–18 GHz range are artefacts due to a failing spectrum analyser. Unfortunately, our 2-20 GHz (Band 2) IF box (with which the measurements could be repeated more cleanly) was out of commission at the time of the measurement.

In figure 35, the image rejection traces are plotted together in the traditional way, as function of on-sky RF frequency, for three different IF ranges. The top panel shows the composite of the 4–20 GHz band. As already clear from figure 34, the extremes of this band ruin the picture, so the second panel limits the IF band to 4–18 GHz. In order to compare this with earlier “narrow-band” results, the third panel shows the same data, but now limited to the

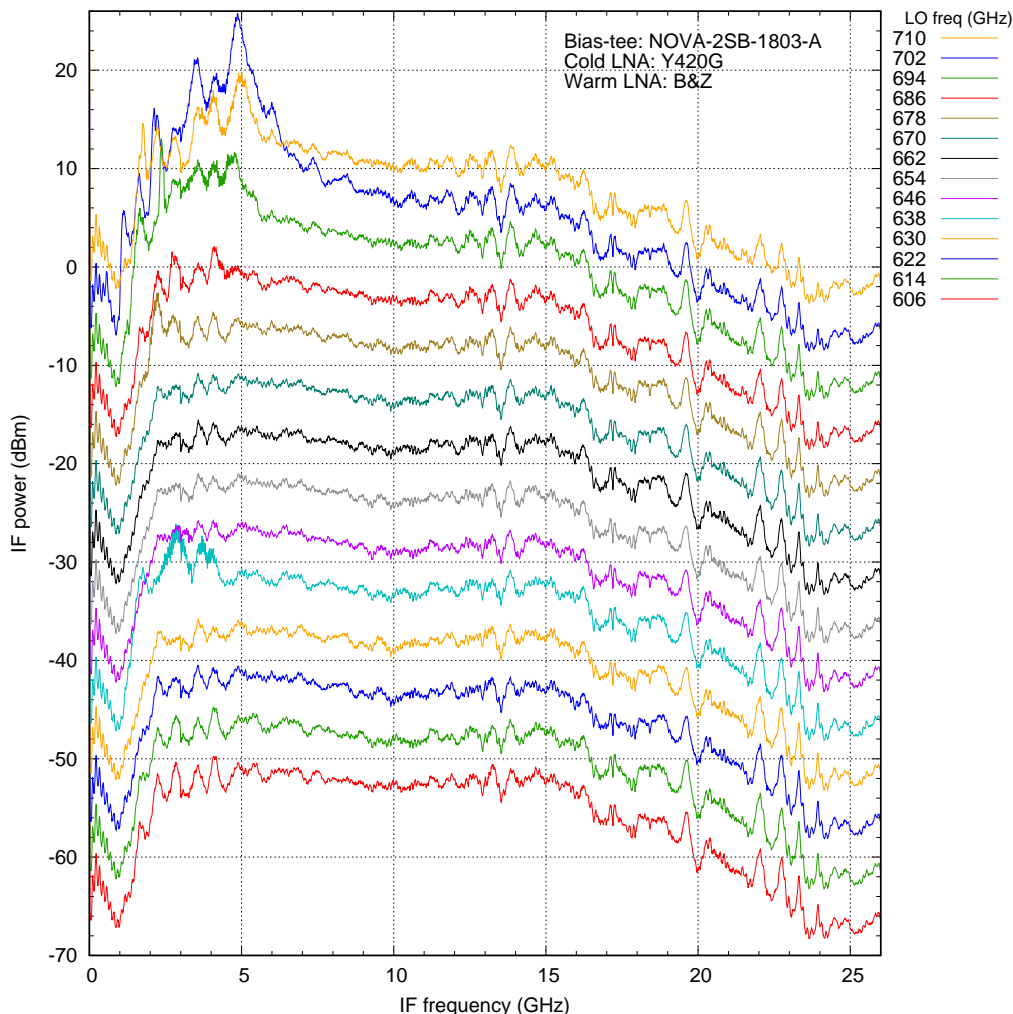


Figure 33: IF power for different LO frequencies using the new Yebes Y420G LNA, looking at a 300 K load. Each curve is offset vertically by a multiple of 5 dB to separate them. This result should be compared to the one shown in figure 28, taken with the previous generation of LNA.

traditional 4–12 GHz range. The bottom panel finally shows the IRR of the same mixer pair obtained during the SEPIA/LLAMA test campaign.

The comparison of the lower two panels requires some consideration. In the first place, apart from the SIS devices, almost all other components in the two systems are different: the RF hybrid block (the original having been delivered), the IF hybrid and LNAs, and the measurement setup itself (YIG filters rather than spectrum analysers). Incidentally, the latter accounts mostly for the different degree of “hairiness” on the data (due to the narrower channel bandwidth), as was observed many times before. Nevertheless, there seems to be a systematic discrepancy of 4–5 dB in IRR between the two data sets which should be accounted for, as there is no obvious reason for a degradation due to the use of wider-band components. The RF hybrid block used in the current measurement (manufactured by MPIfR in Bonn as precursor to the nFLASH Band 10 block) is of exactly the same design as the ones used in SEPIA

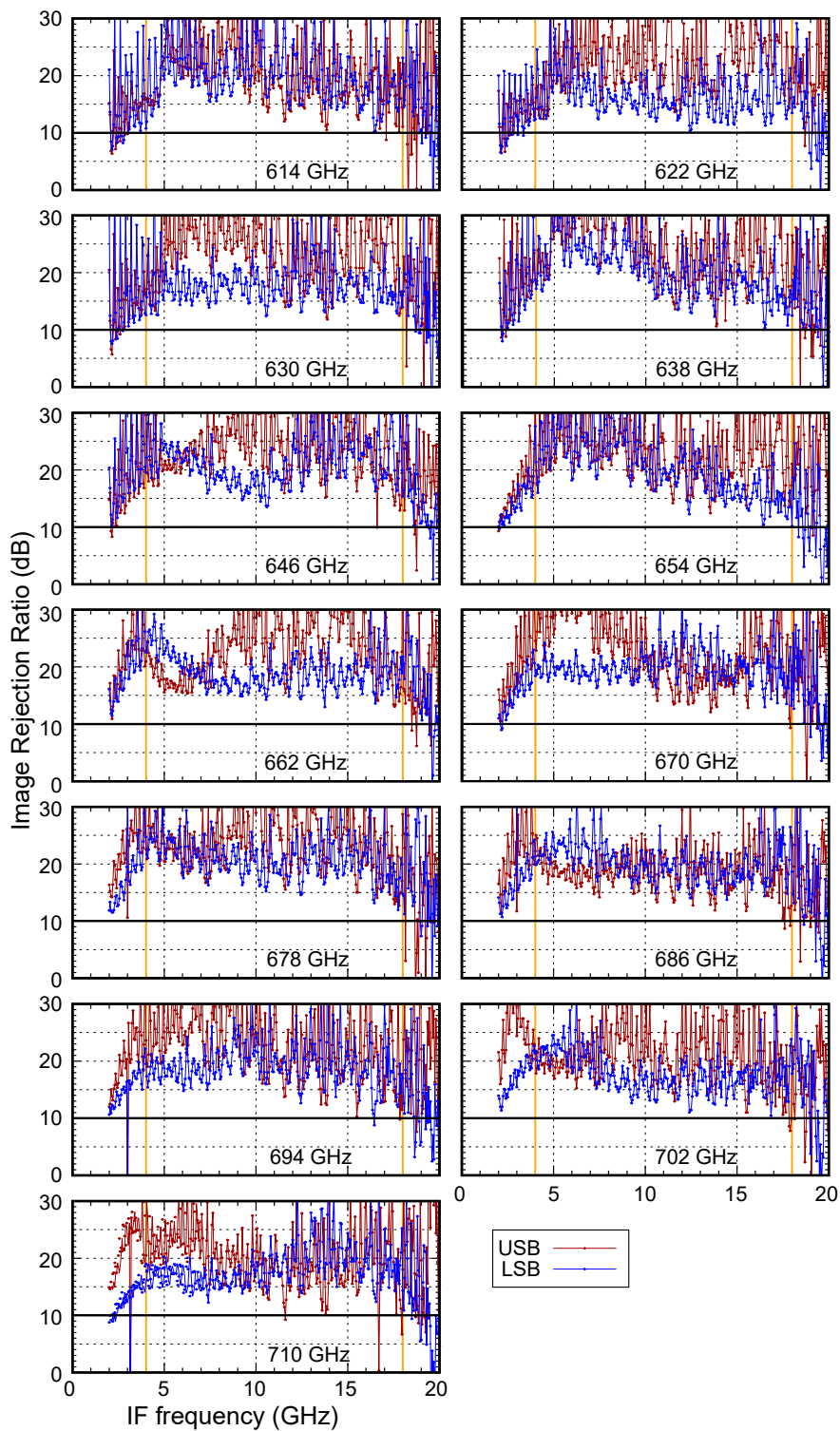


Figure 34: The Image Rejection Ratio as function of IF frequency for different LO frequencies. The thick lines at 10 dB show the typical (current) ALMA spec.

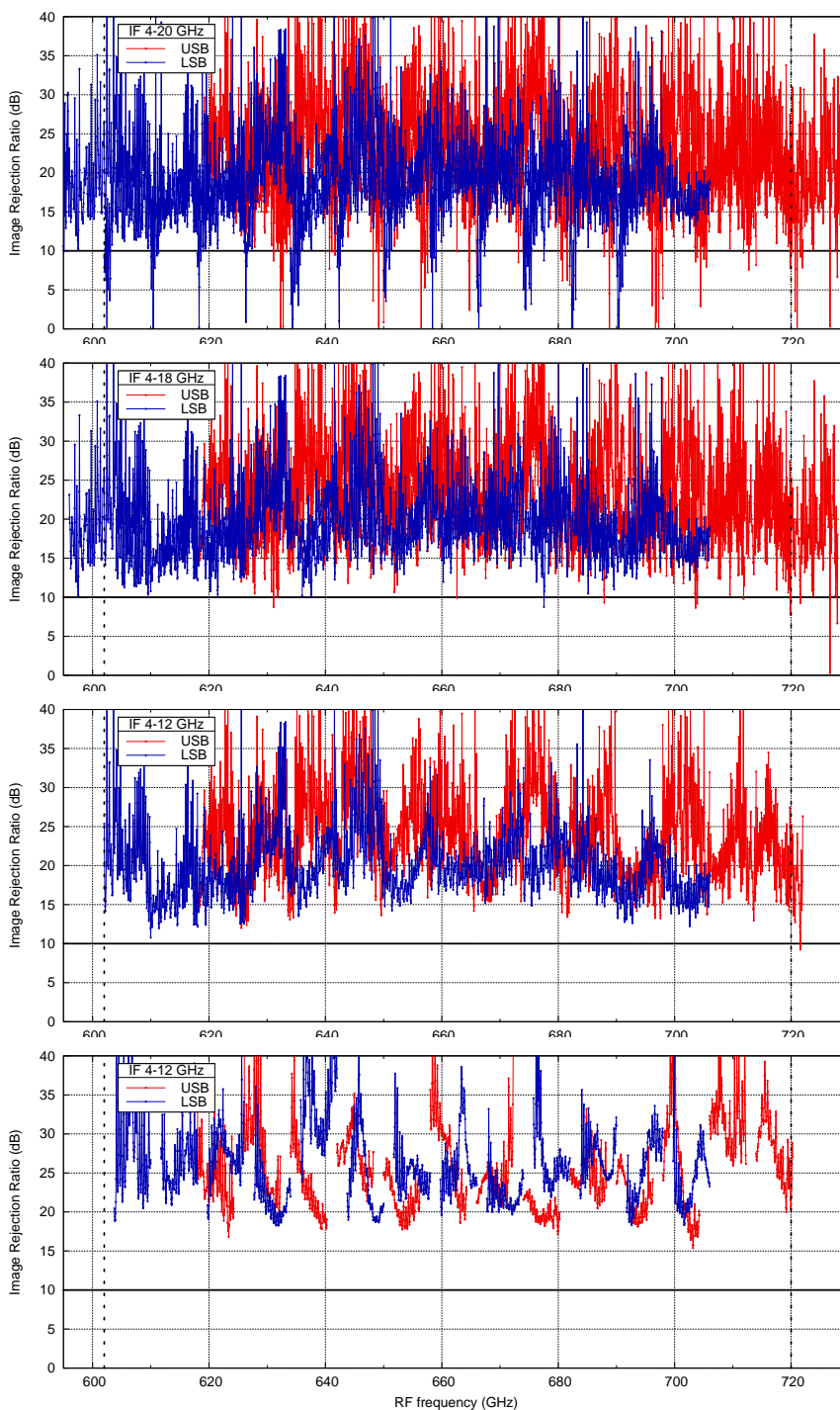


Figure 35: The combined IRR data for the tested mixer pair. Top panel: full IF range (4–20 GHz). Second panel: IF range 4–18 GHz. Third panel: IF range 4–12 GHz. Bottom panel: the same pair of SIS devices measured (over 4–12 GHz) during the SEPIA/LLAMA test campaign, with a different RF hybrid block, different IF hybrid, and different LNAs (with integrated bias-tees).

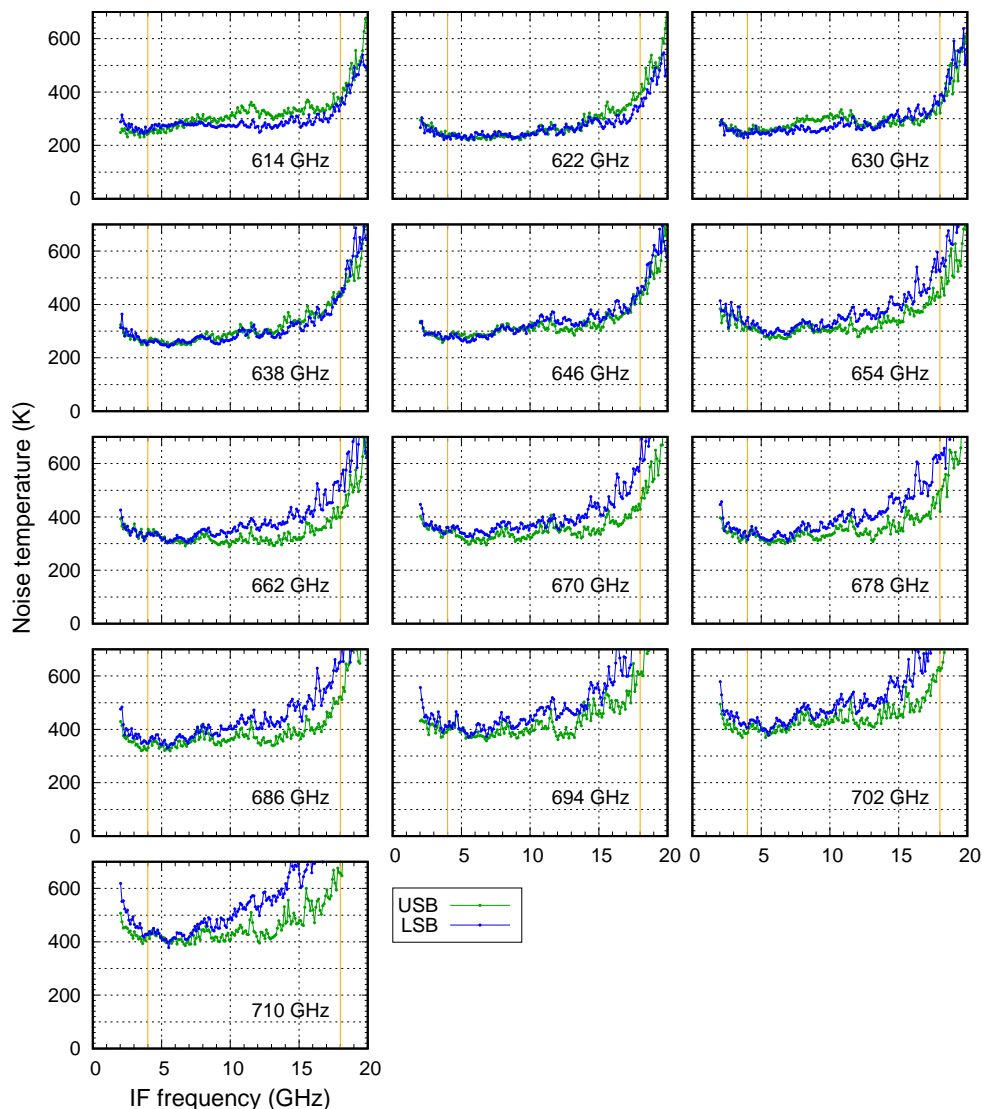


Figure 36: The SSB noise temperature of the 2SB mixer as function of IF frequency for different LO frequencies.

and it showed SEPIA-class IRRs in earlier measurements. Also the new IF hybrid and IF LNAs show performances at least as good as the 4–12 GHz models used in SEPIA/LLAMA, especially in impedance matching. Our suspicion is that the insertion of the external bias-tees is the main factor in the decreased overall IRR, even if they are behind the IF hybrid. As argued before [6], the IRR is determined as much by parasitic reflections as by the phase- and amplitude imbalances in the system, even if outside the hybrid-to-hybrid loop. We realize that this argument by elimination is no conclusive proof, but unfortunately in the time frame of this study this is as far as we can go. If this conclusion is indeed valid, it underscores once more the importance of integrated bias-tees and optimization of impedance matching.

The measured noise temperatures, again over the 2–20 GHz band for 8 GHz-spaced LO frequencies is shown in figure 36. Note that these are now SSB noise temperatures which are twice as high as corresponding DSB ones. When compared (taking the factor of two into account)

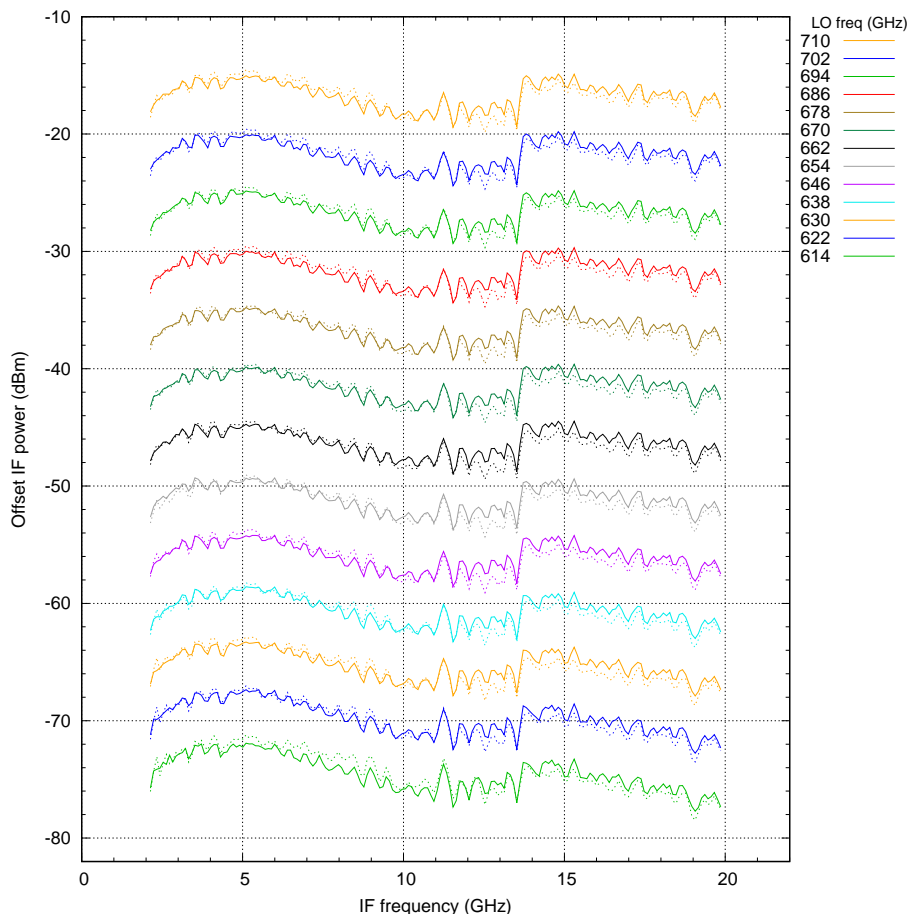


Figure 37: IF power for different LO frequencies for the 2SB mixer, looking at a 300 K load. Each curve is offset vertically by a multiple of 5 dB to separate them. Solid line: USB, dotted line: LSB.

with the DSB measurements in figure 32, the levels are similar or slightly higher. An exact comparison is not possible here, as the respective mixer devices are not identical. The extra loss introduced by the RF hybrid block could explain a remaining systematic difference. The displayed overall noise temperatures are of course higher than what we would like to deliver in real upgraded receivers.

Figure 37 shows the output power over the IF band for different LO frequencies, looking at a 300 K load. Compared to the DSB result in the wet cryostat (figure 33), these are much cleaner: the short-period ripple is at least a factor of two smaller, and the pronounced roll-off (almost 10 dB over 15–20 GHz) is reduced to about 2 dB over the same range in the new situation. This strengthens our belief that many of the issues seen in the DSB measurements were due to the IF infrastructure, not inherent limitations of the mixer or the amplifier.

It should be noted that these mixers were not selected on best noise performance, one mixer turned out to have a series resistance which makes (automatic) tuning more difficult, manually tuning a 2SB mixer (bias points, LO power) is rather laborious, and time was short and the mixers were possibly not very well matched in LO requirement, making noise optimization in both devices difficult. It was a reject pair from the SEPIA campaign, and was chosen here

	<p><b>ALMA Band 9 Sideband Separating Upgrade</b></p> <p>—</p> <p><b>Study Report</b></p>	<p>DocID: FEND-40.02.09.00-1974-C-REP</p> <p>Version: C</p> <p>Date: 2023-02-07</p> <p>Status: Released</p> <p>Page: 44 of 105</p>
---	---	--

because it still presented good IRR. However, we did not put particular effort here into optimizing the noise temperature as the main objective was the demonstration of image rejection over a widened IF band. From past experience with the SEPIA and LLAMA mixers, our estimate is that the transition from DSB to 2SB with comparable SIS devices will incur a SSB noise penalty of about 20 K ( $\pm 10$  K) over the simply doubled DSB noise temperature of the individual mixers. [7].

## 2.4 Discussion

Both the presented DSB and 2SB measurements show that the existing Band 9 SIS mixer design is certainly capable of a much larger IF bandwidth than the original design specification. With confidence we can state that at up to 16 GHz and probably up to 18 GHz the performance will be very similar to that with the band up to 12 GHz.

Whether the useful band can be extended further to, say, 2–20 GHz is an interesting question. On the lower side, the mixer does not seem to be the limiting factor, as for instance is evident from figure 27. For 2SB operation, however, which requires particularly well-matched amplifiers, this may complicate their design considerably, as discussed below. On the high end of the band, we seem limited by increasing losses in the IF path, probably partially in the mixer itself, in addition to the rest in the IF components and cabling. This is something that we encounter in the development of the Band 2 receiver and measurement system as well: most standard coaxial cables and components used up to now are specified up to 18 GHz, and many already start deteriorating well below that. Also, phase matching for 2SB operation becomes more and more critical with increasing IF frequency.

One of the reasons for the high performance of the 4–12 GHz Yebes amplifiers used in the SEPIA receiver (apart from the input matching itself) is the fact that they have built-in bias-tees which greatly mitigates many matching problems by eliminating intermediate components. However, after discussion with Yebes it became clear that they do not have the capacity within the current development program to integrate bias-tees as well. We consider such a development essential for high-performance sideband-separating receivers, and hope that in the future opportunities arise that will facilitate such developments.

### 2.4.1 Desired vs. practical IF band

In general, it is desirable to make the IF band such that the per-sideband IF bandwidth is an integer multiple of the inter-band gap in order to facilitate the tiling of spectral surveys. Upon discussion with ESO, specifically an IF band of 2–18 GHz was considered to be favorable (bandwidth:gap = 4:1), to which small guard bands of about 100 MHz should be added to make seamless overlap possible. A 1.9–18.1 GHz band was proposed as a “desirable” goal of the study.

We discussed this with our colleagues at Yebes. From them we understand that making a 2–18 GHz single-ended LNA with good input matching will be very difficult. For an IRR comparable to the SEPIA receiver (15–25 dB) with the current mixers, we need an LNA with an input return loss ( $S_{11}$ ) of about  $-15$  dB or better. Building a 2–18 GHz LNA with this performance almost certainly requires a balanced design, with a doubled power dissipation and significantly larger envelope. Technologically, this should be feasible as Yebes already built a balanced 1.5–15.5 GHz LNA with an input matching better than  $-17$  dB. If issues of space

	<b>ALMA Band 9 Sideband Separating Upgrade</b> <hr/> <b>Study Report</b>	DocID: FEND-40.02.09.00-1974-C-REP Version: C Date: 2023-02-07 Status: Released Page: 45 of 105
---	---	---

limitations, dissipation and the doubling of the required LNA bias circuits can be addressed, a balanced LNA (possibly thermally anchored to the 15 K stage) would be an attractive option.

According to Yebes, and demonstrated in the mean time, a 4–20 GHz single-ended LNA with the required  $S_{11}$  is much more feasible, although still a serious challenge. So, from a technical point of view a 3.9–20.1 GHz band would be a more realistic goal than 1.9–18.1 GHz. Since it also fulfils the integer bandwidth/gap criterion (with a 2:1 ratio), we anticipate further discussion of the trade-offs with the user community.

The experimental evidence shows a probable obtainable DSB bandwidth of at least 0.1–20 GHz for the current ALMA Band 9 mixer devices. A virtual gapless “spectral grasp” of 40 GHz would provide an unprecedented power for wide-band wide-field spectral surveys. On the other hand, because of the immense relative bandwidth that this encompasses, it is unlikely that the full range can be employed in a practical 2SB receiver. Apart from the issues with the LNAs, the IF hybrid would become prohibitively large, as its dimensions scale roughly with the lowest frequency to be covered. For a lower limit of 0.1 GHz and an effective  $\epsilon_r \approx 10$  for the hybrid structure, this would imply a size of around 30 cm.

One possible way out for the latter problem could be to eliminate the analogue hybrid altogether and move the sideband-separation into the digital domain [18]. Whether this could be extended to such a huge relative bandwidth as well is an interesting question, but fundamentally speaking there should be no limit.

	<b>ALMA Band 9 Sideband Separating Upgrade</b>	DocID: FEND-40.02.09.00-1974-C-REP Version: C
	<b>Study Report</b>	Date: 2023-02-07 Status: Released Page: 46 of 105

## 3 Study goal 2 — Extending the RF bandwidth

### 3.1 Scientific driver

The reason that the band edges of ALMA Band 9 originally were chosen to be 602 and 720 GHz is the presence of strong water vapour absorption lines at about 557 and 750 GHz, each pressure-broadened to something of the order of 50 GHz. In practice, however, very dry conditions still allow useful observations slightly outside of this range, especially if the source is sufficiently bright. A good example, obtained with the SEPIA660 2SB receiver at APEX, is a spectral line survey of the Orion-KL star-forming region [19]. Here, the focus was specifically on the frequency ranges around and just outside of the ALMA Band 9 band edges (*viz.* 581–607 GHz and 701–727 GHz). Even with non-ideal atmospheric conditions, over 100 lines of various molecular species were observed in a matter of minutes of integration time per LO setting. Although many of these molecules can also be observed in the current ALMA Band 9 frequency range (or even in other bands) [20], this clearly demonstrates the feasibility of such observations, especially when combined with a high image-rejection ratio (better than 20 dB at most frequencies for SEPIA660). It should be noted, however, that for an interferometer like ALMA (more so than for a single dish like APEX), sufficient signal-to-noise is needed to observe the scarce and faint calibration sources available in this band, intrinsically handicapping observations at low atmospheric transmission.

Another scientific driver is the expanded access to atomic cooling lines of, e.g., [CII] and [OIII] in distant galaxies over a larger range of redshifts. The mentioned lines appear in Band 9 around  $z = 2$  and  $z = 4$ , respectively, just about bracketing the peak of star formation, making this aspect relevant in the realization of one of the three ALMA 2030 science goals (Origins of Galaxies) [13].

For these reasons, despite the limited observational opportunities offered by atmospheric conditions, the extension of the RF band was included in this study, especially since it should be achievable at relatively moderate cost.

### 3.2 Technical aspects

As demonstrated in the SEPIA660 receiver, the existing AlN-barrier SIS junctions that make up most of mixer in the delivered Band 9 cartridges typically have an RF bandwidth extending significantly beyond the 602–720 GHz range of the Band 9 specification, way into the water vapour absorption lines that in practice limit the observation band. Also the reflective optics in the cartridge as well as the corrugated feedhorns have much wider bands than the specification ( $\sim 25\text{--}30\%$ , while Band 9 requires only 12% relative bandwidth). On the other hand, the older AlO<sub>x</sub>-barrier junctions, of which there are 30 in the Band 9 array (15 cartridges), display a marked upturn in noise temperature at the lower part of the band and they will be replaced anyway. This is taken into account in section 4 when the availability of junctions is discussed. In the scope of this study, apart from the mixers qualified for SEPIA and LLAMA, about 28 extra AlN-barrier mixers have been tested successfully in the extended RF band. We therefore assume that this is representative for all Band 9 mixers.

Since the junctions and surrounding components already have sufficient RF bandwidth, the only modification needed is the extension of the local oscillator (LO) tuning range. Most of the LO resides in the Warm Cartridge Assembly (WCA) just outside the vacuum flange of

	<p><b>ALMA Band 9 Sideband Separating Upgrade</b></p> <hr/> <p><b>Study Report</b></p>	<p>DocID: FEND-40.02.09.00-1974-C-REP  Version: C  Date: 2023-02-07  Status: Released  Page: 47 of 105</p>
---	--	--

the front-end cryostat. This part consists of three main components: a YIG-tuned oscillator (YTO), an active multiplier chain (AMC) and a power amplifier (PA). The final part, the  $\times 9$  multiplier, is located in the Cold Cartridge Assembly (CCA) inside the front-end cryostat. It was demonstrated before [8], during the construction and technical commissioning of the SEPIA and LLAMA cartridges, that AMC, PA and multiplier are indeed usable beyond the ALMA band edges. For these two receivers, a new LO tuning range of 586–730 GHz was defined. With an IF band of 4–12 GHz, this yields an RF band of 574–742 GHz. Since the edges of this band lie deep within the pressure-broadened tails of the water vapour lines, we can state that the receiver RF bandwidth is then totally atmosphere-limited. In fact, the SEPIA660 receiver has recently been used over this extended range to perform a high-resolution study of the atmospheric transmission itself [21]. In the lab (at sea level), the absorption lines limit the measurement range to about 580–735 GHz.

It should be noted that, despite having demonstrated their performance in four cases (two CCAs with two polarizations), several components (AMC, PA, multiplier) are used outside their specified range, which could pose lifetime risks. This was in fact discussed with NRAO before extending the SEPIA and LLAMA bands, but from their side they did not foresee problems in this respect. Nevertheless, for a full upgrade, this would be good to verify further with the respective suppliers of the various components.

The remaining limit on the LO range in the Band 9 WCAs is the tuning range of the YTO, which is a commercial product (Micro Lambda Wireless, Inc., “MLW” hereafter). The tuning range, basically defined by the voltage range of the 12-bit digital-to-analog converter that drives the magnetic tuning coil for the YIG resonator, is set by the manufacturer at the time of production. The YTO currently used in the Band 9 WCAs has a tuning range of 22.5–26.45 GHz, yielding an LO range of 607.5–714.2 GHz. With a conventional IF upper limit of 12 GHz, this translates to an RF coverage of about 596–726 GHz.

The supplier, who was consulted, tells us that the YTOs can be delivered and even refurbished for an extended range. The resulting LSB step size of the DAC is still small enough to ensure capture of the PLL at any tuning frequency. This procedure was successfully applied for SEPIA660, where the YTO range was extended to 21.55–27.04 GHz, resulting in an LO range of 582–730 GHz. With an IF up to 20 GHz (section 2), this would lead to an RF range of 562–750 GHz, deep into the water absorption bands.

It should be noted that just extending the IF Band will intrinsically extend the RF Band without any LO modifications. For instance, an IF band up to 20 GHz would already widen the RF band to about 588–734 GHz.

### 3.3 Practical implications

There have been initial discussions with MLW about possible upgrading schemes for the YTOs. According to them it will not be easy to train ALMA personnel to do this during regular maintenance of the front ends. Their advice is (obviously) that it should be done by their technicians, either at the OSF or at MLW in the USA. Because of the logistical implications of an off-site upgrade, it may be worthwhile to try and re-negotiate with MLW at a later stage. Alternatively, the YTOs could be reconfigured by OSF technicians based on available reverse-engineering data (which cannot be made public, however). Since the Band 9 YTOs are long out of warranty, there is no additional risk in case of failure for reasons not related to the upgrade.

	<b>ALMA Band 9 Sideband Separating Upgrade</b> <hr/> <b>Study Report</b>	DocID: FEND-40.02.09.00-1974-C-REP Version: C Date: 2023-02-07 Status: Released Page: 48 of 105
---	---	---

If this option is not available, one possible scheme is that a small number of extra YTOs (say, 10) are purchased as exchange stock. Then, the YTOs coming out of the WCAs during the upgrade can be shipped in batches to MLW for upgrading. The exact number of required exchange-YTOs depends on the logistical scheme and the front-end service cycle. At the end of the upgrade, the left over YIGs could possibly be sold on the open market or kept as spares.

### 3.4 Costing

For reference, the cost of a new YIG oscillator is of the order of 4k€ in small quantities. The cost reduction we got quoted for 80 units of a similar type was about 10%. This number is of course not very relevant for an upgrade except for the extra exchange-stock mentioned above.

The price that the supplier<sup>3</sup> asked for the extension of the SEPIA660 YTO was EUR 526 for a single unit, which becomes EUR 470 applying the discount. It is not unlikely that for larger numbers in batches this price will go down somewhat. Assuming a price of EUR 470 per unit for 75 WCAs, this would boil down to something of the order of 35k€, plus some shipping costs, for the entire upgrade.

Note that the cost of the 10 exchange units as proposed above ( $\approx 40$  k€) exceeds the likely cost of the extension itself, if the units cannot be sold at a reasonable price.

The replacement of the YTOs in the WCAs is a pretty straightforward action, and should be easily performed at the OSF. The YTO replacement is independent of the IF chain upgrade and the warm IF infrastructure lives in a separate plate that can be swapped as one unit. Estimated work: maybe half a day per unit for the hardware replacement including administrative overhead; 1–2 days for testing and re-qualification. The latter would most conveniently be done at the OSF on a cold Band 9 CCA in a front-end cryostat.

Because the YTO frequency limits are not hard-coded into the ALMA software, but defined in XML tables, no significant software costs are expected because of the increased YTO range in itself. To actually make use of the extended LO range in observations, however, some software modification and re-qualification may be required.

---

<sup>3</sup>The Dutch representative for Micro Lambda, AR Benelux BV

	<b>ALMA Band 9 Sideband Separating Upgrade</b>	DocID: FEND-40.02.09.00-1974-C-REP Version: C
	<hr/> <b>Study Report</b>	Date: 2023-02-07 Status: Released Page: 49 of 105

## 4 Study goal 3 — Availability of SIS mixer devices

First to determine some terminology: in this section, we make a distinction between (SIS) *junctions* or *devices*, which are the quartz chips with the actual tunnel junctions plus superconducting wiring and contact pads, and (DSB) *mixers*, which are SIS junctions mounted in backpieces that can be tested in heterodyne mode. The junctions are produced on *wafers*, each containing 4 or 8 *sectors* (depending on the mask design) of 88 junctions each. About 10% of these junctions are test devices (e.g., to make accurate measurements of the wafer's  $R_N \cdot A$  product) which are not suitable for use as mixers. Sometimes the word *batch* is used synonymously with wafer. The wafers/batches are labelled with a batch number XXYY, where XX represents the mask design and YY a serial number. Within each sector, junctions are labelled SZZ, with S the sector letter (A–H) and ZZ the junction number.

For each Band 9 2SB cartridge we will need four mixers. So, for 73 cartridges, and spares for 7 more, in total we need a minimum of  $4 \times (73 + 7) = 320$  mixers for the upgrade of the ALMA Band 9 DSB cartridges to 2SB cartridges. About half of this number will be made up by re-used DSB mixers. Because of their limiting IF bandwidth, the 30 or so  $\text{AlO}_x$ -barrier mixers that exist in the current DSB array are not considered for re-use. A brief description of the conversion of a DSB mixer into a 2SB one is given in section 1.4.2.

At the moment we do not have enough mixers available for such an upgrade, but, assuming that we keep the 2SB assemblies compatible with the DSB ones, we can of course re-use part of the mixers in the ALMA cartridges and the delivered spare mixers. In addition, we have around 10 000 junctions on un-diced wafers or sectors in stock, as well as a number of mounted junctions left over from the Band 9 production phase.

The process of harvesting junctions, as was done for the current DSB Band 9 cartridges is as follows. Wafers were produced at the Technical University of Delft, and at NOVA the individual SIS junctions were diced (cut and polished to required thickness) from these wafers. To dice one sector of 88 junctions takes about 1 week (5 days). Subsequently, a DC-test is done by dip-sticking them in helium and measuring the IV curves (with and without Josephson suppression). This is a fast measurement: about 30 junctions can be tested per day, so for the entire sector this takes about 3 days. This brings the total time for dicing and DC-testing of one sector to 8 days, or an average throughput of about 55 junctions per week.

Junctions are selected based on the IV curves, where open and shorted junctions are rejected right away. The accepted junctions are then mounted in backpieces to become mixers, and placed in a mixer holder for (DSB) heterodyne noise measurement. Two mixers can be tested in one cooldown using a test-bed CCA, and a full noise measurement of the two mixers takes one day. Cooling down and warming up the receiver each take one night, and the intervening day is used to change the mixers. In total, if nothing goes wrong, a two-day cycle of mounting/replacing (day) — cooldown (night) — measurement (day) — warmup (night) can be maintained. So, in total (taking week-ends into account), we can measure the noise temperature of 10 mixers per two weeks, or an average of 5 per week.

### 4.1 Available mixers for the Band 9 2SB upgrade

Because we don't have enough mixers available right away, we made a statistical estimate of the number of junctions that can be harvested from the wafers we have in stock. There are around 10 000 SIS junctions on un-diced (or partially diced but un-measured) wafers that

	<b>ALMA Band 9 Sideband Separating Upgrade</b>	DocID: FEND-40.02.09.00-1974-C-REP Version: C
	<b>Study Report</b>	Date: 2023-02-07 Status: Released Page: 50 of 105

potentially can be used for the Band 9 upgrade.

First we estimate the yield of the selection of junctions based on the existing DC and noise measurements. The DC yield is basically a pre-selection of the junction based on the IV-curve, the final selection is based on the noise measurement. The noise must be below 168 K over the whole RF band. This is a more strict specification than the current ALMA Band 9 specification where 80% of the band should be below 168 K and the whole band below 250 K. This is to ensure that the performance will be at least as good as with the current DSB mixers, as we eliminate the worst performing mixers in the current array.

During the operations in this process, from dicing to final mounting in the backpiece, junctions may be lost for various reasons. Based on recent experience, we estimate a loss 6% of the junctions during preparation for the DC dipstick measurement, and another 5% in preparation for the noise measurement. We expect that with increasing experience these numbers will go down over time. In our records, more junctions, sometimes entire sectors, are unaccounted for. Since a large part of this is probably due to particular experiments to improve junction quality or handling procedures, this was not further taken into account in our estimates.

Table 2 shows the DC and the noise yield for all wafers from which at least 20 junctions made it to the noise measurement. There are wafers from which there is insufficient data available to calculate the yield reliably, and which therefore do not occur in this table.

With the yield from table 2 an estimation can be made on the number of mixers that could be produced from the unmeasured junctions. Table 3 shows the number of unmeasured junctions, the estimated number of mixers and the number of available mixers from the ALMA cartridges and ALMA/NOVA spares.

The total number of DC-accepted junctions is the sum of the estimated and available:

$$N_{DC,tot} = N_u \cdot Y_{DC} + N_{DC,avail}$$

The total number of noise-accepted mixers is

$$\begin{aligned} N_{n,tot} &= N_{DC,tot} \cdot Y_n + N_{n,avail} \\ &= N_u \cdot Y_{DC} \cdot Y_n + N_{DC,avail} \cdot Y_n + N_{n,avail} \end{aligned}$$

In these expressions,  $N$ 's are numbers of junctions/mixers,  $Y$ 's are yields (0–1). Subscript  $u$ : untested,  $DC$ : DC-accepted,  $n$ : noise-accepted; the rest of the subscripts are self-explanatory.

Wafer	DC				Noise			
	Acc	Rej	Lost	Yield (%)	Acc	Rej	Lost	Yield (%)
2803	75	79	10	46	24	23	2	49
2904	193	115	20	59	78	97	9	42
2906	42	12	3	74	9	11	1	43
2910	198	126	21	57	90	79	9	51
3002	39	4	3	85	4	16	1	19
3007	111	5	7	90	11	35	2	23
3201	128	17	9	83	6	34	2	14
3306	68	6	5	86	3	22	1	12

Table 2: DC and Noise yields of junctions/mixers from different wafers (Acc: accepted, Rej: rejected).

	<b>ALMA Band 9 Sideband Separating Upgrade</b>	DocID: FEND-40.02.09.00-1974-C-REP Version: C
	<b>Study Report</b>	Date: 2023-02-07 Status: Released Page: 51 of 105

Wafer	Available junctions not measured $N_u$	$Y_{DC}$	Estimate DC OK $Y_{DC}N_u$	Available DC OK	Total estimate available DC OK $N_{DC,tot}$	$Y_n$	Estimate noise OK $Y_n N_{DC,tot}$	Available noise OK	Total estimate noise OK $N_{n,tot}$
2803	169	46%	77	15	92	49%	45	18	63
2904	16	59%	9	0	9	42%	4	75	79
2906	264	74%	195	20	215	43%	92	9	101
2910	0	57%	0	15	15	51%	8	84	92
3002	580	85%	492	9	501	19%	95	4	99
3007	381	90%	344	61	405	23%	93	11	104
3201	430	83%	357	65	422	14%	60	6	66
3306	450	86%	387	30	417	12%	48	3	51
Total									655

Table 3: Total numbers of junctions per wafer, available and estimated to be available, with a noise temperature below 168 K.

Wafer	Barrier	# mixers in ALMA CCAs
2311	AlO <sub>x</sub>	18
2314	AlO <sub>x</sub>	2
2315	AlO <sub>x</sub>	10
2803	AlN	9
2904	AlN	65
2906	AlN	2
2910	AlN	24
3007	AlN	10
3201	AlN	6
Total		146

Table 4: Number of mixers, for each wafer, used in current the Band 9 DSB CCAs. The barrier technology (AlO<sub>x</sub> or AlN) is indicated.

## 4.2 Comparison of average noise with current Band 9 mixers

As an added goal, we state that the average noise temperature of available and estimated mixers should be as good as or better than the mixers in the current DSB cartridges. Table 4 shows the number of mixers per wafer in the ALMA cartridges to which the comparison will be made.

Figure 38 shows the average noise temperature and the standard deviation of the mixers in the existing ALMA Band 9 cartridges, for both AlN and AlO<sub>x</sub> mixers combined. For each mixer the noise per LO frequency was determined by averaging over 4-12 GHz IF. In figure 39, the average over the AlO<sub>x</sub> and AlN mixers is calculated separately. The difference in average noise temperature between AlO<sub>x</sub> and AlN at the lower part of the band explains the increased standard deviation visible between 614 and 638 GHz in figure 38.

To determine the average noise temperature of available and estimated mixers we calculated the average noise temperature per wafer. We ordered the average noise from low to high per wafer as shown in table 5. We also added the number of estimated and available mixers (from table 3).

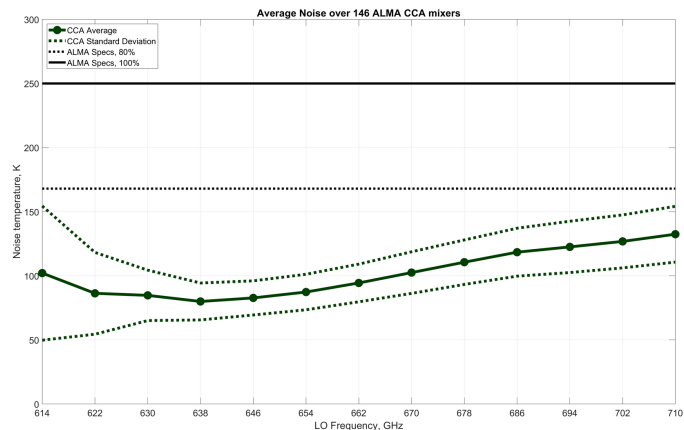


Figure 38: Average DSB noise temperature of mixers installed in the current Band 9 DSB cartridges.

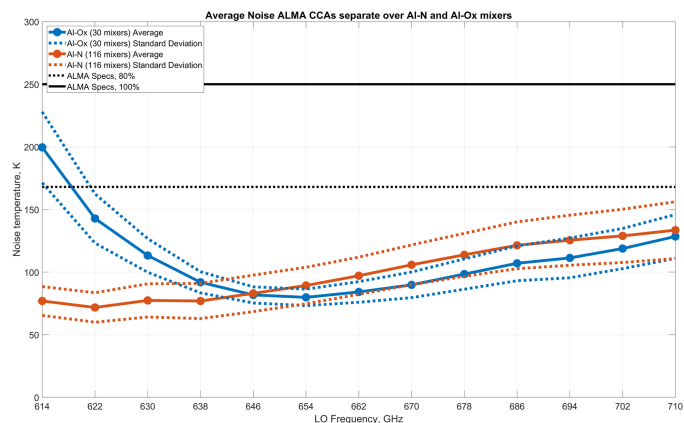


Figure 39: Average DSB noise temperature as in figure 38, but separated out for the AI<sub>O<sub>x</sub></sub> and AI<sub>N</sub> barrier mixers.

As stated before, the minimum number of mixers needed for the upgrade is  $4 \times (73 + 7) = 320$ . However, for an optimum image rejection ratio, the mixers need to be matched on several aspects. A very rough assumption is that we need 50% extra mixers for matching. This means we would need  $320 \times 1.5 = 480$  mixers.

To get the minimum needed number of 320 mixers with the lowest noise we use table 5. We need all the junctions from wafers 2803, 2906, 2904 and 77 junctions from wafer 2910. Additionally, to get the estimated number of 480 mixers for matching, we use all the junctions from wafers 2803, 2906, 2904, 2910, 3002 and 46 from wafer 3306.

The average noise ( $\overline{T}_n$ ) of the estimated+available mixers is calculated as follows:

$$\overline{T}_n = \frac{N_A \cdot \overline{T}_{n,A} + N_B \cdot \overline{T}_{n,B} + \dots}{N_A + N_B + \dots},$$

where  $N_A$  is the number of mixers from wafer A and  $\overline{T}_{n,A}$  the average noise from the selected



Wafer	Average Noise (K)	Available and estimated Noise-accepted mixers
2803	86	63
2906	97	101
2904	100	79
2910	102	92
3002	104	99
3306	112	51
3007	115	104
3201	121	66

Table 5: Wafers sorted by increasing average noise temperature, and the total number of available and estimated mixers.

mixers of wafer A; similarly for B, etc.

The standard deviation of the noise temperature  $\sigma T_n$  is calculated by

$$\sigma T_n = \frac{\sqrt{(N_A \cdot \sigma T_{n,A})^2 + (N_B \cdot \sigma T_{n,B})^2 + \dots}}{N_A + N_B + \dots},$$

where  $\sigma T_{n,A}$  is the standard deviation of the noise from the selected mixers of wafer A, etc.

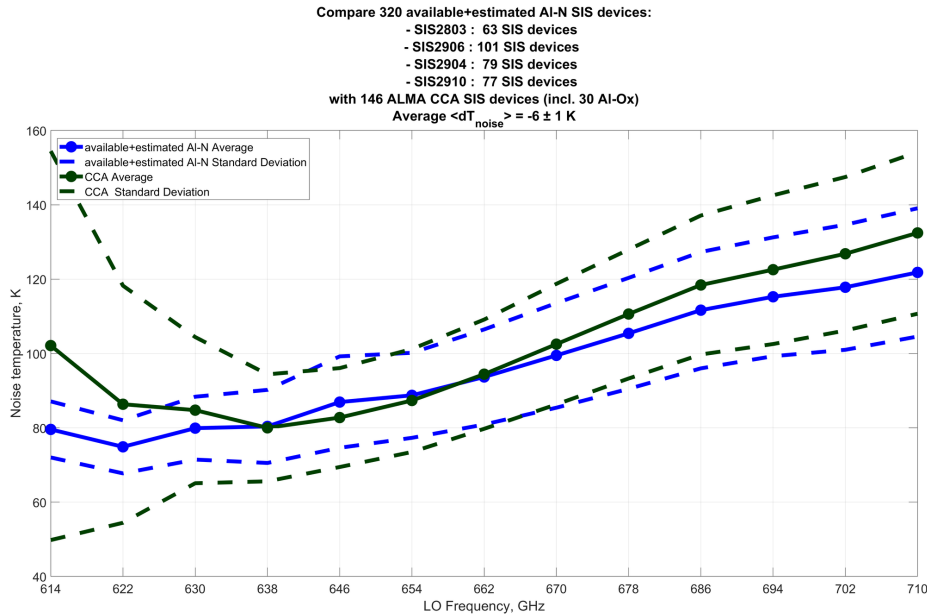


Figure 40: Average Noise temperature of 320 available and estimated mixers compared to the Band 9 cartridge average.

Figure 40 shows the average and standard deviation of the noise for the minimum number of mixers needed for the upgrade compared with the mixers from the existing Band 9 CCAs. A complete replacement of the remaining AIO<sub>x</sub> devices with AlN ones (both because of their limited IF bandwidth and “naturally” because of a generally higher noise temperature) has been taken into account here. Figure 41 shows the same for the estimated 480 mixers needed when the 50% overhead for 2SB pairing is taken into account.

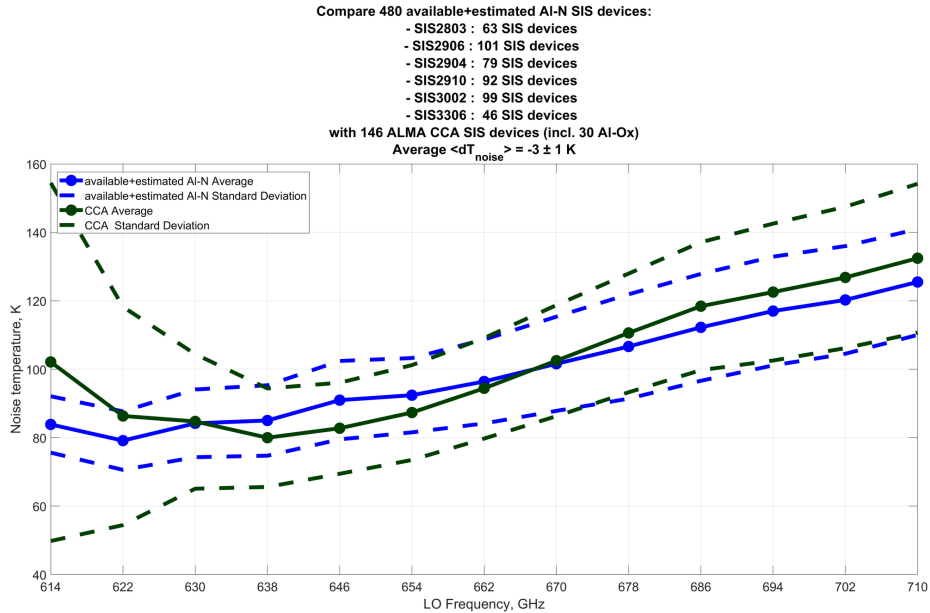


Figure 41: Average Noise temperature of 480 available and estimated mixers compared to the ALMA Cartridge average.

The conclusion is that we estimate to have a sufficient number of available mixers and usable SIS junctions in stock. For the worst case where we need the full 480 mixers for image rejection matching, the estimated average DSB noise temperature is 3 K lower than the mixers of the current DSB cartridges. In case the minimum needed 320 mixers is sufficient, the average noise temperature is estimated to be 6 K lower. Note that these are (equivalent) DSB noise temperatures, and extra loss due to the RF hybrid structure is not taken into account.

### 4.3 Estimation of the time needed for harvesting

Here an estimate will be made on the time needed for harvesting the 320 and 480 mixers as described in the previous chapter. This estimate is based on the availability of one test system for noise measurement.

Table 6, based on tables 3 and 5, shows the estimated harvesting times. Only the wafers needed to harvest up to 480 mixers are shown, and ordered by increasing average noise temperature as previously in table 5. As discussed before, the dicing and DC-testing have a combined throughput of about 55 junctions per week, the noise testing 5 mixers per week.

From this table we can conclude that harvesting the 320 mixers will take  $21 + 48 + 2 + (77/92) \cdot 3 \approx 74$  weeks, or roughly one and a half year. Harvesting the full 480 mixers will take  $21 + 48 + 2 + 3 + 111 + (46/61) \cdot 92 \approx 254$  weeks, roughly five years.

It is possible that in the future we can improve the pre-selection based on the IV-curves which will increase the yield of the noise measurements, which will in turn decrease the harvesting time.

	<b>ALMA Band 9 Sideband Separating Upgrade</b>	DocID: FEND-40.02.09.00-1974-C-REP Version: C
	<b>Study Report</b>	Date: 2023-02-07 Status: Released Page: 55 of 105

Wafer	Available mixers not measured $N_u$	Harvest time DC (weeks)	Total estimate available DC OK $N_{DC,tot}$	Harvest time noise (weeks)	Total estimate available noise OK $N_{n,tot}$	Total harvest time (weeks)
2803	169	3.1	92	18.4	63	21
2906	264	4.8	215	43.0	101	48
2904	16	0.3	9	1.8	79	2
2910	0	0.0	15	3.0	92	3
3002	580	10.5	501	100.2	99	111
3306	450	8.2	417	83.4	61	92

Table 6: Estimated harvesting times per wafer.

#### 4.4 Estimation of the time needed for pairing

Apart from the time that is estimated here for finding a sufficient number of DSB mixers to construct the 2SB mixer assemblies, the pairing process itself will also take time. How much this will be is not quite certain yet. From our experience with SEPIA and LLAMA we probably already can make decent (initial) pairings based on the DSB data, before doing actual 2SB measurements. A very rough estimate is that we need 30% overhead. This number is likely to go down as we gain experience during the production. The pairing will be part of the total CCA qualification test campaign, as, upon finding a pair with good IRR, other key parameters like stability have to be verified as well.

#### 4.5 Summary

For the band 9 2SB upgrade we need 320 pair-matched DSB mixers. For the matching, needed to optimize the image rejection ratio, we expect to need up to 50% more, i.e., a worst-case maximum of 480. The actual number needed for the upgrade will most likely be in between these two extremes. We intend to re-use as many of the AlN-barrier mixers from the existing DSB Band 9 cartridges as possible, as well as the delivered spares. Besides that, we will have to produce new mixers. We expect that our current stock of SIS junctions is just enough to achieve this with an average noise temperature very close to the current average in the Band 9 array.

Harvesting extra junctions to get a total of 320 mixers is estimated to take about one year and a half of testing. This is the best case where all mixers can be paired for good image rejection with no left-overs. The average (equivalent DSB) noise temperature of the resulting array is then expected to be 6K lower than with the current mixers in the ALMA cartridges. In the estimated worst case of 50% dropout due to pairing, harvesting the extra required junctions to get a total of 480 DSB mixers will take about five years of testing. In this case, with the current knowledge of the expected individual mixer noise temperatures, the average noise temperature of the resulting array will be about 3K lower than with the current mixers in the DSB cartridges. The estimated resulting noise temperatures do not take into account the extra waveguide losses due to the 2SB structures. These waveguide losses are of the order of 10–15% for the current 2SB blocks.

The estimates of the throughput time presented here are based on the use of one test system.

	<b>ALMA Band 9 Sideband Separating Upgrade</b> <hr/> <b>Study Report</b>	DocID: FEND-40.02.09.00-1974-C-REP Version: C Date: 2023-02-07 Status: Released Page: 56 of 105
---	---	---

When two (or even more) setups can be run in parallel, the total end-to-end time can be reduced accordingly, given sufficient FTEs.

## 4.6 The search for the Golden Wafer

On several occasions, including the mid-term review, a strong desire was expressed to investigate the chances of significantly improving on the current array noise temperature. For this to happen (without production of new, improved junctions), a currently hidden and overlooked supply of “golden junctions” would have to be found in our existing stock. Although we considered the probability of this not very high, we did agree to perform a limited investigation of this.

### 4.6.1 Statistical analysis of I-V curves

As a first step, we managed to obtain a full data dump (about 12000 files) of *all* historical SIS measurement data from the Technical University of Delft, salvaged from an abandoned measurement computer. This consist mainly of sector test data, which are I-V curves obtained from a subset (about one in ten) of the SIS devices on each sector that have special outside connections on the sector edge. The great advantage of the sector test data is that it can be obtained without the laborious process of dicing and polishing the sector into individual junctions. The test junctions themselves are not usable in operational mixers, but are intended to assess the overall quality and health of the wafer. The main added value of this archive is that it contains data of wafers that, for some reason or other, were not measured in detail in Groningen.

A preliminary look at this data suggested that using it for pre-selection of promising wafers is feasible. Because of the sheer volume, some form of automation was required to extract the most relevant parameters (e.g., the gap voltage, the normal-state resistance and the leakage current). On the other hand, it was also clear that the Delft data are not as complete as we would like. A small number of wafers (order of five) was lacking any kind of I-V data.

A statistical analysis of the combined Delft-Groningen I-V data was performed to try and find a set of criteria, or at least a ranking, for the prediction of good noise temperature. Since the data set consists of a huge number of curves, an automatic fitting and ranking procedure was developed, described in some detail in Appendix A. To our disappointment, but hardly against expectation, no wafers jumped out as candidates for overall noise-improvement of the array. Despite the great pressure at the time of Band 9 production, we apparently were still quite effective in mining out the best wafers, as all “promising” candidates have largely been used already.

### 4.6.2 Measurement of additional unknown junctions

Since, as just mentioned, no wafer that was not characterised earlier showed high promise of significantly improved noise temperatures, as a last-ditch effort we started processing the few wafers of which no heterodyne data was available at all. One of the most interesting was SIS2804, which was manufactured right after SIS2803. The latter batch, although produced for development rather than production, yielded some of the lowest noise temperatures ever observed in a Band 9 junction (down to about 60 K). Like SIS2803, SIS2804 also had production

	<b>ALMA Band 9 Sideband Separating Upgrade</b> — <b>Study Report</b>	DocID: FEND-40.02.09.00-1974-C-REP Version: C Date: 2023-02-07 Status: Released Page: 57 of 105
---	--	---

issues (bad adhesion of gold films, etc.). Nevertheless, one sector was diced and polished, and the I-V curves measured by dipstick. Unfortunately, out of 15 junctions, only one showed a recognizable I-V curve, and with very bad parameters. Based on this result, this particular batch can be written off. Besides this experimental batch, two others, SIS2911 (the companion of the highly successful SIS2910 batch) and SIS3001 (one of the early full-production batches) were diced and dip-sticked, without any positive result. Testing of the last one or two unknown candidates was cut short by a fatal breakdown of our dicing machine, and since the probability of finding the “golden batch” among them is microscopic anyway, we decided that this thread of investigation was hereby concluded.

	<b>ALMA Band 9 Sideband Separating Upgrade</b>	DocID: FEND-40.02.09.00-1974-C-REP Version: C
	<b>Study Report</b>	Date: 2023-02-07 Status: Released Page: 58 of 105

## 5 Study goal 4 — Improving the polarization purity

As mentioned before, the cross-polar performance of existing Band 9 receivers could be improved (current spec is  $-17$  dB). In addition to a relatively large beam squint, as will be discussed below, this leads to an on-sky performance that is not really suitable for extended-source polarimetry. We try to touch upon two questions here: is polarimetry in Band 9 scientifically desirable, and what should happen to make Band 9 proficient at polarimetric observations?

To a certain degree there seems to be a chicken-and-egg situation here, as there are hardly any facilities in the world (probably none, actually), including ALMA, that *can* do polarimetry on extended sources at these frequencies. This also means that compelling science cases will rarely be considered by the community. It is very well conceivable that any offer of this capability may bootstrap the interest in it.

### 5.1 Scientific rationale

The ESAC recently considered the case of polarimetry in Band 9 and reported on it. Unfortunately, this report is not public, so we can not quote from it at this point. In one of the progress meetings, Ciska Kemper (ESO) summarised the main science cases that were identified as follows:

- The study of magnetic fields in very dense environments of circumstellar envelopes around evolved stars and high mass star-forming regions through the vibrationally excited water maser line at 658 GHz (a unique feature of Band 9).
- The study of dust polarization at high frequency, in combination with similar measurements at low frequency (ultimately in Band 1), provides a powerful tool to constrain the sizes of dust grains, and thus to study processes such as dust settling and grain growth in protoplanetary disks around young stellar objects.

We expect that more use cases will come up once enhanced polarimetry capabilities are established. For the time being, we interpret this as a serious interest from the user community.

### 5.2 Technical issues

During the June and July 2020 progress meetings, Neil Phillips (ESO) presented the eye-opening insight that for wide-field polarimetric observations in ALMA (or any other similar instrument), the limiting factor in most cases is actually the beam squint rather than the polarization purity of the receiver itself. The two reports he presented are included in appendix B. Briefly summarized, there is a clear distinction between the beam squints of the ALMA bands with grids for polarization-splitting (bands 7, 9 and 10), and the other bands that employ OMTs (which we will call the “single-horn architecture”), where the former are worse by at least an order of magnitude.

As demonstrated below, unless the alignment accuracy (and probably the mechanical stability) of the grids can be improved drastically, it seems that the key to wide-field polarimetry is the single-horn architecture, which implies the use of an OMT. The downside of this is that OMTs in waveguide technology are certainly not lossless, if only due to the relatively long waveguide runs required for interfacing them with the mixer blocks. To get an idea of the noise temperature trade-off involved, we both measured the transmission loss in a traditional

	ALMA Band 9 Sideband Separating Upgrade	DocID: FEND-40.02.09.00-1974-C-REP
	—	Version: C
	Study Report	Date: 2023-02-07
		Status: Released
		Page: 59 of 105

Band 9 grid and made a simple straw-man design of two Band 9 2SB mixers coupled to a minimal-sized OMT.

As an alternative, we investigated the possibility of improving the beam squint by narrowing the tolerances on the grid's orientation. For this, we set up an electromagnetic model of the existing Band 9 optics using the GRASP software, which allows us to simulate the cross-polar and aberration performance of the system, the impact of the grid on these, and the expected beam squint when we introduce inaccuracies in the alignment of the grid.

### 5.3 Electromagnetic modelling of the Band 9 optics

The electromagnetic model has been implemented according to the values reported in Ref. [22] and it includes two feedhorns, three ellipsoidal mirrors (M3, M4 and M4') and the polarization grid, as shown in Fig. 42. The sky signal is incident on the M3 reflector with an off-set angle of  $0.974^\circ$  relative to the central telescope axis, due to the off-axis position of the Band 9 cartridge window on the ALMA cryostat. The grid works in transmission for the P1 beam (pink rays) and in reflection for the P0 beam (light blue rays). The two polarization branches are identical, but rotated relative to the point of beam incidence on the grid by  $125^\circ$ . The LO beams for each polarisation are coupled to the respective feed horns using a  $45^\circ$  beam splitter placed between the M4 reflectors and the feedhorns. The beam splitters and LO optics are not considered in the analysis presented hereafter. Each feedhorn is modelled as a hybrid-mode feedhorn based on the values from the drawings. This is a good approximation to the actual corrugated horn. The mirrors shape is defined by the mechanical drawings assuming the values for the cold structure. The grid is modelled as a regular grid of conducting parallel wires.

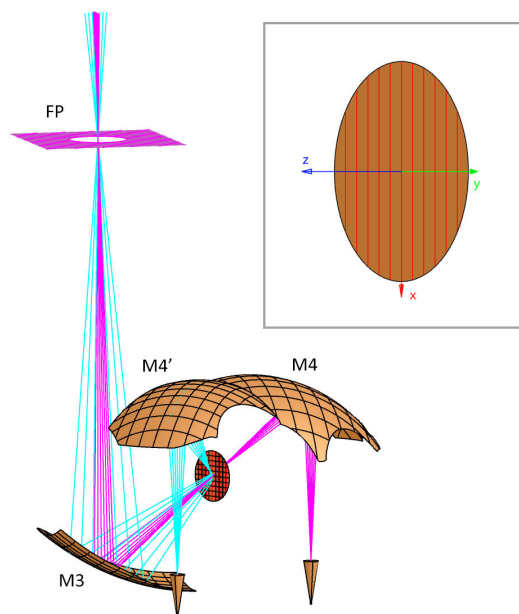


Figure 42: Model of the Band 9 optics as implemented in GRASP. Light blue rays represent polarization P0, which is reflected by the grid. Pink rays represent polarization P1, which is transmitted by the wire grid. The top-right panel shows an enlargement of the polarizing grid with its reference coordinate system.

	<b>ALMA Band 9 Sideband Separating Upgrade</b>	DocID: FEND-40.02.09.00-1974-C-REP Version: C
	<b>Study Report</b>	Date: 2023-02-07 Status: Released Page: 60 of 105

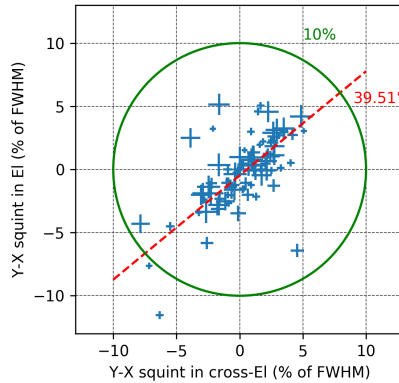


Figure 43: On-sky Y-X polarisation beam squint in cross-elevation vs. elevation coordinates in units of the beam FWHM at 661 GHz. The 10% limit is shown as a green circle and the red line is the fit to the measured data, which highlights a preferred angle of about  $39.5^\circ$ .

## 5.4 Simulation of the beam squint

The Band 9 dual orthogonally polarised beams are divided using a wire grid. As described in section 5.3, the two beams follow separate paths from the grid to the related feedhorn. Displacement of the optical components can cause a beam squint between the two main beams on the sky, potentially affecting the receivers calibration procedure as discussed in Appendix B.1. The report in the Appendix shows also that the beam squint for OMT-based bands is generally within 2%, while the current configuration of Band 9 with the wire grid has a larger scatter. In addition, the on-sky beam squint for Band 9 shows a preferred direction. Fitting the data with a straight line, we find an angle of  $\sim 39.5^\circ$  (see figure 43).

Since the inaccuracy in the mounting of the grid could be one of the causes of the scatter, we tried to reproduce this effect using the GRASP model to simulate the squint. We computed the beam squint in the focal plane for a random tilt of the grid around the  $x$  and  $y$  axes shown in figure 42 and we quantified the offset of the beam in the focal plane to make a comparison with measured data. We assumed two independent gaussian distributions for the tilt in the two perpendicular directions, which makes sense since the sources of these tilts are almost totally decoupled due to the mechanical construction. In order to find the best description to the measured data, we repeated the same simulation changing the values of the standard deviation of the two gaussian distributions (see figure 44).

By optimizing the values of the two independent standard deviations to match the data, we found that a gaussian distribution with a standard deviation  $\sigma_\theta = 0.28^\circ$  in one direction and  $\sigma_\phi = 0.19^\circ$  in the orthogonal one can give a similar scatter of the beam squint, as shown in figure 45. Therefore, inaccuracies in the grid mounting could be responsible for the observed beam squint scatter.

Nevertheless, an angle of  $0.25^\circ$  transposed to the size of the grid, whose diameter is 17.5 mm, means an accuracy of  $20 \mu\text{m}$  per side, which is the tolerance of the grid clamps. This uncertainty could be also an error of the grid foil mounting angle in its frame. In both cases, it is very challenging to obtain a significant improvement by requiring tighter tolerances, especially if we want to reuse these components. Since the observed beam squint remains stable with



Figure 44: Simulation of the beam squint in azimuth-elevation coordinates in units of the beam FWHM at 661 GHz. Each plot corresponds to a different set of values for the standard deviation of the gaussian distributions which describes the tilt of the grid in the two perpendicular directions. Blue dots represent the measured data, red dots are the results of the simulations and the green line is the fit to the simulated data. The inclination of this line can be compared to the one of the measurement, i.e.,  $39.5^\circ$ .

time (according to the measurements over several years), we could consider shimming the grid holder to achieve the beam coalignment as shown in figure 46. The initial shim foil thicknesses can be obtained from measurements done by using the established model. In this way the beam squint can be practically corrected at an upgrade stage. This single-shot adjustment will need to be verified experimentally, of course. A potential risk of such procedure would be an additional shimming attempt and beam pattern measurement, which would be needed if the required accuracy can not be achieved during the first attempt. This extra qualification time should be budgeted in the preparation for a possible upgrade program.

A complication is the observed level of correspondence between the beam squint values obtained

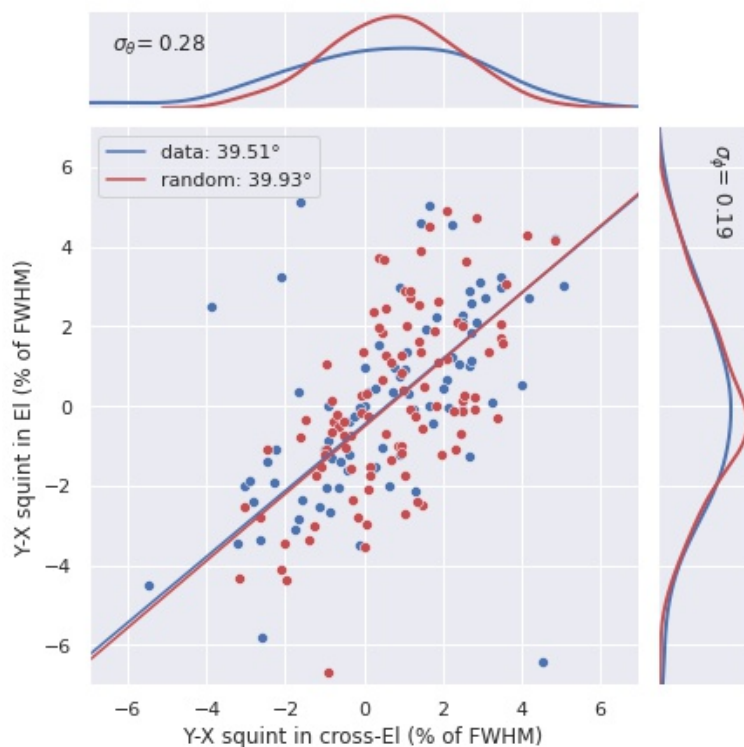


Figure 45: Comparison of the measured and simulated on-sky polarization beam squint. Blue dots are the data from Appendix B.2, while red dots are the results of the simulations with a random tilt with a gaussian distribution in the two orthogonal directions with  $\sigma_\theta = 0.28^\circ$  in one direction and  $\sigma_\phi = 0.19^\circ$ . Both measurements and simulation data have been fitted with a straight line to compare the direction of the beam squint in the sky.

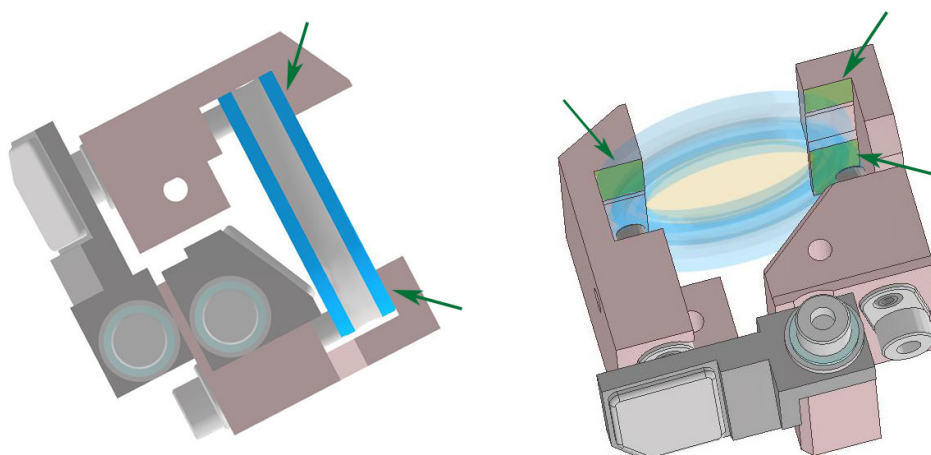


Figure 46: Views of the model drawing of the grid and its holder. The green arrows indicate where the shimming could be done.

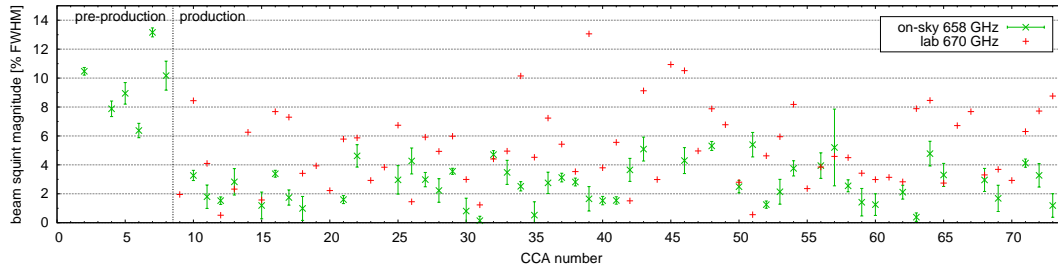


Figure 47: Comparison of the beam squints (as percentage of the beam FWHM diameter) of the deployed Band 9 receivers, derived from near field lab data (red +es) and from on-sky measurements (green ×-es). Figure and data processing courtesy Neil Phillips, ESO.

in the lab (from near-field beam-pattern measurements) and those found on-sky. Figure 47 shows these two data sets for the currently operating Band 9 receivers. It is clear that the correlation is sub-optimal, to say the least. Since the confidence of the on-sky data is quantified (see error bars in the plot), apparently the uncertainty is in the lab results. For the latter, several data processing methods were tried in the past, but the one used in the end for receiver qualification, although it clearly does not *underestimate* the beam squint, is probably not the best for the quantitative accuracy needed for shimming. If any attempt along this direction is to be pursued, the first priority should be to obtain a better correspondence here.

In addition to the grid tilt, we also modelled the effect of a rotation of the upper and lower mirrors blocks with respect to each other around their mutual alignment pin. This is one of the obvious and straightforward errors that could have crept into the optics block production. Since this is a one-dimensional source of error, it gives in first approximation a straight error pattern on the sky. Without showing this result in detail, we simply state that the resulting on-sky projection is not compatible with the observations at all, and can therefore be ruled out.

There are of course more complicated aberrations possible in the mirror surfaces machined in the blocks. In principle these could be analysed, as mechanical probe measurements are available for all blocks. However, we found it very hard in the past to link these probe reports to actual aberration of the surfaces, although they turned out to be quite usable for pass/reject workmanship qualification. Since an investigation like this is actually not going to answer the central question in this study goal, we will leave it at that.

## 5.5 Simulation of the cross-polarization performance

Using the electromagnetic model of Band 9, we tried to quantify the improvement in the cross-polarization performance by changing the way in which polarization separation is performed, i.e., by removing the grid and using an orthomode transducer (OMT) to separate the two orthogonal polarizations. This means considering only the straight, transmitted branch without the grid (P1 in figure 42).

We started the analysis considering the nominal optics to determine the reference cross-polarization level. We performed main beam simulations using Physical Optics (PO) and Physical Theory of Diffraction (PTD) on all the reflectors. Physical optics is a method that gives an approximation to the surface currents and is valid for perfectly conducting scatterers,

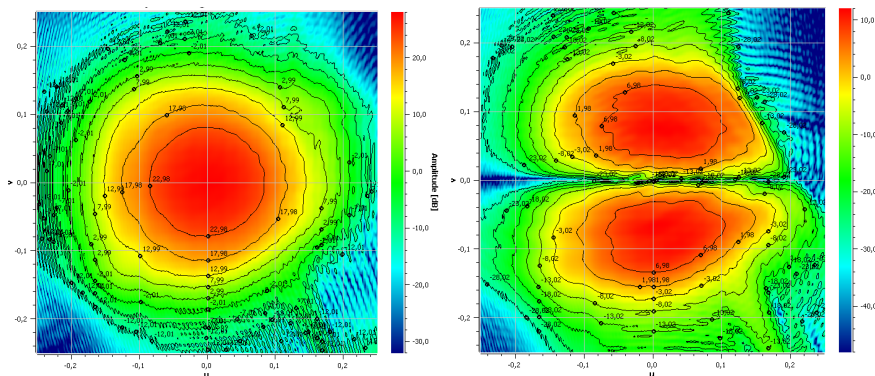


Figure 48: Co-polar (left) and cross-polar (right) beam computed in the far-field at 661 GHz.

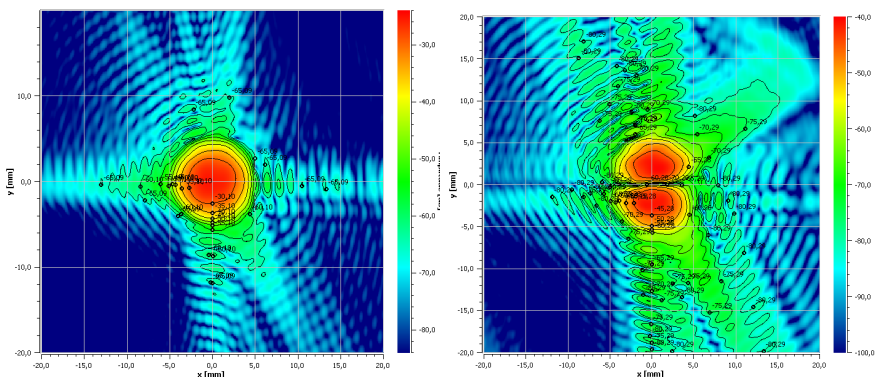


Figure 49: Co-polar (left) and cross-polar (right) beam computed in the focal plane at 661 GHz.

which are large in terms of wavelengths. The induced currents are then used to evaluate the total radiated field. This method is the most accurate to predict beams propagating from reflector antenna systems and it may be used in all angular regions of the space surrounding the system. Figure 48 shows the co-polar and cross-polar components of the far-field computed at 661 GHz, while Fig. 49 shows the same components of the field computed in the focal plane. All the beams have been simulated without taking into account the infrared filters and cryostat window apertures, which may modify the beam shape far away from the pointing direction. Figure 50 shows the two orthogonal cuts of the P0 (reflected) and P1 (transmitted) polarisation beams at the same measurement location, i.e., in the focal plane.

Since the available measurements of the cross-polarization level are integrated values, we integrated the map shown in Fig. 49 to get the comparison. The measured and simulated values are very close to each other, with a value of  $\sim -17$  dB, which gives a check of the validity of the electromagnetic model.

Then we repeated the simulations removing the grid from the model to get an idea of the best cross-polarization obtainable with the existing optics when this is re-used in a single-horn configuration. With this configuration we get a cross-polarization level of  $\sim -23.8$  dB, i.e., within the original specification established for most ALMA bands. This result includes only the influence of the mirrors and feedhorns and does not include other components of the signal chain such as IR filters and vacuum window, which can potentially contribute to the final system cross polarization value as well.



	<b>ALMA Band 9 Sideband Separating Upgrade</b>	DocID: FEND-40.02.09.00-1974-C-REP Version: C
	<b>Study Report</b>	Date: 2023-02-07 Status: Released Page: 66 of 105

For comparison within ALMA, the closest band that uses an OMT is Band 8 (385–500 GHz), built by NAOJ in Japan [24]. The basic OMT structure is very similar to the Band 5 one, which should not come as a surprise since both are derived from the Band 4 OMT [23]. The scaling ratio between Band 9 and Band 8 is about 1:1.5. The polarization requirements for Band 8 [25] are

- –18 dB over 70% of the frequency range, and
- –17 dB over the rest of the band.

Sampling a couple of Band 8 test reports, it seems that the actual obtained performance was typically in the –18 to –20 dB range. This should be considered a remarkable feat, since the Band 8 OMT, which is integrated with one of the RF hybrids, is highly complex. The geometrical tolerances specified for the waveguide structures are  $\pm 5 \mu\text{m}$ , which is the same number as in the Band 5 OMT. Considering that the Band 5 cartridges typically reached their cross-pol spec (–23 dB) while the waveguides being about two times larger, this suggests that the obtainable cross-pol level indeed scales more or less with the relative machining tolerances. Note that in both cases this also includes effects of the optics (the Band 5 OMTs by themselves obtained typically 26–27 dB cross-pol, for instance).

Summarizing, we can state that further scaling of the Band 8 OMT to Band 9 dimensions is probably an option. However, to reach a polarization purity of 23 dB or better, the tolerances should be significantly tightened, and the design is complex. In addition to that, the long waveguide runs intrinsic in the design will not help keeping the noise temperature down.

### 5.6.1 Proposition: Dunning’s OMT

Several discussions on the manufacturability of OMTs were held with RPG, part of the Rohde & Schwarz company, who manufactured the Band 5 OMTs and hybrid blocks, as well as the band 9 corrugated horns and one of the Band 9 prototype RF hybrid blocks.

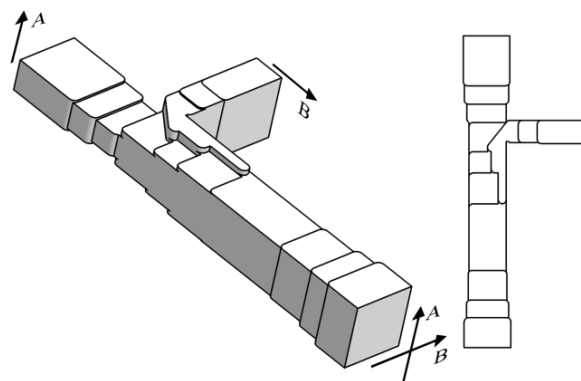


Figure 52: Structure of the OMT by Dunning, Srikanth and Kerr. Image from [26].

During one discussion about the feasibility of scaling a Band 5 OMT to Band 9 size, Bertrand Thomas of RPG pointed us to a very interesting design presented by Dunning, Srikanth and Kerr at the ISSTT in 2009 [26], shown in figure 52. Although this design (“Dunning architecture”) certainly has its own fabrication challenges when scaled to Band 9 (it was designed and tested for the WR10 band), it has certain features which make it attractive in our case. Its main advantage is that it does not rely on the recombination of two waveguides on either side

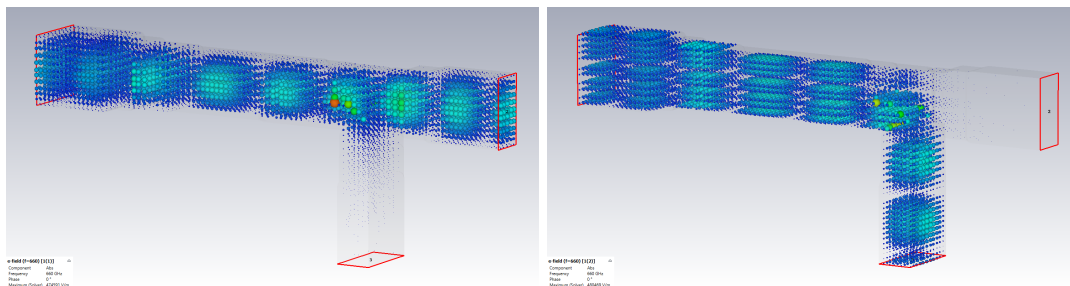


Figure 53: Simulated E-field distribution in the Dunning OMT for horizontal (left) and vertical (right) input polarization. The input (port 1) is on the left in each case, and the two outputs on the right (port 2) and the bottom (port 3).

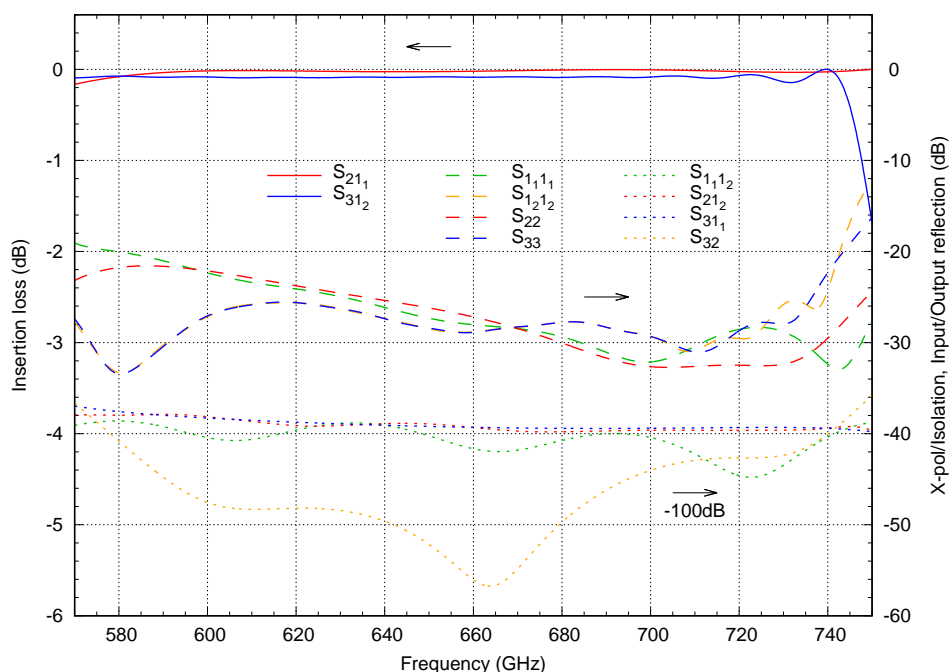


Figure 54: Simulated S-parameters of the Dunning OMT. The solid lines are the co-polar transmissions (i.e., the insertion losses), the dashed lines the return losses, and the dotted lines (offset by 100 dB) the cross-pol and isolation factors. Ports:  $1_1$  input H,  $1_2$  input V, 2 output H (straight), 3 output V (side). This is a simulation of the ideal structure; neither tolerances nor material losses were taken into account.

of a septum, as in the Band 4/5/8 OMT. This means that the long waveguide runs needed to bring the two sides together can be avoided. Actually, the Dunning OMT looks pretty much like a minimum-length T-splitter, and a more compact design can hardly be imagined. Since waveguide losses are the main argument against using an OMT at our frequencies, a design like this seems a good candidate for a Band 9 single-horn architecture.

Some initial simulations were performed, using an ideal (tolerance-free) structure made of perfect metal. This to verify understanding of the structure, and as a precursor to future studies on, e.g., sensitivity to tolerances and material losses. Figures 53 and 54 show images of the fields propagating through the structure and a set of representative S-parameters, respectively;

	<b>ALMA Band 9 Sideband Separating Upgrade</b>	DocID: FEND-40.02.09.00-1974-C-REP
	<b>Study Report</b>	Version: C
		Date: 2023-02-07
		Status: Released Page: 68 of 105

see captions for more details. Apart from noting that the device clearly acts as an OMT, we like to defer further investigation to a future study.

Manufacturability of an OMT like this at Band 9 size is still far from trivial, as tolerances of the order of  $2\ \mu\text{m}$  are likely to be needed. As can be expected, the people at RPG are cautious but not without hope that this could be achieved.

### 5.6.2 Straw-man single-horn design

To estimate how compact the outer envelope of the Dunning OMT could be made, a little packing-exercise was performed. Figures 55 and 56 show two SEPIA-style 2SB mixers packed closely around a block that is supposed to contain the OMT. The in-plane dimensions of the block as shown are  $12\times 12\ \text{mm}$ . The OMT structure itself, scaled to Band 9, is only about 2 mm long, so the limiting factor is the space needed for interfacing. Clearly, with their current envelope, the two mixer block interfere with each other, and the mechanical interfacing will be a challenge. On the other hand, at this distance, none of the crucial parts (e.g., the backpieces and magnetic conductors) are intersecting, and we are confident that with a careful redesign of the mixer envelope a packing like this (possibly down to  $10\times 10\ \text{mm}$ ) should be possible.

Of course, other geometries can be envisioned. A bit more complicated but maybe attractive option is to integrate a  $90^\circ$  twist in the straight output waveguide (which in the simple case has an unfavourable split in the H-plane) right after the OMT structure itself. This would actually cause more problematic interference of the mixer blocks, but if this is combined with

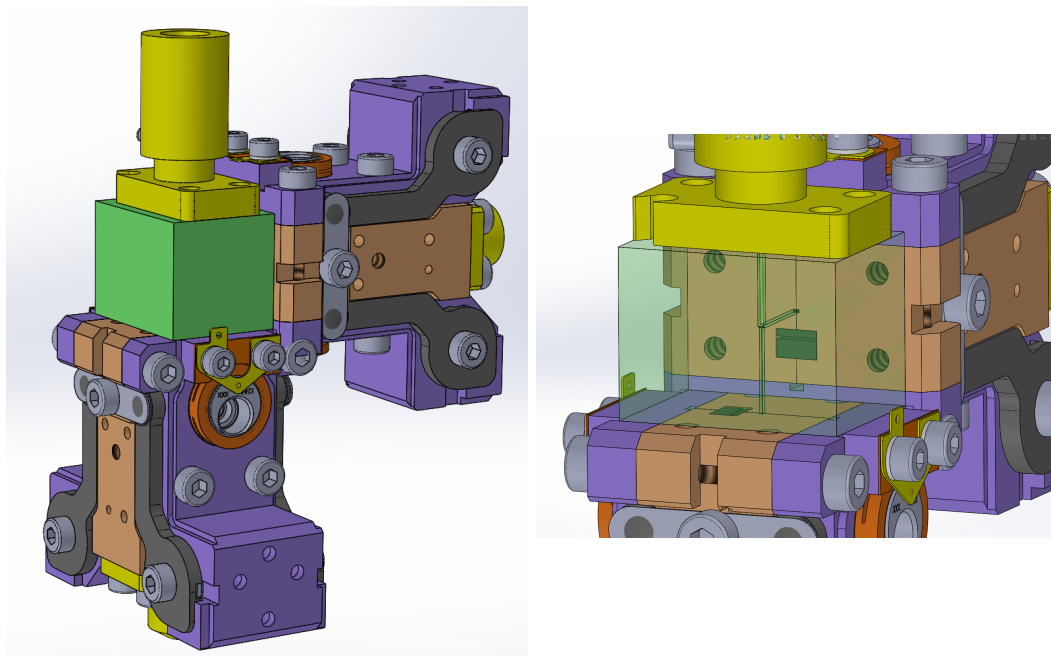


Figure 55: The basic geometry of two SEPIA Band 9 2SB mixers around a block (green) that could contain a Dunning-type OMT. On the right a detail showing the basic waveguide runs. The OMT structure itself is not drawn, but since it will be about 2 mm long, it will certainly fit in a block like this. The split will be in the vertical plane.

	<b>ALMA Band 9 Sideband Separating Upgrade</b>	DocID: FEND-40.02.09.00-1974-C-REP Version: C
	<b>Study Report</b>	Date: 2023-02-07 Status: Released Page: 69 of 105

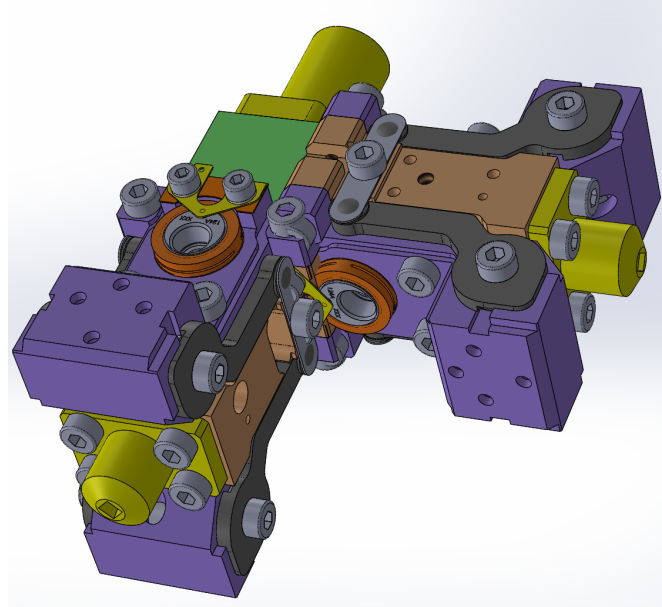


Figure 56: A view of the straw-man single-horn assembly from below, showing that, although there are some intersections, no vital parts (backpieces, magnet conductors, etc.) are interfering in a fundamental way.

a bend, the two mixers would diametrically oppose each other. This could also facilitate LO injection because of the much higher symmetry.

The extra waveguide length introduced would anyway be 10–12 mm, giving an estimated loss of roughly 0.4–0.5 dB [27], corresponding to 9–13 K for 100–120 K mixers. Although clearly higher than the losses in a grid (see section 5.7), this is not so far off the mark to dismiss it out of hand. According to the authors, this OMT has a polarization purity of better than 37 dB, assuming perfect manufacturing. A simple two-mirror optical configuration with small bending angles and slow surfaces, like in Band 5, would keep the added cross-polar in front of the OMT low.

A very preliminary EM simulation has been set up and run already, using the dimensions from the paper. This more or less reproduces the findings of the authors. The challenge will be to adapt the design to the Band 9 waveguide size, which is larger than usual (i.e., the upper limit of the band is quite close to the second-mode cutoff at 750 GHz). This large size was chosen to minimize waveguide losses, but they could also easily lead to trapped modes as soon as the structure deviates from a straight waveguide.

## 5.7 Measurement of grid losses

Any estimate of extra losses introduced by a waveguide OMT should of course be weighed against the losses currently introduced by the polarization grid. The Band 9 grids were manufactured by QMC Instruments Ltd. (UK) and consist of thin copper lines (width  $10\ \mu\text{m}$ , pitch  $20\ \mu\text{m}$ ) photolithographically deposited on thin ( $\approx 1\ \mu\text{m}$ ) PET film. To determine their loss, we performed a simple measurement: the noise temperature of a representative mixer was measured in a DSB Band 9 cartridge in polarization 1 (the one transmitted through the

grid) both with and without the grid present. The results are presented in figures 57 and 58. Although the mixer misbehaves a bit at a couple of LO frequencies, there is a rather consistent increase in the DSB noise temperature by 3–4 K caused by the grid. Considering an average DSB noise temperature of 120 K, this corresponding to a loss of, say, 0.1 to 0.15 dB. Reflection measurements were not performed (technically more difficult as the grid has to be replaced by a mirror), but we do not expect significant differences there.

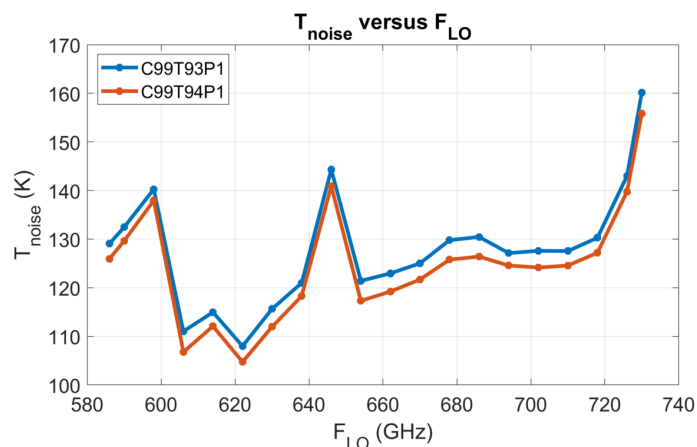


Figure 57: Noise temperature of an arbitrary Band 9 mixer measured with and without the polarization grid.

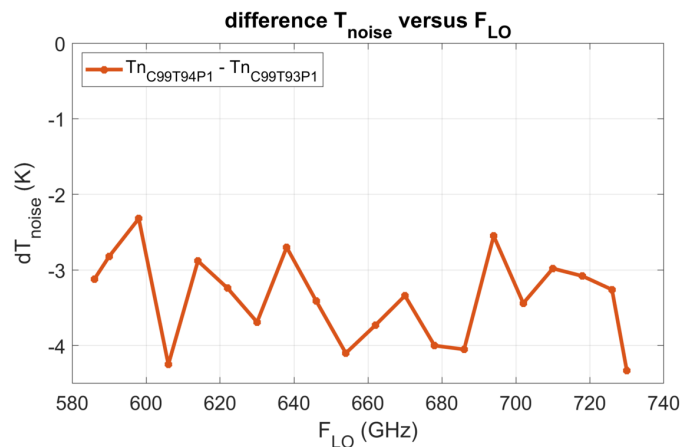


Figure 58: Difference between the measurement with and without the grid.

## 5.8 Achievable cross-polar level with existing Band 9 optics

Although the existing two-mirror configuration itself is designed to correct cross-polar contributions between the two mirrors, the actual insertion of the grid in between breaks this compensation. One question when going to a single-horn architecture is whether the existing optics *without grid* is good enough to obtain an in-spec cross-polar level, assuming a high-quality OMT.

For this we performed a cross-polar measurement with exactly this configuration. Without the grid the RF signal is only going to polarisation 1, which is therefore the only polarisation shown. The measurements were done with two different horns: S02-C-021 and S02-C-022. The cross polarization measurement procedure is described in [28].

The co- and cross-polar plots for one of the horns are shown in figure 59, and table 7 summarizes the results. Between the horns these are quite consistent: without the grid about  $-21$  dB, with the grid about  $-17$  dB. Clearly the breaking of the cross-polar compensation by inserting the grid in between the two mirrors costs about 4 dB.

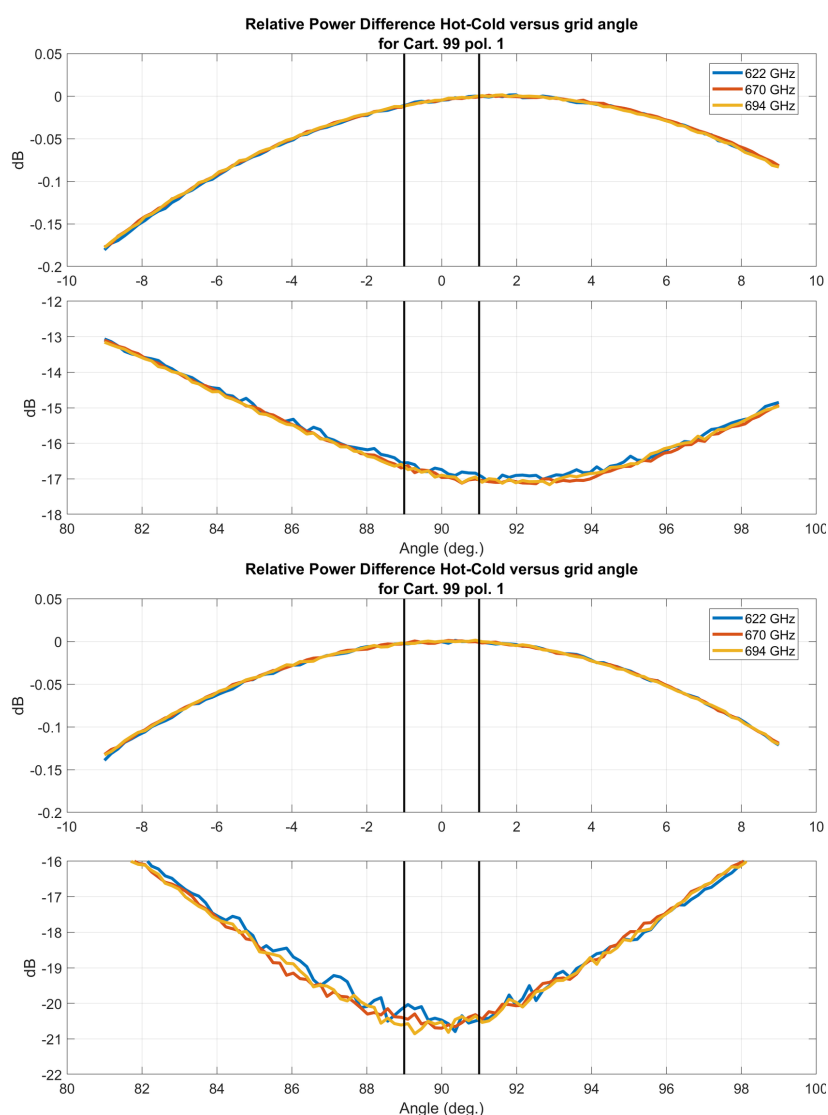


Figure 59: Co- and cross-polar level of the Band 9 optics *with* (upper pair) and *without* (lower pair) polarizing grid. The corresponding curves are normalized for 0 dB at the co-polar maximum, so the minimum in the cross-polar curves immediately gives the best possible cross-polar level. Each curve was measured at three different frequencies, and no significant frequency dependence is observed.

	<b>ALMA Band 9 Sideband Separating Upgrade</b> — <b>Study Report</b>	DocID: FEND-40.02.09.00-1974-C-REP Version: C Date: 2023-02-07 Status: Released Page: 72 of 105

$F_{LO}$ (GHz)	Horn S02-C-021 with grid Crosspol (dB)	Horn S02-C-021 without grid Crosspol (dB)	Horn S02-C-022 with grid Crosspol (dB)	Horn S02-C-022 without grid Crosspol (dB)
622	-17.1	-21.5	-17.2	-20.9
670	-17.3	-21.2	-17.4	-21.1
694	-17.1	-21.3	-17.3	-21.1

Table 7: Cross-polar levels of the existing Band 9 optics with and without polarizing grid, measured with two different horns.

There is a good match between simulations and measurements for the case with the grid. However, the measured cross-polar without the grid is  $-21$  dB, whereas we expected  $\sim -23$  dB from the simulations (see Section 5.5). Calculating backwards, the reduction of the simulated cross-polar level of  $-23.3$  dB to the measured (average) one of  $-21.2$  dB requires an additional contribution of about  $-25$  dB. Adding this same contribution to  $-17$  dB (simulation) should yield about  $-16.4$  dB (measured). The latter is probably within the measurement accuracy of the used method (rotating a grid in front of a hot-cold load), so we consider it to be consistent. Moreover, the comparisons between software and measured electric field patterns is reported in [29], where we can see that experimental and simulated data agree very well.

The additional  $-25$  dB cross-polar contribution could come from the IR filter or (less likely) the quartz window. Also the external grid used in the measurement could be more leaky than is corrected for, or the hot-cold load could be very slightly polarized (e.g. mirrors, etc.). However, with the measurement as done here, it is hard to determine the actual responsible. More accurate measurements with, e.g., a rotating source (as done in Band 5) could be done, but that requires a significant hardware and calibration effort. We could consider setting up an improved beam measurement system for future studies in a follow-up project.

Given these results, even with a hypothetical ideal OMT and ideal feedhorn (see section 5.9), with the current configuration of the mirrors we cannot hope to reach the desired cross-polar levels of around  $-23$  dB. A redesign of the optics (with slower mirrors and smaller bending angles) would be in order, irrespective whether the polarisation separation will be done by grid or by OMT.

## 5.9 Cross-polar performance of the bare Band 9 horn

Another question is how good the cross-polar performance of the original Band 9 actually is, if it were to be used in combination with an OMT. Note that for this purpose we are only interested in the part of the horn with cylindrical symmetry, as the built-in transition to single-moded waveguide at the output of the horn obviously has to be omitted. For this reason also, there is no measurement data available, as we never had a horn without transition in our hands. Of course, measured cross-polar data could at least put an upper limit on the cross-polar level. Unfortunately, if this data was ever available, we have not been able to recover it. What we do have are the original design simulations of the cylindrical part of the horn. There were performed early in 2003 using a mode-matching program (CWGSCAT, old FORTRAN code) provided by the late Matt Carter of IRAM. The calculations give the expected E-field distribution at the mouth of the horn, and these have been propagated mathematically to the far field, for cross sections in both the E and H planes. Interestingly, the historical far field plots also include the cross-polar level over a diagonal section of the far-field, where its contribution is expected to be maximal due to symmetry. Figure 60 shows all three levels (Co-pol E- and



H-plane and X-pol on diagonal D-plane) for 660 GHz, the middle of the band. Clearly, the cross-polar is at an exceedingly low level here, peaking at  $-50$  dB. In figure 61, the same calculation for 760 GHz shows that the cross-polar level stays below  $-45$  dB even here, which is beyond the extended RF band as considered for this study. On the low extreme of the band (560 GHz, not shown), the X-pol level remains around the  $-50$  dB level. Concluding, we can say that based on these calculations, the current Band 9 horn will not have a significant negative effect on the cross-polar level from a design point of view. Of course, the real performance hangs on the accuracy of the manufacturing.

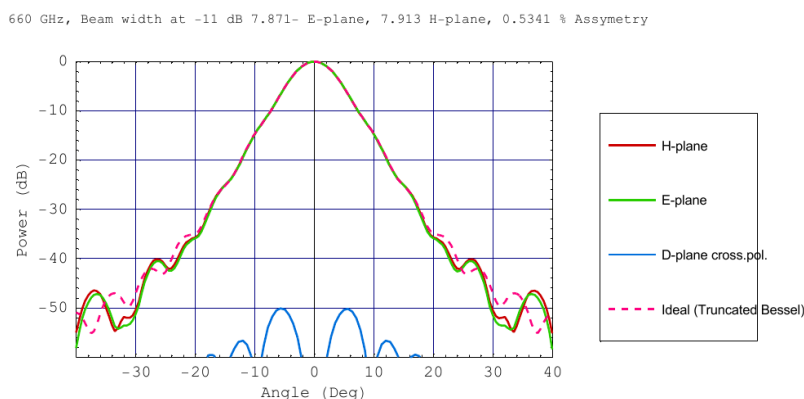


Figure 60: Calculated co-polar far-field intensity in E- and H-plane cuts, and cross-polar in a diagonal (D-plane) cut, for the original Band 9 feedhorn, obtained by propagating the field distribution in the mouth of the horn, in its turn obtained by mode-matching calculations. This example is for 660 GHz, the middle of the 600–720 GHz band.

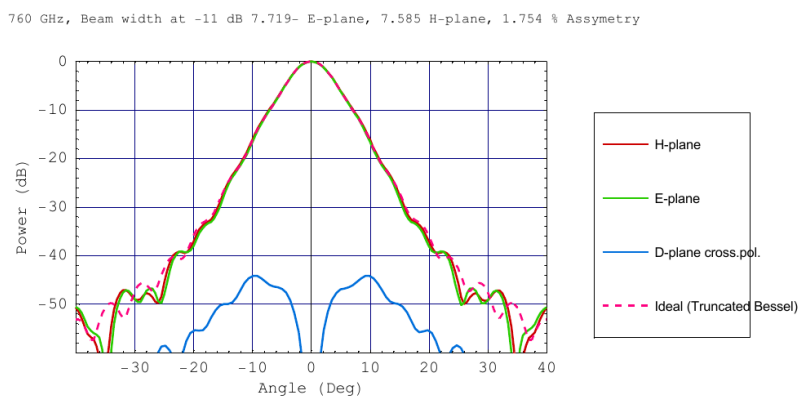


Figure 61: Similar data as in figure 60, but now for 760 GHz, which is beyond even the most extended RF band considered in this study.

## 5.10 Discussion and costing

In the sections above various possibilities and expected results are presented, and here we will try to put them in perspective. For that, in table 8 an overview is given of the various optical upgrades options, with their expected benefits and costs.

	<b>ALMA Band 9 Sideband Separating Upgrade</b> <hr/> <b>Study Report</b>	DocID: FEND-40.02.09.00-1974-C-REP Version: C Date: 2023-02-07 Status: Released Page: 74 of 105

Solution	Expected beam squint	Expected cross-pol	Expected noise incr	Expected cost per CCA
Single-horn with new optics	1%	-23 dB	6-10%	10 k€
Single-horn with existing optics	1-2%	-20 dB	6-10%	5 k€
Shimming of grids only	2-3%?	-17 dB	nil	2 days labour
No optical upgrade	5-10%	-17 dB	nil	nil

Table 8: Expected benefits and costs of various optical upgrade options.

Some comments on the numbers:

- The beam squint improvement is based on the observed on-sky measurements (appendix B.2) of comparable bands; the expected improvement of shimming is a hand-waving estimate.
- The cross-pol levels correspond to those found experimentally; for single-horn with existing optics 1 dB deterioration w.r.t. the value in table 7 is given to the OMT.
- The expected noise increase for single-horn is taken as 0.5 dB (for the OMT) - 0.1 dB (for the grid) = 0.4 dB, or about 10% in worst case, and as 0.4 - 0.15 dB (about 6%) in the best.
- In our experience, the monetary cost of high-tech machined products like OMTs and optics blocks usually ends up roughly around 5 k€, no matter what.
- The labour cost for the grid shimming includes the work shimming itself (including removing and inserting the cartridge, disassembly and assembly of the optics and determining the shim values) plus one day to obtain an extra beam pattern.

There are of course other costs in smaller parts. For instance, the corrugated feedhorns have to be reworked differently in the single-horn case and in the conventional case. These costs are likely to be very similar.

Also not taken into account are the one-time development costs for the various options, where applicable. For a full upgrade, these should be budgeted (or covered in a specific follow-up study project, for instance).

	<b>ALMA Band 9 Sideband Separating Upgrade</b> <hr/> <b>Study Report</b>	DocID: FEND-40.02.09.00-1974-C-REP Version: C Date: 2023-02-07 Status: Released Page: 75 of 105
---	---	---

## 6 Study goals 5 and 6 — Upgrade costing

In this section, estimates will be given on the cost (both monetary and concerning labour). It should be noted that any monetary estimate is volatile by nature, especially with the recent economical developments. Most of the prices mentioned in this section should be considered valid roughly for the 2020 epoch. Some of the hardware prices are based on quotations from former projects, scaled by best guess to this epoch.

### 6.1 Introduction

When upgrading a few scenarios can be evaluated:

1. Ship existing receivers to NOVA to be upgraded;
2. Make upgrade kits to be used at the OSF and perform dis- and re-assembly and testing at the OSF;
3. Disassemble critical parts which can be reused from the receiver and ship those to NOVA;
4. Make entirely new receivers and do not re-use any parts.

All these options could be investigated in detail. However, the general feeling is that only very limited technical work can be done on the receivers at the OSF. Sending over specialized NOVA people to the OSF is not practical, as the whole upgrade scheme most likely will be done over a longer period of time, mainly dictated by the annual refurbishment/maintenance of the frontends. So for now only option 1 is investigated here.

Option 4 would only be interesting if so few (expensive) parts can be re-used that the extra cost needed for a rolling upgrade does not outweigh the cost of those parts.

### 6.2 Parts to re-use, newly procure or discard

For a brief summary of the modifications to be made on the CCA level, see section 1.4.3. A more extensive discussion is in [8].

The aim is of course to reuse as many parts as possible of the existing Band 9 DSB receivers. Most important are:

- Mixers (SIS devices)
- Corrugated feedhorns (have to be reworked)
- Optics blocks (if not upgraded)
- LO multipliers with associated horns, optics and waveguides
- Vacuum feedthroughs
- 300K base plates
- Temperature sensors (surprisingly expensive)
- Fiberglass cartridge spacers (difficult to procure)
- The WCAs (except for the warm LNAs)

The following parts certainly have to be made new or procured:

- 2SB mixer blocks
- Mixer backpieces (the double number is needed)

	<p><b>ALMA Band 9 Sideband Separating Upgrade</b></p> <p>—</p> <p><b>Study Report</b></p>	<p>DocID: FEND-40.02.09.00-1974-C-REP</p> <p>Version: C</p> <p>Date: 2023-02-07</p> <p>Status: Released</p> <p>Page: 76 of 105</p>
---	---	--

- Rework of corrugated feedhorns, i.e., cutting off the rectangular (single-pol) waveguide part (including transition) to interface directly with the cylindrical waveguide, probably with a new transition, and add a mounting flange
- LO redirection mirrors (if the old optics is re-used, these are needed because the LO beams in the DSB cartridge are not co-aligned with the mixers as needed for the 2SB mixers.)
- IF hybrids
- IF LNAs
- IF cabling and thermal anchoring (double number of channels)
- DC cabling and thermal anchoring (ditto)
- Optics cradle and other structural parts (the original optics blocks have to be reworked on the bottom side to make space for the larger 2SB mixer assemblies)
- 4K, 12K and (probably) 90K cartridge plates
- Warm LNAs

The following parts cannot be re-used in any way and will be left over:

- DSB mixer blocks
- LO beamsplitters (can simply be removed)
- 4-12 GHz cryogenic LNAs (maybe sellable?)
- 4-12 GHz warm LNAs (ditto?)
- 4K and 12K cartridge plates and other small hardware

Optional new components:

- OMTs (if going to single-horn architecture)
- Optics blocks (if upgraded)

Optics: The baseline design, which is the same as the one which is installed in APEX/SEPIA, reuses the existing Band 9 DSB optics. The problem with these optics is the poor Cross polarization quality, as discussed in section 5. However, at this moment this is basis of the costing analysis. Recent investigations show that redesigning the optics could be useful.

### 6.3 Cost of full upgrade

The main cost items are:

- Transport, including insurance;
- New hardware;
- FTEs for the upgrade at NOVA
- FTEs at JAO for integration

Note that the cost estimates given in the following subsections are for the basic upgrade; those for optional extras are presented in section 6.4.

	<b>ALMA Band 9 Sideband Separating Upgrade</b>	DocID: FEND-40.02.09.00-1974-C-REP Version: C
	<b>Study Report</b>	Date: 2023-02-07 Status: Released Page: 77 of 105

### 6.3.1 Transport and insurance

It is assumed that the transport of the receivers can be done at the same way as “normal” shipments to the OSF. This means:

- NOVA organizes the transport to and from the JAO;
- ESO/JAO organizes the transport to and fro between the OSF and the SCO;
- NOVA organizes the assurance for the entire route;
- ESO/JAO assists in custom clearance issues in Santiago de Chile.

Costing estimate for transport:

1. Transport from NOVA to the JAO: 500 Euro per shipment.
2. Transport from SCO to OSF:  $A$  Euro per shipment.
3. Insurance costs are 0.3% of the insured value. We assume 140 kEuro per shipment, leading to 420 Euro insurance fee per shipment
4. Personnel costs of labor at the JAO:  $B$  Euro per shipment

So, per shipment the transport costs are:  $920 + A + B$  Euro, where  $A$  and  $B$  are unknowns at the moment. Each receiver needs two transports, of course: from Chile to NOVA and back. So per receiver the total transport costs are:  $1840 + 2A + 2B$  Euro. It is estimated that the total cost for shipment to NOVA and back from the OSF to be 4 kEuro per CCA. Shipment costs of 73 CCAs then leads to a cost of about 0.3 MEuro.

Required preparations: the aid of JAO needs to be sought for organizing the export of receivers from Chile to The Netherlands and importing upgraded versions. Whether or not this can be treated as temporary export remains to be seen.

### 6.3.2 New components

A detailed bill of materials for the current upgrade design, including cost estimates, needed for an upgrade is given in the tables 10 and 11.

Summarizing: the cost estimates for a Band 9 2SB upgrade are approximately 65 kEuro per CCA. Note: these are approximately 2020 prices; corrections for inflation and world market prices will have to be made.

Upgrading 73 receivers from the current DSB version to a 2SB version according to the current design will cost:  $73 \times 65$  kEuro = 4.7 MEuro. With some cost for spares: roughly 5 MEuro.

### 6.3.3 Spares

At the moment, there is no concrete plan for the number of spare components to deliver. However, with DSB Band 9 operational at ALMA now for more than ten years, a reasonable estimate can be made of failure rates. Table 9 lists lists the number of items taken over the years out of the Band 9 spare parts stock (which, while property of ALMA, is maintained at NOVA).

These are the only failures that have come to our knowledge. Since, as expected, the active components (mixers, LNAs) are the most vulnerable, it seems prudent to keep a sufficient

	<b>ALMA Band 9 Sideband Separating Upgrade</b> <hr/> <b>Study Report</b>	DocID: FEND-40.02.09.00-1974-C-REP Version: C Date: 2023-02-07 Status: Released Page: 78 of 105

Spares	Failed	Item	Cause	Re-use
10	1	grid	in-situ damaged by impact	Yes <sup>1</sup>
40	2	mixer (backpiece + SIS)	unknown	Yes
5	1	cryo LNA	unknown	No
20	All	DC (MDM) feedthrough	non-vacuum-compatible design	Yes <sup>2</sup>

Table 9: Items used out of the Band 9 spare parts stock from initial deployment up to time of writing. Notes: <sup>1</sup>not re-used in case of single-horn architecture (see section 5); <sup>2</sup>all DC feedthroughs have been replaced on-site by another type (not from spare stock, as these had the same design flaw); no further failures have been reported to NOVA.

number of spares of these. For the LNAs, doubling the number (because of the doubled number of channels) to ten should be adequate; this is also the number used in Band 5. For the mixers, this is a bit more complicated. These are probably the most likely to fail over time (2 cases for Band 9 DSB, but the number of SIS devices is doubled for 2SB). Especially if on-site drop-in replacement is desired, the most straightforward way would be to stock complete qualified 2SB assemblies (as done, e.g., in Band 5). On the other hand, these are expensive items (table 10). If more extensive re-qualification effort (e.g., at NOVA) is acceptable, it may be more cost-effective to stock matched backpiece+SIS pairs, and resupply failed 2SB assemblies with those. It is very unlikely that other components in the 2SB mixer assembly will fail. Still, keeping 1–2 complete units in stock would be prudent.

Considering the volatility of hardware costs at the moment, we don't think that a more detailed costing of spares at this stage is feasible. This should be considered carefully, however, if/when detailed plans for an upgrade are worked out.

### 6.3.4 FTE of the upgrade at NOVA

Based on the experience of the Band 9 and Band 5 effort three phases can be identified for a project like the Band 9 2SB upgrade.

Each receiver project has three phases:

1. Prototype;
2. Small Pre-production series;
3. Production.

Roughly speaking, phase 1 takes 25% of the time. This phase can maybe be considered to be done when the current design is followed (i.e., no optics upgrade). We roughly expect that the NOVA group of 6 people is needed for a period of 5 years to achieve enable this upgrade. So, a rough estimate would be 30 FTE for the manpower at NOVA.

### 6.3.5 FTE at JAO

This is difficult to estimate for NOVA at this moment. But for each receiver 0.05 FTE (about 2 manweeks) maybe. 75 Receivers would then be about 4 FTE.

	<b>ALMA Band 9 Sideband Separating Upgrade</b>	DocID: FEND-40.02.09.00-1974-C-REP
	—	Version: C
	<b>Study Report</b>	Date: 2023-02-07
		Status: Released
		Page: 79 of 105

Item	Part number	Description	Material	Manufacturer	Need	Unit price	Price mixer	Notes
1	NOVA-2SB-0101-A	Mixer body bottom	CuTeP	RPG/GARD	1	3000	3000	half split-block
2	NOVA-2SB-0102-A	Mixer body top	CuTeP	RPG/GARD	1	3000	3000	half split-block
3A	NOVA-2SB-0103-A	RF horn	Cu+Au	RPG	1	2100	0	to be re-worked
3	NOVA-2SB-0203-A	RF horn assembly		RPG/TK	1	500	500	re-flanged B9 horn
4	NOVA-2SB-0104-A	LO Horn	Cu+Au	RPG/TK	1	1200	1200	
5	NOVA-2SB-0105-B	Sidepiece	CuTeP	mech	2	300	600	
6	NOVA-2SB-0106-A	Backpiece cap	P-bronze	mech	2	100	200	
7	NOVA-2SB-0107-A	Centering ring	P-bronze	mech	2	20	40	
8	NOVA-2SB-0108-A	Pole piece	Vacoflux 50	mech	4	40	160	
9	NOVA-2SB-0109-A	Magnet conductor 1	Vacoflux 50	mech	2	150	300	
10	NOVA-2SB-0110-A	Magnet conductor 2	Vacoflux 50	mech	2	150	300	
11	NOVA-2SB-0111-A	Magnet core	Vacoflux 50	mech	2	50	100	
12	NOVA-2SB-0112-A	Heater Contact	Spring steel+Au	mech	2	20	40	
13	NOVA-2SB-0113-A	Contact Insulation	Kapton	mech	2	20	40	
14	NOVA-2SB-0114-A	Polepiece Spring	Spring steel	mech	2	10	20	
15	NOVA-2SB-0115	PCB	FR4	PCB	2	20	40	
16	NOVA-2SB-0116-A	Horn Adapter	CuTeP + Au	mech	1	300	300	
17	NOVA-2SB-0217-A	Magnet coil	Al/NbTi	Witronic	2	150	300	
18	NOVA-2SB-0118-B	Connector clamp	Al-6082	mech	1	100	100	
19	NOVA-2SB-0119-A	Insulating bush	Vespel	mech	4	10	40	
20	NOVA-2SB-0120-A	LO load	Eccosorb MF112	mech	2	20	40	
21	NOVA-2SB-0121-A	RF load	Eccosorb MF112	mech	1	20	20	
22	NOVA-2SB-0122-A	Thermal compensator	Ti	mech	3	20	60	
23	NOVA-2SB-0123-B	Connector spring	Spring steel	mech	2	20	40	
24	NK-2D2-009-225-TH00	Nano connector 9-way		Airborn	2	100	200	
25	TBD	Resistor 0805 100R		Farnell	2	1	2	
26	TBD	Resistor 1206 560R		Farnell	2	1	2	
27	DT-670-A-SD	Temperature sensor		Lakeshore	1	420	420	
28	S-00005-A	Mixer backpiece		NOVA	2	700	700	one re-used
29	SISxx-yySzz	SIS junction		TUD	2	5000	0	"virtual" price
30	TBD	Hex Screw M1-6 x 105	SS		3	1	3	
31	TBD	Hex Screw M1-6 x 65	SS		14	1	14	
32	TBD	Hex Screw M2 65	SS		16	1	16	
34	TBD	Hex Screw UNF 0-80	SS		4	1	4	
35	TBD	Dowel pin	SS		2	1	2	
TOTAL							11103	

Table 10: Hardware cost of a 2SB mixer assembly. Each CCA needs two of these.

### 6.3.6 Summary

Hardware costs: about 5 MEuro

Shipment costs: about 0.3 MEuro

30 FTE at NOVA: about 3 MEuro

4 FTE at JAO/OSF: about 0.4 MEuro

Total: about 9 MEuro

## 6.4 Expected price increase for optional upgrades

In section 5.10 some estimates are given of extra costs of optional upgrades to the optics. Material-wise these come out at about 5kEuro for a single-horn solution and about 10kEuro for an additional upgrade of the mirror block. If the choice is made to just shim the existing grids, about 2 extra days of labour should be taken into account. The cost for the extension of the YTO for 73 WCAs, of the order of 35k€, has to be taken into account, as discussed in section 3.4.

A summary of these options with their costing and labour estimates, for an entire upgrade of 73 receivers, is given in table 12.

	<b>ALMA Band 9 Sideband Separating Upgrade</b>	DocID: FEND-40.02.09.00-1974-C-REP
	—	Version: C
	<b>Study Report</b>	Date: 2023-02-07
		Status: Released
		Page: 80 of 105

Item	Part number	Description	Manufacturer	Unit price budget	Unit price quote	Needed /CCA	Total /CCA
1	NOVA-2SB-0200	Mixer	NOVA	11103		2	22206
2	YH90X	IF hybrid	Yeibes	1000		2	2000
3		Isolator	Quinstar	1500		0	0
4	YXA 4-12	LNA opt 1	TTI	3500		0	0
5		LNA opt 2	Yeibes/LNF	5000		4	20000
6		Bias-tee		200		0	0
7		Mirror block rework	0.5 day	300		1	300
10	B9-2SB-1030-A	IF cables mixer-hybrid	SSI	150	101	4	600
11	B9-2SB-1011-A (11-14)	IF cables hybrid-LNA	SSI	150	51	4	600
12		IF cables hybrid-isolator	SSI	150		0	0
13		IF cables isolator-LNA	SSI	150		0	0
14	B9-2SB-1015-A (15-18)	IF cable LNA-4K	SSI	150	30	4	600
15	B9-2SB-1055-A (55-56)	New IF cables 4K-12K	SSI	150	22	4	600
16	B9-2SB-1101-A	New IF cables 12K-90K	SSI	150	10	4	600
17	B9-2SB-1151-A (51-54)	New IF cables 90K-300K	SSI	150	42	4	600
8	B9-2SB-1001-A	Cradle	Kenter	500		1	500
	B9-2SB-1002-A	Cradle post 1	Kenter	50		1	50
	B9-2SB-1003-A	Cradle post 2	Kenter	50		1	50
9	B9-2SB-1020-A	LO redirection mirror	Kenter	1000		2	2000
18	B9-2SB-1007-A (1010)	IF cable clamps 4K	Kenter	200		1	200
	B9-2SB-1051-A	IF cable clamps 12/90K	Kenter	200		2	400
	B9-2SB-1006-A	4K plate	Kenter	400		1	400
	B9-2SB-1050-A	12K plate	Kenter	400		1	400
	B9-2SB-1100-A	90K plate	Kenter	400		1	400
	B9-2SB-1004-A	Optics posts	Kenter	50		4	200
	B9-2SB-1005-A	IF hybrid bracket	Kenter	50		1	50
	B9-2SB-1009-A	LNA bracket	Kenter	100		2	200
	B9-2SB-1052-A, etc.	Covers	Kenter	100		1	100
		DC connector bracket	mech	50		1	50
		Ti compensators	mech	100		1	100
		DC cable anchors	mech	100		2	200
		Set fibreglass rings	RAL	1000		1	1000
19		Warm IF amplifiers	AML/TTI	1500		4	6000
20		Interstage DC harness	AirBorn	650	791	2	1300
21	DT-670C-CU	12/90K tempsensor	Lakeshore	317		2	634
22		4K DC cable harness	Tekdata	480		2	960
23	DT-670A-CU	4K tempsensor	Lakeshore	550		1	550
	NM-212-009-161-JCAQ	Connector	AirBorn	110	110	8	880
TOTAL							64730

Table 11: Hardware costs of new parts needed for the entire upgrade. Note that the mixer cost of item 1 are copied from table 10

Subsystem	Option	Improvement	HW Cost Euro/73	Labour FTE
RF (section 3)	YTO range extension	RF range	35k	0.5
Optics (section 5)	Shimmed grids	Beam squint	—	0.75
	Single-horn, old optics	Beam squint, bit X-pol	365k	0.75
	Single-horn, new optics	Beam squint, X-pol	730k	1

Table 12: Overview of estimated monetary and labour costs of upgrade options, for 73 receivers.

## 6.5 Cost of upgrading four CCAs only

The first approximation for upgrading four Band 9 CCAs is mainly the ratio of these four CCAs with respect to the 73 CCAs for a full upgrade. But with a 20% higher value for hardware components due to smaller quantity orders than in case of ordering for 73 CCAs.

	<b>ALMA Band 9 Sideband Separating Upgrade</b> <hr/> <b>Study Report</b>	DocID: FEND-40.02.09.00-1974-C-REP Version: C Date: 2023-02-07 Status: Released Page: 81 of 105
---	---	---

This means that the total costs would be:

- Hardware costs:  $(5 \text{ MEuro} \times 4 / 73) + 20\% = 330 \text{ kEuro}$
- Other costs:  $(4 \text{ MEuro} \times 4 / 73) = 220 \text{ kEuro}$

The total costs would then be 550 kEuro. This is quite comparable with the 537 kEuro cost estimate of the original bid by NOVA in 2019.

Note that the purpose of building four 2SB CCAs for the Total Power antennas, as proposed there, turns out not to be so attractive, as it interferes with the scheduled turnaround of front-ends during maintenance. Nevertheless (apart from fulfilling study goal 6), it is good to have an indication of the cost of a small series, for instance when a small upgrade pool is needed, as discussed in sections 7.3 and 7.4.

	<b>ALMA Band 9 Sideband Separating Upgrade</b>	DocID: FEND-40.02.09.00-1974-C-REP Version: C
	<b>Study Report</b>	Date: 2023-02-07 Status: Released Page: 82 of 105

## 7 Study goal 7 — Upgrade strategies

### 7.1 Technical and logistical issues — introduction

One possible alternative to the total unavailability of Band 9 during an upgrade, which was discussed briefly, is the temporary re-combination of the upper and lower sideband IF signals between the output of the WCA and the input of the front-end IF switch. This could simply be done with an inexpensive 3 dB power combiner. During the upgrade campaign, Band 9 could then be offered in continued DSB configuration. At its conclusion, all combiners could be removed on-site in a relatively short time, say the engineering time between cycles, to start working in 2SB mode with a complete array in one go. The implications for re-qualification of the front ends are not clear at the moment and should be discussed more extensively with ESO and/or JAO.

Of course, the most attractive option from the hardware point of view would be to introduce no intervening modification to the IF system at all, and simply let the DSB and 2SB receivers coexist during the upgrade. According to recent information<sup>4</sup>, it may be possible to limit correlation to either the USBs or LSBs of both the DSB and 2SB receivers (thereby temporarily halving the continuum sensitivity of the former). Potentially, a switch between USB and LSB correlation could even be made without hardware modifications: if the bias polarity of one of the junctions in the 2SB mixer is inverted, the LSB and USB change places on the front-end output ports. It should be noted, however, that up to now, all Band 9 mixers have been qualified with only one bias polarity. If this mode is desired during the upgrade, qualification of the new 2SB CCAs with inverted bias should be added to the test plan, at the cost of a certain amount of extra labour. Also on the side of the ALMA front-end software there will be investment needed to operate in inverted-bias mode (alternative tuning tables, etc.).

On 2021-08-26 an open discussion between stakeholders from NOVA, ESO and JAO/OSF was held concerning the possible on-site strategies to upgrade the existing Band 9 DSB CCAs to a 2SB configuration<sup>5</sup>. In the following sections, rather than summing up all individual contributions, the main arguments and some provisional conclusions will be discussed here in an integrated way. New thoughts that came up after the meeting are also incorporated.

Participants of the discussion:

- NOVA Ronald Hesper, Andrey Baryshev, Joost Adema;
- ESO Carlos De Breuck, Pavel Yagoubov, Neil Philips;
- JAO/OSF: Norikazu Mizuno, Rodrigo Cabezas, Giorgio Siringo, Roberto Price.

### 7.2 Availability during upgrade

As already mentioned in the introduction, the main issue is the availability of Band 9 during the upgrade, which is likely to take at least 2–3 years. Three global options can be envisioned:

- Take Band 9 completely off-line for the duration of the upgrade;
- Recombine the LSB and USB of the upgraded 2SB Band 9 cartridges before the IF switch for (part of) the duration of the upgrade, remove upon completion;

<sup>4</sup>Post-review email exchange with Christophe Risacher (IRAM) and Neil Phillips (ESO).

<sup>5</sup>This section is based on the separate meeting report FEND-40.02.09.00-1967-A-MIN which was circulated before. The version presented in the current Study Report supersedes the meeting report.

	<p><b>ALMA Band 9 Sideband Separating Upgrade</b></p> <p>—</p> <p><b>Study Report</b></p>	<p>DocID: FEND-40.02.09.00-1974-C-REP</p> <p>Version: C</p> <p>Date: 2023-02-07</p> <p>Status: Released</p> <p>Page: 83 of 105</p>
---	---	--

- Let the 2SB and DSB CCAs coexist and only use either the USB or LSB of the 2SB CCAs (possibly switchable by bias-inversion) for the duration of the upgrade.

The first one is obviously highly undesirable, and will not be considered here.

### 7.2.1 Recombination of USB and LSB during upgrade

During the discussion it became clear that having temporary hardware installed during the upgrade (as in option 2) is possible, but gives rise to several complications. For instance, if a simple power combiner is installed (either in the WCA or between the WCA and the IF switch), it has to be removed at some point, which will very likely be only practical if the entire front-end is taken off the telescope. In any case, after removal, the receiver has to be re-qualified in 2SB mode, which requires its presence at the OSF, and cost additional labor. Finally, this also means that during the upgrade period, 2SB operation will not be available even for on-sky testing purposes. Even if this approach is chosen, there will still be a fairly long transition period during which the combiners are removed front-end by front-end. In this period the array is effectively in a mixed DSB/2SB configuration (see next section). Altogether, this makes this option rather unattractive.

Alternatively, a switchable power combiner could be installed (i.e., switchable between LSB / USB straight through and LSB+USB power-combined into one of the outputs). The advantage is that front-end qualification of both modes can be performed at the OSF, and also that the upgraded part of the array can either function in full 2SB configuration with a limited (but growing) number of receivers, or participate with the remaining receivers to maintain the full array's sensitivity in DSB mode. The disadvantage is that it requires an additional control input to the front-end. Question is if such a control is available, either in the IF switch or the WCA MCDPLL unit. Adding an additional control outside the existing infrastructure is pretty much out of the question. One solution could be a mechanism that actuates the DSB/2SB switch by a "magic command", say a special sequence of YTO frequency settings that should never occur during normal operation. Still, this would require modification of the control software, which can be a laborious process due to requirements of robustness and associated review procedures. However, it does allow operation of the Band 9 array at its maximum momentary potential during the upgrade. Also, after the upgrade is concluded, there is no rush to remove the additional hardware (if at all necessary).

### 7.2.2 Co-existence of 2SB and DSB receivers during upgrade

From the front-end point of view, the simplest solution is to let a growing population of 2SB receivers co-exist with a shrinking number of DSB ones. In this case, the already upgraded receivers would always export both USB and LSB, but when correlated with the DSB receivers, only one of the sidebands would be used. Also here two operation modes could be offered: full 2SB with the growing number of upgraded receivers, or the full array with reduced sensitivity due to the missing sideband. An advantage of the latter mode is that, although the sensitivity is reduced, all baselines contribute to filling the U-V plane.

The correlator should have no problem handling the mixed array, but a mechanism should be devised to flag the distinction between the two types of receiver in the data archive. Possibly the simple absence of power in the missing sideband is sufficient for this. Alternatively, the electronic serial number of the CCAs could be stored in the metadata, and a record kept of the upgrade status of each receiver.

	<p><b>ALMA Band 9 Sideband Separating Upgrade</b></p> <p>—</p> <p><b>Study Report</b></p>	<p>DocID: FEND-40.02.09.00-1974-C-REP</p> <p>Version: C</p> <p>Date: 2023-02-07</p> <p>Status: Released</p> <p>Page: 84 of 105</p>
---	---	--

During finalization of this report, Neil Phillips of ESO contributed an in-depth analysis of the point-source sensitivity, making suitable assumptions, of a mixed DSB/2SB array. Rather than trying to integrate this here, it is reproduced in its entirety in Appendix C.

### 7.3 Logistics of the upgrade procedure

Since it is NOVA’s intention to re-use several of the most precious parts of the DSB receivers (notably the SIS mixers, but also the LO multipliers and probably the optics), a buffer pool of off-line CCAs is needed. This number of units will then be in the process of being upgraded and re-qualified at NOVA, or in transit between the continents.

During initial Band 9 DSB production, an additional seven CCAs (on top of the 66 required for the array) were delivered as spares. Of these seven, at any time, four are circulating in the regular front-end maintenance cycle at the OSF. This leaves three available for the upgrade pipeline, which is clearly insufficient for an efficient operation. This means that either a number of units have to be built from scratch (which is a monetary investment and a burden on the mixer pool), or the number of receivers active in the array must be reduced. It is estimated that at around 8–10 CCAs are needed in the pipeline, although this number has not been deeply researched. This would mean an additional 5–7 units should be built, or the same number extracted from the array. The latter could be potentially viable given the availability of several spares, the low CCA failure rates, the number of antennas at OSF (or long-term out of service for other reasons), the fact that the Total Power array not used for DSB bands, and careful seasonal planning. As a side note, even if a small number of CCAs is absent during the upgrade, it is important that the corresponding WCAs are still mounted on the front-ends, as the Band 9 WCAs contain the Faraday rotation mirrors used for phase compensation of the photonic reference for all the bands. A sufficient number of dummy CCAs should be available at the OSF for this.

Apart from the detachable IF plate (which has to be upgraded both in bandwidth and number of channels), the WCAs themselves do not have to be modified for 2SB operation proper. Only if the “Extended RF Range” option (goal 2 of this study) is selected for roll-out, the YIG oscillators in the WCAs have to be modified (probably by the manufacturer). Of course, if a DSB/2SB switch is integrated in the WCA, as discussed above, more extensive modifications are needed. However, probably this could be limited to the IF plate as well, if properly miniaturized warm LNAs are available, and the replacement can then be handled on-site.

It was noted that rather than being a handicap, working on two bands at the same time at the OSF could actually save a considerable amount of labor, as a lot of double work is avoided. This would make it attractive to schedule the Band 9 upgrade in parallel with the upgrade or installation of other bands (e.g., Band 2). This would call for some rather tight coordination and schedule-keeping on the side of the respective CCA producers, however.

Generally speaking, the period in the year at which most of the engineering on the front-ends is possible is roughly from December up to March (southern Summer). Also, at any time that the array is in a long-baseline configuration, Band 9 is not likely to be used extensively. On the other hand, the band-to-band phase transfer is reported to become available soon, so this advantage may disappear to some extent.

	<p><b>ALMA Band 9 Sideband Separating Upgrade</b></p> <p>—</p> <p><b>Study Report</b></p>	<p>DocID: FEND-40.02.09.00-1974-C-REP</p> <p>Version: C</p> <p>Date: 2023-02-07</p> <p>Status: Released</p> <p>Page: 85 of 105</p>
---	---	--

## 7.4 Possibilities of a pre-production series

In another standing proposal to ESO, the consideration of which is on hold until the end of the current study, is to build a small series of Band 9 2SB pre-production receivers. Apart from the possibility to use these for on-sky interferometric tests (something that SEPIA660 on APEX cannot do), these would be particularly beneficial for the four total-power antennas used for flux calibration. Rather than discussing the merits and challenges of this endeavor (which are covered in the proposal), just a few notes that are relevant for the current discussion:

- If the pre-production units are built from scratch, they add to the upgrade pool of receivers.
- The use of these CCAs specifically for the total-power antennas complicates the front-end maintenance schedule, as these receivers are now earmarked, and can not rotate freely among the stations anymore.

## 7.5 Scheduling and FTE issues

The period of time needed for the upgrade is comparable to the production of a new band, mainly due to the need for full lab qualification. A period of at least 2–3 years should be envisioned. The lower limit of this estimate will be very challenging to meet, but on the other hand, testing efficiency at NOVA is also increasing steadily, for instance by the use of the “Advanced Tuning Algorithms” [17] developed during an earlier ESO-funded study.

At NOVA, Band 2 production will be difficult to combine with Band 9 upgrade work, but probably these two activities will not overlap for other reasons as well (e.g., cash flow at the funding agencies). Production of a small pre-production series during Band 2 should be possible, however.

It would be desirable to give upgrade priority to CCAs with  $\text{AlO}_x$ -barrier mixers to gain early benefit of increased sensitivity. On the other hand, this limits the number of AlN mixers available in the initial phase for matching into 2SB pairs.

On the side of the OSF, staff effort should be considered, and training for the upgrade AIV and maintenance should not be neglected.

Finally, any method chosen to let the DSB and 2SB receivers coexist in some form will almost certainly require modifications in the front-end, observing and data handling software. As software is a complex and critical part of the observatory, the effort of this, including testing, reviewing and required management approval, should be part of any serious plan for the upgrade.

	<b>ALMA Band 9 Sideband Separating Upgrade</b>	DocID: FEND-40.02.09.00-1974-C-REP Version: C
	<b>Study Report</b>	Date: 2023-02-07 Status: Released Page: 86 of 105

## 8 Conclusions and outlook

### 8.1 Conclusions

By the end of this study, we think we can draw the following conclusions:

Goal 1: The SIS mixers allow an extension of the upper limit of the IF band to at least 18 GHz (possibly 20 GHz with some reduced performance). The challenge is obtaining a well-matched LNA with integrated bias-tee; the IF hybrid made by Yebes is fully up for the job. Extension downwards below 4 GHz is probably not limited by the mixer (which goes almost to DC) but by the IF infrastructure (LNAs and hybrid) as the fractional bandwidth becomes huge.

Goal 2: Widening of the RF bandwidth to 580–735 GHz is demonstrated in SEPIA660. Main cost is the refurbishment (commercially or on-site) of the YIG oscillators in the WCAs.

Goal 3: A sufficient number of SIS devices for a 2SB upgrade with comparable noise performance are probably available, but not by a large margin. Main uncertainties are statistical extrapolation of historical test results and the 2SB pairing yield.

Goal 4: The limitation of the current polarimetric performance can be explained by the deviation of grid mounting angle for the beam squint and by presence of the grid in combination with mirrors for the cross-pol level. The most radical way to improve this is to remove the grid and use a single feed horn architecture, possibly together with new optics for improved cross-pol level. With this, the on-sky polarization purity for extended sources can probably be improved by an order of magnitude. The performance cost is an expected increase in the noise temperature of the order of 10%. Alternatively, only the beam squint could be improved by shimming the grid upon upgrade, based on measured beam squint data. If this is found sufficient for polarimetric observation, it would be the most cost efficient way to address the issue.

Goal 5: As a rough estimate, about 9 M€ is needed for the entire DSB to 2SB upgrade, with baseline optical performance.

Goal 6: As a rough estimate, for about 550 k€ four pre-production units could be built.

Goal 7: A “rolling” upgrade scheme requires an upgrade pool of the order of 10 receivers to enable a smooth flow. During the upgrade, the co-existing DSB and 2SB receivers can most likely still be correlated together, with only moderate performance loss. Alternatively, the upper and lower sidebands could temporarily be recombined (switchable) in the WCA (no infrastructural changes in the front-end required).

### 8.2 Outlook

Several things come to mind that would be worthwhile follow-ups on the current study:

- Construct a small set of prototypes using the current 4–12 GHz IF bandwidth (but in all four channels, SEPIA-style) for, e.g., the total-power antennas in ALMA. Alternatively, a bandwidth of, say, 4–18 GHz could be implemented to make these receivers future-proof, and possibly also to enable using them as test-bed for IF upgrades at the ALMA site. A project like this has been proposed already.



**ALMA Band 9 Sideband  
Separating Upgrade**  
—  
**Study Report**

DocID: FEND-40.02.09.00-1974-C-REP  
Version: C  
Date: 2023-02-07  
Status: Released  
Page: 87 of 105

- Experimentally verify the feasibility of improving the beam squint by shimming the grid. Even if there are other aberrations in the existing optics, this should be able to correct for most of the first-order ones. Find out if a single beam-pattern measurement (or perhaps even existing qualification data) is sufficient for a one-cycle optimization. As mentioned in section 5.4, this would require a better understanding of the transformation of lab beam-pattern measurement to expected on-sky beam squint.
- Make a more concrete design of the single-horn architecture and associated optics. Construct and test a prototype.
- Design and produce new SIS devices, either for the case that the current stock turns out to be marginal or to try and make a significant improvement in the SIS performance. This is a substantial project which includes finding a junction fab to collaborate with. At the moment, a limited effort in an ESO study performed by GARD (Chalmers University of Technology, Sweden) is devoted to produce new Band 9 junctions (in this part, NOVA is directly involved already).
- Build a full (2-polarization 2SB) prototype with latest LNAs and optimise the performance over a wide IF to determine what specifications may really be achievable. It would also provide a (dual-pol) test bed for other ideas like improving the x-pol/beam squint (alternative optics, OMT demonstrator etc.).



## A Appendix — Statistical SIS I-V curve analysis

*In which a description is given of the statistical SIS batch quality analysis referred to in section 4.6.1.*

During production of the ALMA Band 9 receivers, many batches of SIS junctions have been produced in the TU Delft clean room facilities. Amount of produced junctions was much more than needed for production of 200+ SIS mixers needed for delivery. Several wafers were only tested to the level of DC I-V characteristics. For the purpose of upgrading ALMA band 9 receivers to a 2SB configuration we need produce an additional 200+ SIS DSB mixers and find matching pairs to form a 2SB mixer assemblies. Since heterodyne testing of representative amount of SIS mixers from each batch is beyond the scale of this study project we attempt here to use the available measured DC I-V characteristics to predict heterodyne performance of mixers based on these junctions.

In order to accurately predict SIS mixer performance, Tucker theory should be used, which allows to predict SIS mixer noise temperature and gain based only on the knowledge of the shape of an unpumped DC I-V characteristic, a pumping level and an embedding impedance of SIS mixer support both at RF and IF frequencies. The embedding impedance is the most variable (unstable) quantity as it depends on produced SIS mixer chip geometry, thickness of superconducting and dielectric layers, accuracy of the mixer chip positioning in a mixer block and machining accuracy of a mixer block. All these parameters vary from mixer to mixer and will not allow to accurately relate unpumped I-V curve with expected SIS mixer noise temperature. A statistical approach should be used by analyzing significant number of measured mixers.

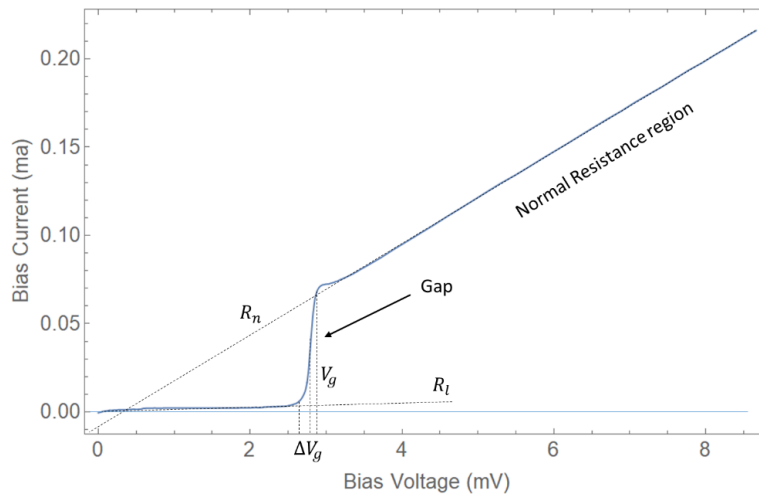


Figure 62: DC I-V curve of SIS junction with analysis parameters indicated as follows:  $R_n$  is normal resistance,  $V_g$  is Gap voltage,  $R_j = R_l$  is subgap resistance,  $\Delta V_g$  is width of gap region.

As an initial step of such an analysis we propose to use set of integral I-V curve parameters which were used to judge the junction's quality during ALMA Band 9 production. As shown in figure 62, we introduce: a normal resistance  $R_n$  as slope of I-V curve at voltages above superconducting gap voltage  $V_g$ ; a leakage resistance  $R_l$  or  $R_j$  which is the minimum  $dI/dV$  for the voltages below  $V_g$  and the energy gap width  $\Delta V_g$  as a width of energy gap defined as shown in figure 62. All these parameters influence performance SIS junction as mixer. We

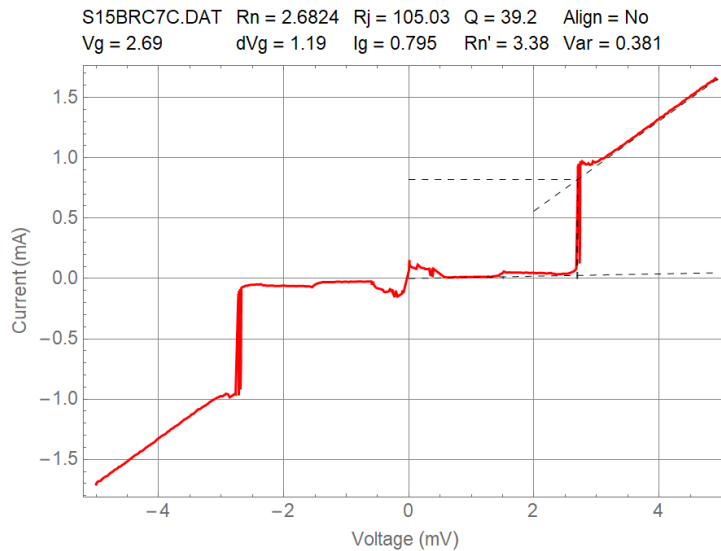


Figure 63: Example of measured I-V curve with key parameters (see figure 62) automatically determined.

have developed a software routine that determines these parameters automatically on the basis of fitting of measured I-V curve. Example of typical fit is shown in figure 63 together with automatically determined parameters.

As next step, we use a database of heterodyne measurements of delivered ALMA Band 9 mixers. From that database we use junction code to retrieve the corresponding unpumped I-V curve measurement from dipstick data and we also produce an average of a measured noise temperature over all available LO and IF frequency. Thanks to the fixed delivery measurement

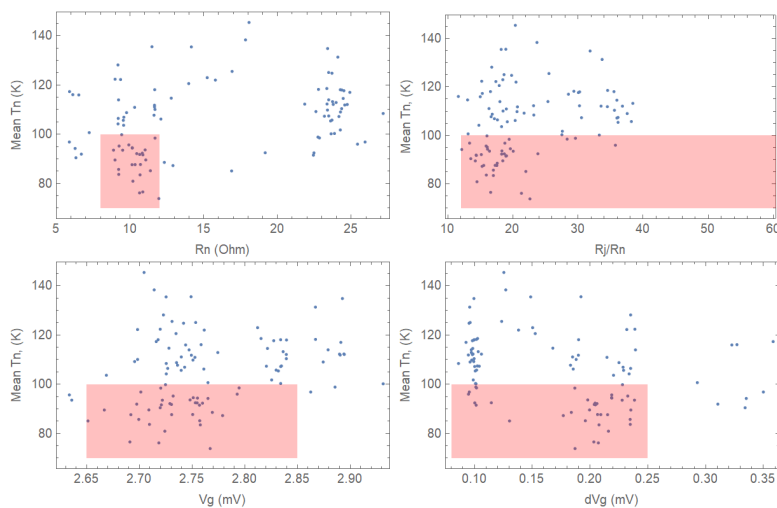


Figure 64: A noise temperature average over LO frequencies of NbTiN ALMA Band 9 mixers as delivered to ALMA as a function of automatically determined unpumped DC I-V parameters: top left  $R_n$ , top right  $R_j/R_n$ , bottom left  $V_g$ , bottom left  $\Delta V_g$ . Red shaded areas indicate regions of optimum performance which will be used for merit function.

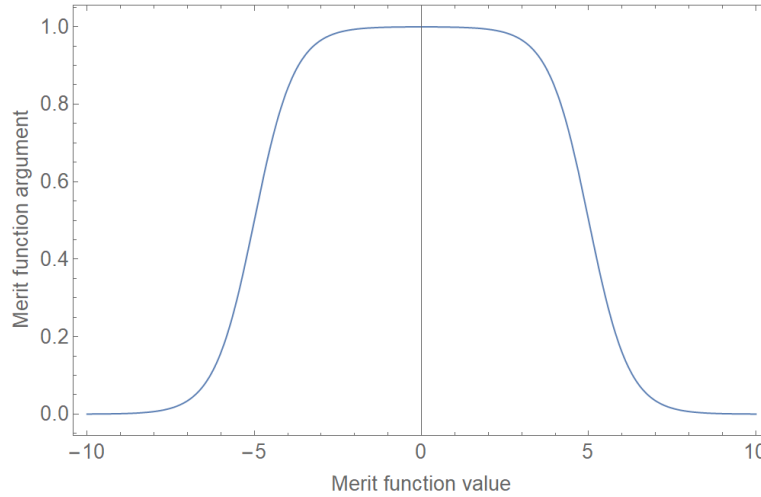


Figure 65: A Pi-shaped merit function for the argument range of -5,5.

protocol and setup we have uniform data over many mixers. From unpumped I-V curves we determine integral parameters as described earlier and show average noise temperature vs.  $R_n$ ,  $V_g$ ,  $\Delta V_g$  and quality factor  $Q = R_j/R_n$  in figure 64. Of course, the Q factor is only one of the parameters determining the performance of an SIS mixer. It is used here because it is easily qualifiable. A better approach would be to use the full Tucker theory, which takes as input the entire I-V curve<sup>6</sup>. As seen in the figure 64, we can associate certain parameter ranges as necessary condition to achieve a low average noise temperature ( $< 100$  K), shown as red shaded areas. Note that indicated conditions are not sufficient to achieve low noise temperature as we also have mixers with much higher noise temperatures associated with the same parameter range. Nonetheless, we can still attempt to use these parameters to provide a statistical selection criteria for measured batches, because mixer noise temperatures corresponding to the I-V curves outside the indicated ranges are guaranteed to have values above 100 K.

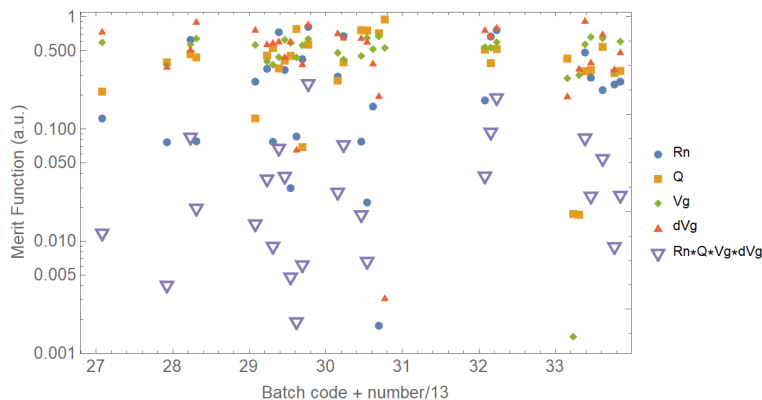


Figure 66: Merit function for automatically determined I-V curve parameters,  $R_n$ ,  $Q = R_j/R_n$ ,  $V_g$  and product of merit functions for  $R_n$ ,  $Q$ ,  $V_g$ ,  $\Delta V_g$  (open down triangles). The data is shown as function of batch code + batch number/13, i.e. all available SIS27xx batches are located between 27 and 28 on the horizontal axis.

<sup>6</sup>Given sufficient resources, this could be done, e.g., using the QMIX package or even a neural network for optimization.

	<b>ALMA Band 9 Sideband Separating Upgrade</b> <hr/> <b>Study Report</b>	DocID: FEND-40.02.09.00-1974-C-REP Version: C Date: 2023-02-07 Status: Released Page: 91 of 105
---	---	---

Let us define a merit function which has value 1 when its argument falls within a certain parameter range and it has value 0 outside this range with a smooth transition; see the example in figure 65. Then we can take all available DC I-V curves of a certain batch and use the value of this function for a certain parameter range (as shaded in figure 64), averaged for all of them to estimate the probability of the batch to have a good noise temperature. We plot the merit function vs. the batch code plus batch number as shown in figure 66. It can be done for all available parameter types  $R_n$ ,  $V_g$ ,  $\Delta V_g$  and quality factor  $Q = R_j/R_n$ . We assume that to get an optimal noise temperature merit function corresponding to all parameters should be 1 simultaneously and we use product of merit functions for all parameters as final score to make a choice of good batch candidates. This score function is shown in figure 66 as an open triangles. The higher the value the larger the probability that noise temperature of mixer with these I-V curve parameters will have a low noise temperature.

It must be noted that both batches that were measured and delivered as part of ALMA Band 9 receivers as well as batches that have only DC I-V curves are present in figure 66. It comes at no surprise that the delivered batches have the highest score. From the available batches that were not excluded on the basis of additional noise temperature measurements, only one batch remains that has a score large enough to try to do heterodyne evaluation. From this we preliminary conclude that it is highly likely that we have depleted all the batches delivering good noise temperatures.

The method that we use have significant simplification as only a few parameters of DC I-V curve are taken into consideration. We are developing two more sophisticated methods to predict noise temperature: a Tucker-theory based prediction as well as a neural network based prediction. We will discuss results of these methods in the future.

## B Appendix — Polarimetry with ALMA

*In which two short reports are given on the effect of beam squint (rather than cross-polar level) on the polarimetric performance of ALMA; referred to in section 5.2.*

### B.1 Analysis cross-pol vs. beam squint

*Neil Phillips (ESO), 2020-06-19*

In summary, variations of beam squint between cartridges must be tightly controlled if not to hamper wide-field polarisation observations. On-axis cross-polar calibrates out, so the main concern there should just be noise contribution (similarly to imperfect image rejection). Systematic variation of cross-polar over the beam can be calibrated out too, but variation of the cross-polar pattern between receivers must be tightly controlled (same argument as beam squint). Tightly controlled here means at least an order of magnitude better than the 10% of the FWHM of the accepted ALMA beam squint specification, if we are serious about wide-field polarisation.

Following some discussion with Pavel Yagoubov (ESO), we realised that the basis for this topic has actually been covered in the project previously, in a polarisation supplement to the System Technical Requirements [30].

Based on that, it was proposed to significantly tighten the beam squint requirement, but it was considered too late in the construction receiver development to impose such a change. For new bands and upgrades we should probably review this.

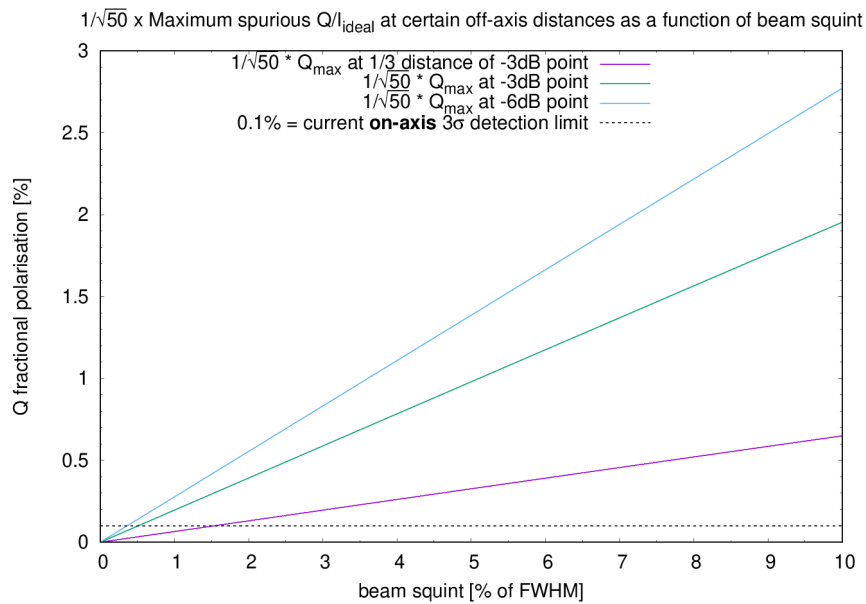


Figure 67: Spurious  $Q$  vs. beam squint

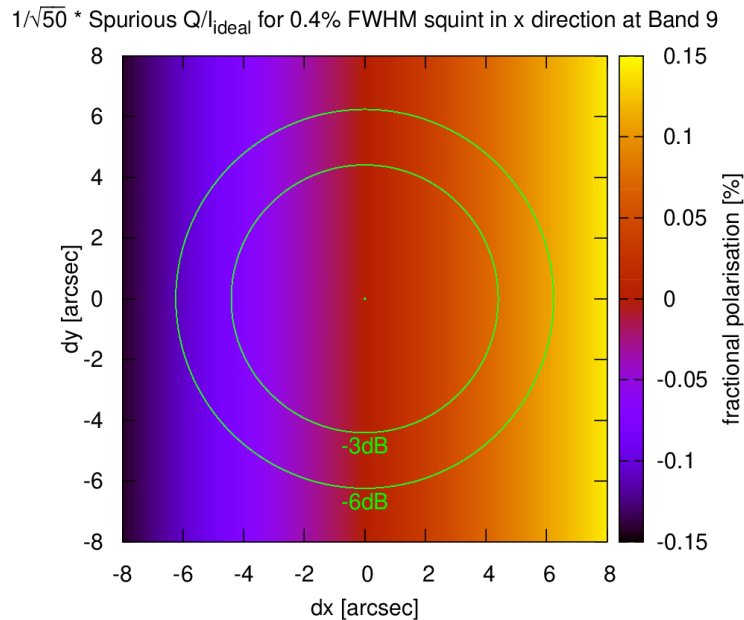


Figure 68: Spurious  $Q$  map

In terms of calibration, essentially any *systematic* small level (few % or less) errors in polarisation properties across the two instrumental polarised beam patterns can be calibrated out. By *systematic* I mean common to all array elements, allowing a single general model to be used in correction of data prior to or during imaging (analogous to primary beam correction). This includes cross-polar variations and beam squint. Even if receivers had perfect polarisation characteristics, such systematics anyway need to be accounted for due to the ALMA optical design with feeds offset from the centre of the focal plane, which gives a significant effective squint between circular polarisation beams (see, e.g., ALMA memo 115 [31]).

The on-axis cross-polar for each antenna (even if not systematic across the array) can also be straightforwardly calibrated out if it is reasonably small (few % or less, i.e., something like  $-15$  dB or better, such that high order terms in the maths can be neglected). Correction terms (on-axis “ $D$ -terms”) are measured by observing a calibrator source on-axis over a wide range of parallactic angles during each polarisation observation, such as to separate the instrumental cross-polar and the astronomical source polarisation.

What is very difficult to calibrate out is spatial variations across the beams that are not common to all array elements, i.e., to all receivers. This includes beam squint. Doing so in a similar way to how we handle on-axis variations would imply huge observing overheads to make polarisation beam maps for each antenna (if that’s even possible routinely for high frequency bands), and greatly increased complexity and run times of data processing to apply the per-antenna correction maps.

Squint of the linear feeds translates directly into a gradient of Stokes  $Q$  error across the field of view (e.g., figure 67). This directly impedes wide field polarisation measurements, as measurements off-axis have spurious Stokes  $Q$  (which is derived directly from  $XX - YY$ ). Polarised sources off-axis also undergo a mixing of Stokes terms.

	<p><b>ALMA Band 9 Sideband Separating Upgrade</b></p> <hr/> <p><b>Study Report</b></p>	<p>DocID: FEND-40.02.09.00-1974-C-REP  Version: C  Date: 2023-02-07  Status: Released  Page: 94 of 105</p>
---	--	--

In [30] they suggest that the random beam squint differences between receivers should be below 0.4% in order to suppress spurious polarisation (Stokes  $Q$  in particular) to 0.1% out to  $-6$  dB in the beam when averaging over an array of 50 antennas. The  $-6$  dB point is perhaps a little conservative, but taking the half-power point only increases the random squint tolerance up to about 0.6% (see figure 68, a plot of peak  $Q$  error at various distances from on-axis as a function of squint, after averaging 50 antennas). Note that at present we do achieve and offer on-axis linear polarisation accuracy of 0.1% (3-sigma), but we limit users to proposing polarisation experiments only within 1/3 of the half-power point, within which calibration errors are considered reasonable, which implies the average random squint variations between antennas for the offered receiver bands (3–8) being under about 1%. Increasing the field of view for polarisation is indeed a sticking point in ALMA.

Regarding measurement of beam squint, for Band 9 we can measure with an accuracy of around 0.2% FWHM using basic single dish techniques and a suitable planet. As an example see JIRA ticket AIV-15651 (in this case measuring a squint of 3.6% — in spec, but not ideal for wide field polarisation). We could therefore quite easily verify a very tight beam squint requirement such as 0.4% for Band 9.

Apart from the obvious noise impact of cross-polar leakage, I don't yet see any clear downside to calibration, as long as any angular variation across the beam is systematic for all receivers, and the worst-case leakage is small enough (few %) that the usual  $D$ -term calibration formalism, assuming high order terms can be neglected, is sufficiently valid. Systematic cross-polar would of course still limit polarisation measurement accuracy without  $D$ -term correction, but unless the cross-polar is better than  $-30$  dB,  $D$ -term correction is anyway needed to reach the level of accuracy needed for most science cases (calibration accuracy better than 0.1%).

## B.2 Beam squint statistics of the ALMA bands

*Neil Phillips (ESO), 2020-06-19*

Figure 69 shows the linear polarisation beam squint (cross-elevation and elevation offset between the  $Y$  and  $X$  polarisation beams on the sky) in units of percentage of the beam FWHM at the observing frequency, for each band. These measurements were from recent interferometric pointing calibration scans that occur at the end of focus calibration observations. These measurements have the advantage of being pretty consistently made (many antennas observing simultaneously) and it was less tedious than having to copy+paste values out of many AIV/AIV+ reports. For Band 10 there are few of these measurements available, and it is expected that the AIV+ single-dish measurements, will be better for that band. For Band 9 it worked pretty well, although there are not measurements of every cartridge (only observations of masers have sufficient S/N for this in Bands 9 and 10, and these only started being used for such calibration scans in Cycle-7). For lower frequency bands it works very well as there are many measurements and very high S/N.

As can be seen, the OMT-based (single-horn) bands are generally well within 2% of the FWHM for all but rare outliers. This includes Band 8. Bands 7 and 9 with wire grids show a much larger scatter. There are a couple of pre-production Band 9 cartridges that exceed the 10% limit, at least one of which has a waiver (FEND-40.00.00.00-1008-A-RFW) acknowledging that the 10% specification was introduced after the pre-production run so it was not decided to improve it.

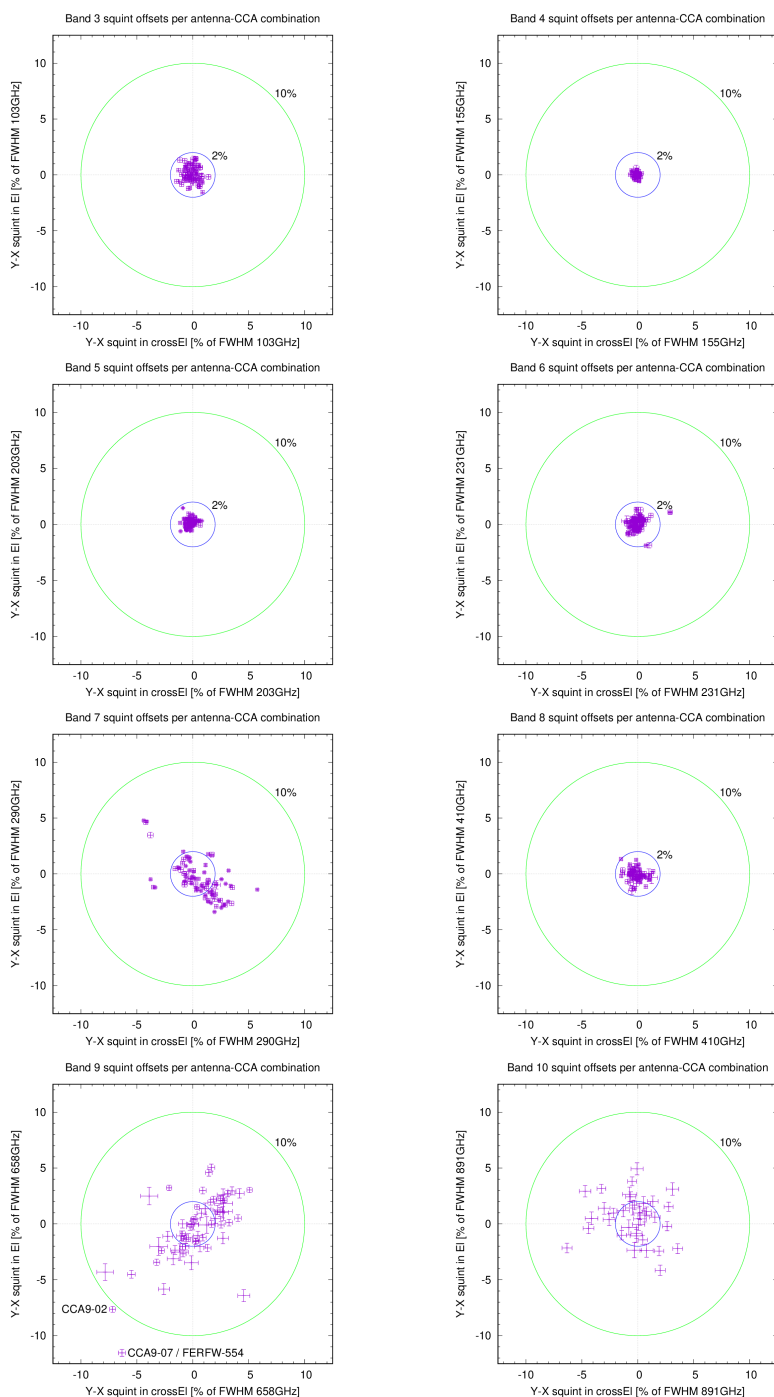


Figure 69: On-sky  $Y-X$  polarisation beam squint in cross-elevation vs. elevation coordinates in units of the beam FWHM at the observing frequency for Bands 3 to 10. Multiple measurements have been averaged per antenna-CCA combination when possible. The 10% specification limit is shown (green circle), in addition to a threshold of 2% which all existing single-horn receivers (Bands 3, 4, 5, 6, 8) could comply with and which may be a practical future goal.

	<p><b>ALMA Band 9 Sideband Separating Upgrade</b></p> <p>—</p> <p><b>Study Report</b></p>	<p>DocID: FEND-40.02.09.00-1974-C-REP  Version: C  Date: 2023-02-07  Status: Released  Page: 96 of 105</p>
---	---	--

Whilst there are systematic offsets from the origin for some bands, including Band 9, these are small compared to the scatter, so it seems that the repeatability variation dominates over any systematic  $Y$ - $X$  squint. As discussed in section B.1, it is the repeatability that is most important to control in the context of wide-field polarisation imaging, in order to avoid needing per-antenna/CCA polarisation beam maps to be obtained and applied as part of the reduction process. Given that the repeatability dominates, it does not seem useful to complicate any future specifications with separate systematic vs. repeatability specifications, and retaining a single simple limit on per-cartridge squint is fine. A limit of 2% would imply an RMS scatter below about 1%, resulting in approximately the sort of calibration error tolerable for high quality wide field polarisation (0.6% for imaging to the half power field of view). This would therefore be a good goal for future receivers.

Although a single-horn+OMT solution clearly does achieve the desired squint performance, it was discussed in the meeting that it may not necessarily be unachievable with a dual-horn+grid solution. Most Band 9 receivers are within about 5% FWHM, and quite a few already fall within 2%, so it was proposed to investigate if the squint could be reduced to within 2% by reducing tolerances in the optics as an alternative to a more significant re-design.

	<b>ALMA Band 9 Sideband Separating Upgrade</b>	DocID: FEND-40.02.09.00-1974-C-REP Version: C
	<hr/> <b>Study Report</b>	Date: 2023-02-07 Status: Released Page: 97 of 105

## C Appendix — Observing during a 2SB upgrade roll-out

*In which an in-depth discussion is presented on the issues of correlating a heterogeneous array of DSB and 2SB receivers; referred to in section 7.2.2.*

*Neil Phillips (ESO), 2022-08-29*

A receiver band upgrade roll-out takes a minimum of 2 to 3 years to be completed, so we need to consider how to keep observing with a band while the number of DSB receivers reduces and the number of 2SB ones increases.

At a minimum this will require the ALMA control software to support both of these two types of receivers in antennas in an array. This is at least theoretically possible as the software controlling each receiver runs within each antenna, but some effort to allow these different configurations to coexist is expected. This issue may be common to the upgrade of any band that will alter the required M&C, i.e., this may be a more general consideration than just the upgrade of DSB bands to 2SB.

How a heterogeneous array of DSB and 2SB receivers may be correlated is the subject of this section. Recall that the LSB signals from the DSB receivers are provided in the single “USB” IF channel (the “USB” label referring to the use of this channel by SSB/2SB bands), while the LSB signals from the 2SB receivers are in the dedicated “LSB” IF channel. In a worst case only the USB could be correlated and offered to users during the transition observing cycles. However, this will prevent observing the bottom of the RF band, will reduce available bandwidth by a factor of two, and reduce tuning flexibility. Thus means are desired for allowing the LSB to also be observed during the transition. An option could be to invert the sign of the bias in the XML configuration files for frequencies in the lower LSB portion of the band, in order to deliver the LSB signal in the USB IF output channel. However, this requires some extra effort and uncertainty to verify the receivers also with reversed bias.

### C.1 Ideal case: per-antenna sub-band configuration

As will be described in the following subsection, using a single signal path configuration in the back-end and correlator for all antennas in the array will lead to complexities and reduced sensitivity and number of baselines for LSB correlations during the upgrade campaign. The reduced number of baselines and sensitivity are due to not producing LSB correlations between DSB and 2SB receivers. However, the proposed ALMA Wideband Sensitivity Upgrade (WSU) system offers a potentially optimal and elegant solution to this. The WSU system is expected to be operational by the time of a Band 9 upgrade roll-out.

The WSU system will have a “first-F” channelisation, which will split the digitised IFs into sub-bands of around 1.6–2.0 GHz of usable bandwidth. There is expected to be flexibility in how these sub-bands are tuned and selected, although this is not defined yet. Here we propose a requirement on this flexibility: that sub-bands from one IF sampler (USB) can optionally be duplicated, taking the place of sub-bands that would normally be generated from the other IF sampler (LSB). This would be performed for the antennas in the array with DSB receivers, while the antennas with 2SB receivers do not, and instead use the same sub-band tunings for both IF samplers (USB and LSB), producing separate sub-bands from each. The correlator will then see from every antenna correlateable USB signal in one half of the sub-bands and correlateable LSB signal in the other half, regardless of the receiver type (just the sideband gains will differ between antennas). Depending on how LO offsetting will be implemented

	<b>ALMA Band 9 Sideband Separating Upgrade</b>	DocID: FEND-40.02.09.00-1974-C-REP Version: C
	<b>Study Report</b>	Date: 2023-02-07 Status: Released Page: 98 of 105

in the “first-F”, the image sideband suppression in the cross-correlations could be performed either by LO offsetting or 90° Walsh switching (with the image sideband output ignored). For LO offsetting to be used it would be necessary to not simply duplicate the sub-bands, but produce a pair of sub-bands with opposite LO offsets, which may or may not be feasible depending on the “first-F” implementation. 90° Walsh would work with sub-bands copied verbatim. Note that with this technique it is also necessary to account correctly for the extra LSB signal path delay terms for the 2SB receivers in the delay model, which do not apply to duplicated sub-bands for LSB correlation from the DSB receivers.

A particular advantage of this technique is that the LSB correlations between all receiver types (DSB×DSB, 2SB×2SB *and* DSB×2SB) end up in the same spectral windows, so there are no complications for combining them in imaging. Both the LSB and USB will have the full number of baselines possible with a given number of antennas, and the sensitivity of both sidebands will only improve as 2SB receivers replace DSB ones.

A caveat, although equally affecting any band with 2SB receivers, is that the total post-correlation bandwidth available for science will be equal to the correlation bandwidth of the correlator. However, given the 8 GHz IF bandwidth of the legacy DSB receivers this would only be an issue if the correlator has less than 16 GHz of correlation bandwidth. It would, for example, be a relevant concern if the existing correlators with just under 8 GHz of correlation bandwidth would be used (with only DSB receivers as now, the post-correlation bandwidth is doubled by sideband separation in the correlator). This issue is common to any scheme that wishes to obtain LSB correlations from 2SB receivers.

To summarise, with sub-band duplication in antennas with DSB receivers there would be the following pros and cons.

**Pros:**

- No reduction in LSB baselines: LSB correlations produced between all receiver types (DSB×DSB, 2SB×2SB *and* DSB×2SB);
- LSB correlations between all receiver types (DSB×DSB, 2SB×2SB *and* DSB×2SB) end up in the same spectral windows (i.e., the data looks normal);
- Maximum sensitivity for any combination of DSB and LSB receivers in the array.

**Complexities / cons:**

- “first-F” to implement sub-band duplication, or better to allow the full number of sub-bands to be generated from a single IF sampler to allow different LO offsets;
- Control software to configure the “first-F” per-antenna based on whether a DSB or 2SB receiver is installed;
- LSB signal path delays need to be used in the delay compensation for LSB sub-bands of 2SB receivers, i.e., the delay model logic also needs to be aware of the receiver type in each antenna;
- Limited by correlated bandwidth of the correlator just as for 2SB bands, although with an upgraded correlator this should not be an issue during the 2SB upgrade.

## C.2 Uniform signal path configuration for the whole array

If the signal path settings (sub-band selection/tuning in the WSU “first-F”, or IF Processor sideband switch settings in the current system) need to be the same for all antennas in the array, or duplicating sub-bands from a single IF input is not feasible, then we need to consider the impact on LSB correlations. There are three post-correlation sideband quantities to consider:



1. USB signal delivered via the “USB” IF receiver outputs (DSB and 2SB receivers);
2. LSB signal delivered via the “USB” IF receiver outputs (DSB receivers only);
3. LSB signal delivered via the “LSB” IF receiver outputs (2SB receivers only).

Note that LSB signals cannot be correlated between DSB and 2SB receivers in this scenario as these originate in different IF signal paths. As the upgrade progresses, the number of baselines in (1) will remain fixed, while the sensitivity will steadily improve due to the reduced image sideband noise from the 2SB receivers; the number of baselines and sensitivity in (2) will steadily decrease; and the number of baselines and sensitivity in (3) will steadily increase. The progression of the number of baselines in each of these three correlations and the sum of both LSB correlations is shown in figure 70. The progression of point source sensitivity is considered later, after mentioning some other relevant factors.

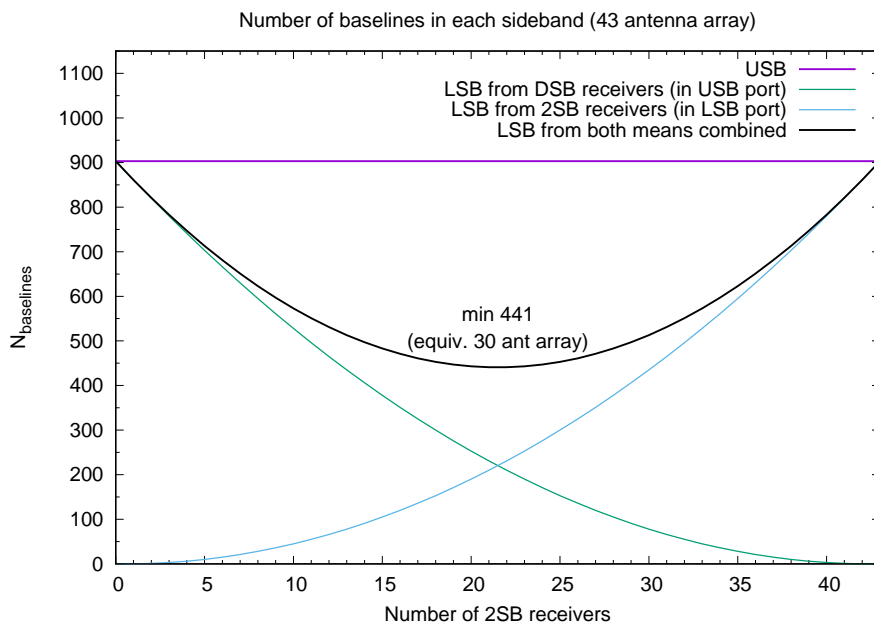


Figure 70: The progression of the number of baselines in each sideband product as the upgrade progresses, assuming an array of 43 antennas and that it is not possible to correlate different IF channels from different antennas. The number of USB baselines remains constant as DSB and 2SB receivers work interchangeably. The number of LSB baselines between DSB receivers, obtained by correlator sideband separation of the USB receiver IF output channel, decreases as DSB receivers are removed. The number of LSB baselines between 2SB receivers, from correlating the LSB receiver output channel, increases as 2SB receivers replace the DSB ones. The total number of LSB baselines from both means reaches a minimum half way through the upgrade of roughly half the number of USB baselines, approximately equal to the number of baselines from an array of 30 antennas.

### C.2.1 Relevant correlator capabilities

In addition to the receivers, the available correlator capabilities in terms of sideband separation and correlated bandwidth are important to consider. By the time of the Band 9 upgrade we anticipate that the correlator will have been upgraded. The correlated bandwidth of the new

	<p><b>ALMA Band 9 Sideband Separating Upgrade</b></p> <p>—</p> <p><b>Study Report</b></p>	<p>DocID: FEND-40.02.09.00-1974-C-REP</p> <p>Version: C</p> <p>Date: 2023-02-07</p> <p>Status: Released</p> <p>Page: 100 of 105</p>
---	---	---

correlator will be at least 16 GHz per polarisation which, considering the 8 GHz IF bandwidth of the legacy DSB receivers, is sufficient to correlate both sideband IF outputs over the common IF range during the upgrade roll-out. The eventual usable bandwidth after the upgrade roll-out, when the full IF range of the new 2SB receivers could be used, will depend on the actual correlation bandwidth delivered.

We expect that sideband separation by 90° Walsh switching will be supported<sup>7</sup>, which is required to obtain both USB and LSB correlations from the DSB receivers. This doubles the recorded post-correlation bandwidth by producing two sideband spectral windows from one correlated IF (this is the case for the existing correlators). With correlator sideband separation it is possible to record all three of the correlation products mentioned above, such that a reasonable number of baselines in LSB can be achieved at any point during the 2SB roll-out (the worst case being about half the number of USB baselines, as shows in figure 70). As the correlator may be quite new during the 2SB upgrade roll-out, and perhaps sideband separation by 90° Walsh switching may not have been made available (e.g., for the existing correlators this mode was only offered after 5 years of ALMA operations), we also consider the situation without this correlator capability.

### C.2.2 Implications on offline processing

A further consideration for the operational use during the transition is whether offline data processing will be able to make use of both the LSB correlations (2) and (3). The current ALMA data processing is generally able to proceed with different antennas flagged in each spectral window, so the reduced number of LSB baselines in both (2) and (3) during the transition should not inherently be a significant issue to handle. It is possible that the unusable baselines with 2SB receivers in (2) and DSB receivers in (3) may anyway be heuristically flagged, but explicit flags could be set if suitable metadata conveying the receiver type in each antenna is made available. The most complex issue to consider would be the combination of baselines from (2) and (3) if both are recorded. These would naturally be produced in different spectral windows by the correlator, and thus calibrated and imaged independently by the pipeline. To deal with this, either the pipeline could be modified to recognise these spectral windows covering the same sky frequency range and image them together or, perhaps more pragmatically, the imaging of the combined LSB SpWs could be performed manually, as this will only be needed for a limited period of time.

### C.2.3 Point-source sensitivity during the upgrade roll-out

A simple model is used here to show how the continuum point source sensitivity varies throughout the upgrade process from DSB to 2SB for an array of 43 12 m antennas. Although continuum observations of point sources are only one use case, the sensitivities per sideband still have relevance for point source spectral line observations, and continuum point source sensitivity is an important quantity for phase referencing. The model uses the following assumptions:

- $T_{\text{RX,DSB}} = 100 \text{ K}$  (roughly the case for current Band 9 mixers);
- $\text{SEFD} = 42 \text{ [Jy/K]} \times (0.7/0.5)$ , where 0.7 and 0.5 are approximate aperture efficiencies at low frequencies at which the 42 Jy/K is reasonable and at Band 9, respectively;
- $N_{\text{pol}} = 2$  polarisations are averaged;

<sup>7</sup>As long as 16 ms duration dumps can be produced by the correlation then it is simple to perform the sideband separation in post-processing.

	<b>ALMA Band 9 Sideband Separating Upgrade</b>	DocID: FEND-40.02.09.00-1974-C-REP
	—	Version: C
	<b>Study Report</b>	Date: 2023-02-07
		Status: Released
		Page: 101 of 105

- Bandwidth per sideband,  $\Delta\nu_{\text{SB}}$  of 8 GHz (limited by the legacy DSB receivers);
- $t_{\text{int}} = 60$  seconds integration duration;
- Atmospheric optical depth for both sidebands,  $\tau_{\text{USB}}, \tau_{\text{LSB}}$ , equal to 1.0 (fairly typical on average);
- $T_{\text{sky}}$  in each sideband computed as  $T_{\text{sky,USB}} = T_{\text{atm}}(1 - e^{-\tau_{\text{USB}}})$ , with  $T_{\text{atm}} = 270$  K (reasonable for the broadband absorbing components, particularly  $\text{H}_2\text{O}$ );
- $T_{\text{sys}}$  for each sideband for DSB and 2SB receivers calculated as:
  - $T_{\text{sys,DSB,USB}} = e^{\tau_{\text{USB}}}(2 T_{\text{RX,DSB}} + T_{\text{sky,USB}} + T_{\text{sky,LSB}})$
  - $T_{\text{sys,DSB,LSB}} = e^{\tau_{\text{LSB}}}(2 T_{\text{RX,DSB}} + T_{\text{sky,USB}} + T_{\text{sky,LSB}})$
  - $T_{\text{sys,2SB,USB}} = e^{\tau_{\text{USB}}}(2.1 T_{\text{RX,DSB}} + T_{\text{sky,USB}})$
  - $T_{\text{sys,2SB,LSB}} = e^{\tau_{\text{LSB}}}(2.1 T_{\text{RX,DSB}} + T_{\text{sky,LSB}})$
  - The factor 2.1 is a bit of a fudge to try to account for added noise from losses in a 2SB design with the same mixers (the ideal case would be 2.0).
- For each sideband in each baseline the weight is  $w_{i,j} = 1/(T_{\text{sys,i}} \times T_{\text{sys,j}})$ , where the appropriate sideband and receiver type  $T_{\text{sys}}$  are used for each antenna;
- The point source sensitivity is  $\sigma = \text{SEFD}/\sqrt{N_{\text{pol}}\Delta\nu_{\text{SB}}t_{\text{int}}\sum w_{i,j}}$ , where the sum is over the relevant baselines for each correlation.

Figure 71 shows how the continuum point source sensitivity varies in each sideband and in total for these assumptions, with and without correlator sideband separation.

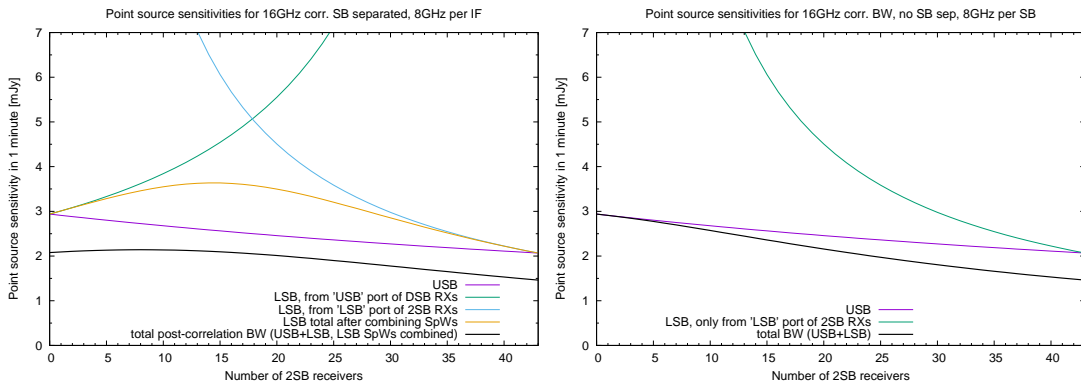


Figure 71: Continuum point source sensitivity progression of a 43 antenna array during a 2SB upgrade roll-out with a correlation bandwidth of at least 16 GHz per polarisation, assuming that it is not possible to correlate different IF channels from different antennas. Lower is better. In both cases 8 GHz of correlation bandwidth is assigned to each IF channel. Left: with correlator sideband separation enabled, which gives 16 GHz total bandwidth for both DSB $\times$ DSB and 2SB $\times$ 2SB baselines but only 8 GHz (only USB) for DSB $\times$ 2SB baselines. Note that the LSB output from the DSB $\times$ DSB and 2SB $\times$ 2SB baselines would appear in different spectral windows. Right: without correlator sideband separation, which produces 16 GHz total bandwidth for 2SB $\times$ 2SB baselines but only 8 GHz (only USB) for all the other baselines.

### C.2.4 Pros and cons

Below are a summary of pros and cons of using a common sub-band or signal path selection for all antennas in the array during the upgrade roll-out.

	<b>ALMA Band 9 Sideband Separating Upgrade</b> <hr/> <b>Study Report</b>	DocID: FEND-40.02.09.00-1974-C-REP Version: C Date: 2023-02-07 Status: Released Page: 102 of 105
---	---	--

**Pros:**

- “first-F” doesn’t need to do anything special;
- ALMA control software doesn’t need to configure different sub-band or signal path settings per antenna;
- LSB can be offered with reasonable (but not maximum) number of baselines and sensitivity during the upgrade.

**Complexities / cons:**

- number of LSB baselines and sensitivity is not maximum due to missing DSB×2SB baselines;
- LSB correlations from DSB×DSB and 2SB×2SB baselines would appear in different spectral windows if both are produced; offline data processing would need to deal with this;
- LSB data would be “sparse” in the sense of only having meaningful data for only a subset of baselines in each SpW; this would need suitable flagging;
- the system will need to gracefully handle the complete lack of power in the “LSB” IF channel from DSB receivers which will be sampled and processed in this scenario.

	<b>ALMA Band 9 Sideband Separating Upgrade</b>	DocID: FEND-40.02.09.00-1974-C-REP Version: C
	<b>Study Report</b>	Date: 2023-02-07 Status: Released Page: 103 of 105

## References

- [1] A. Baryshev, A. Khudchenko, R. Hesper, J. Adema, and W. Boland, “Full 2SB Receiver Upgrade for ALMA Band 9: Implementation Study; Scientific — Technical — Management Proposal,” 01 Sept. 2016.
- [2] R. Hesper, A. Baryshev, A. Khudchenko, J. Adema, and W. Boland, “Amendment to Annex to Call for Proposals CFP/ESO/16/11115/OSZ,” 25 Jan. 2019.
- [3] R. Hesper, J. Barkhof, J. Adema, and A. Baryshev, “ALMA Band 9 Sideband Separating Upgrade — Midterm Study Report,” ALMA document FEND-40.02.09.00-1963-E-REP, NOVA Sub-mm Instrumentation Group, 17 Dec. 2020.
- [4] A. Baryshev, A. Khudchenko, R. Hesper, and W. Boland, “Design Verification and Test Results,” ALMA document FEND-40.02.09.00-1874-A-REP, NOVA Sub-mm Instrumentation Group, 28 Mar. 2012.
- [5] R. Hesper, A. Khudchenko, A. M. Baryshev, J. Barkhof, and F. P. Mena, “A new high-performance sideband-separating mixer for 650 GHz,” in *SPIE Conference Series*, vol. 9914, pp. 99140G–1–99140G–11, 2016.
- [6] A. Khudchenko, R. Hesper, A. M. Baryshev, J. Barkhof, and F. P. Mena, “Modular 2SB SIS Receiver for 600–720 GHz: Performance and Characterization Methods,” *IEEE Transactions on Terahertz Science and Technology*, vol. 7, pp. 2–9, Jan. 2017.
- [7] R. Hesper, A. Khudchenko, A. M. Baryshev, J. Barkhof, and F. P. Mena, “A High-Performance 650-GHz Sideband-Separating Mixer — Design and Results,” *IEEE Transactions on Terahertz Science and Technology*, vol. 7, pp. 686–693, Nov. 2017.
- [8] R. Hesper, A. Khudchenko, M. Lindemulder, M. Bekema, R. de Haan-Stijkel, J. Barkhof, J. Adema, and A. Baryshev, “A Deployable 600–720 GHz ALMA-Type Sideband-Separating Receiver Cartridge,” in *29th International Symposium on Space Terahertz Technology, Pasadena*, 2018.
- [9] Belitsky, V., Lapkin, I., Fredrixon, M., Meledin, D., Sundin, E., Billade, B., Ferm, S.-E., Pavolotsky, A., Rashid, H., Strandberg, M., Desmaris, V., Ermakov, A., Krause, S., Olberg, M., Aghdam, P., Shafiee, S., Bergman, P., Beck, E. De, Olofsson, H., Conway, J., Breuck, C. De, Immer, K., Yagoubov, P., Montenegro-Montes, F. M., Torstensson, K., Pérez-Beaupuits, J.-P., Klein, T., Boland, W., Baryshev, A. M., Hesper, R., Barkhof, J., Adema, J., Bekema, M. E., and Koops, A., “SEPIA — a new single pixel receiver at the APEX telescope,” *A&A*, vol. 612, p. A23, 2018.
- [10] P. Bergman, M. Olberg, D. Meledin, M. Fredrixon, E. Sundin, M. Strandberg, R. Hesper, J. Barkhof, K. Torstensson, J.-P. Perez, F. Montenegro, R. Parra, M. Ciechanowicz, C. de Breuck, and F. Wyrowski, “SEPIA660 (Band 9) Commissioning Report,” APEX Doc. APEX-ESO-TRE-0023, Atacama Pathfinder EXperiment, 29 Jan. 2019.
- [11] A. D. Bolatto, J. Carpenter, S. Casassus, D. Iono, R. Ivison, K. Johnson, H. van Langevelde, J. Martín-Pintado, M. Momose, R. Moreno, K. Motohara, R. Neri, N. Ohashi, T. Oka, R. Osten, R. Plambeck, E. Schinnerer, D. Scott, L. Testi, and A. Wootten, “A Road Map for Developing ALMA — ASAC Recommendations for ALMA 2030,” 2015.
- [12] A. Bolatto, S. Corder, D. Iono, L. Testi, and A. Wootten, “Pathways to Developing ALMA — ALMA Development Working Group Report,” 2015.
- [13] J. Carpenter, D. Iono, L. Testi, N. W. amd A. Wootten, and N. Evans, “The ALMA Development Roadmap,” 2018.
- [14] A. R. Kerr, S.-K. Pan, and J. E. Effland, “Sideband Calibration of Millimeter-Wave Receivers,” ALMA Memo 357, NRAO, 27 Mar. 2001.

	<p><b>ALMA Band 9 Sideband Separating Upgrade</b></p> <hr/> <p><b>Study Report</b></p>	<p>DocID: FEND-40.02.09.00-1974-C-REP Version: C Date: 2023-02-07 Status: Released Page: 104 of 105</p>
---	--	---

- [15] A. M. Baryshev, R. Hesper, F. P. Mena, T. M. Klapwijk, T. A. van Kempen, M. R. Hogerheijde, B. D. Jackson, J. Adema, G. J. Gerlofsma, M. E. Bekema, J. Barkhof, L. H. R. de Haan-Stijkel, M. van den Bemt, A. Koops, K. Keizer, C. Pieters, J. Koops van het Jagt, H. H. A. Schaeffer, T. Zijlstra, M. Kroug, C. F. J. Lodewijk, K. Wielinga, W. Boland, M. W. M. de Graauw, E. F. van Dishoeck, H. Jager, and W. Wild, “The ALMA Band 9 receiver - Design, construction, characterization, and first light,” *A&A*, vol. 577, p. A129, May 2015.
- [16] K. Rudakov, *Development of Advanced Superconductor-Insulator-Superconductor Mixers for Terahertz Radio Astronomy*. PhD thesis, University of Groningen, 8 July 2021.
- [17] R. Hesper, J. Barkhof, and T. Vos, “Improving Band 9 Sensitivity by Advanced Tuning Algorithms — Final Study Report,” ALMA document FEND-40.02.09.00-1944-C-REP, NOVA Sub-mm Instrumentation Group, 10 Jan. 2020.
- [18] R. Finger, F. P. Mena, A. Baryshev, A. Khudchenko, R. Rodriguez, E. Huaracan, A. Alvear, J. Barkhof, R. Hesper, , and L. Bronfman, “Ultra-pure digital sideband separation at sub-millimeter wavelengths,” *A&A*, vol. 584, p. A3, 2015.
- [19] F. M. Montenegro-Montes, K. Torstensson, R. Parra, J. P. Pérez-Beaupuits, L. Å. Nyman, C. Agurto, F. Azagra, M. Cárdenas, E. González, F. MacAuliffe, P. Venegas, C. De Breuck, P. Bergman, D. S. Gunawan, F. Wyrowski, T. Stanke, V. Belitsky, M. Fredrixon, D. Meledin, M. Olberg, M. Strandberg, E. Sundin, J. Adema, J. Barkhof, A. Baryshev, R. Hesper, and A. Khudchenko, “Orion-KL Observations with the Extended Tuning Range of the New SEPIA660 APEX Facility Instrument,” *The Messenger*, vol. 176, pp. 20–24, June 2019.
- [20] F. Kemper e-mail, 2019-11-08.
- [21] J. R. Pardo, C. De Breuck, D. Muders, J. González, F. M. Montenegro-Montes, J. P. Pérez-Beaupuits, J. Cernicharo, C. Prigent, E. Serabyn, T. Mroczkowski, and N. Phillips, “Extremely high spectral resolution measurements of the 450  $\mu\text{m}$  atmospheric window at Chajnantor with APEX,” *A&A*, vol. 664, p. A153, 2022.
- [22] A. Baryshev, “Details of optical layout for band 9,” Tech. Rep. 2, Kapteyn Astronomical Institute, University of Groningen, The Netherlands, January 2004.
- [23] S. Asayama and M. Kamikura, “Development of Double-Ridged Waveguide Orthomode Transducer for the 2 mm Band,” *J. of Infrared, Millimeter, and Terahertz Waves*, vol. 30, pp. 573–579, June 2009.
- [24] N. Satou, “Band 8 OMT Pol1 Hybrid Assy,” ALMA document (drawing) FEND-40.02.08.04-002-D-DWG, NAOJ, 17 Jan. 2011.
- [25] Y. Sekimoto, “Band 8 Cartridge Technical Specifications,” ALMA document FEND-40.02.08.00-001-B-SPE, NAOJ, 8 Aug. 2013.
- [26] A. Dunning, S. Srikanth, and A. R. Kerr, “A Simple Orthomode Transducer for Centimeter to Submillimeter Wavelengths,” in *Proc. 20th ISSTT*, pp. 191–194, 2009.
- [27] A. Khudchenko, R. Hesper, A. M. Baryshev, J. Barkhof, K. Rudakov, D. Montofré, D. van Nguyen, V. P. Koshelets, P. N. Dmitriev, M. Fominsky, C. Heiter, S. Heyminck, R. Güsten, and B. Klein, “Design and Performance of a Sideband Separating SIS Mixer for 800–950 GHz,” *IEEE Transactions on Terahertz Science and Technology*, vol. 9, no. 6, pp. 532–539, 2019.
- [28] A. Baryshev, B. Jackson, and J. Barkhof, “ALMA Band 9 Cartridge Cross Polarization Test Procedure,” ALMA document FEND-40.02.09.00-027-C-PRO, NOVA Sub-mm Instrumentation Group, 27 Aug. 2008.
- [29] M. Candotti, A. M. Baryshev, N. A. Trappe, R. Hesper, J. A. Murphy, and J. Barkhof, “Quasi-Optical Verification of the Band 9 ALMA Front-End,” in *Sixteenth International Symposium on Space Terahertz Technology*, pp. 79–84, 2005.

	<b>ALMA Band 9 Sideband Separating Upgrade</b> — <b>Study Report</b>	DocID: FEND-40.02.09.00-1974-C-REP Version: C Date: 2023-02-07 Status: Released Page: 105 of 105
---	--	--

- [30] R. Sramek and P. Napier, “Revised ALMA System Technical Requirements — Polarization,” ALMA document (draft status) ALMA-80.04.00.00-0038-A-SPE, NRAO, 27 Aug. 2010.
- [31] P. J. Napier, “Polarization Properties of an Open Cassegrain Antenna,” ALMA Memo 115, NRAO, 4 May 1994.